MOTROL

AN INTERNATIONAL JOURNAL
ON OPERATION OF FARM
AND AGRI-FOOD INDUSTRY MACHINERY

Polish Academy of Sciences
University of Engineering and Economics in Rzeszów
University of Life Sciences in Lublin

MOTROL

COMMISSION OF MOTORIZATION AND ENERGETICS IN AGRICULTURE

AN INTERNATIONAL JOURNAL
ON OPERATION OF FARM
AND AGRI-FOOD INDUSTRY MACHINERY

Vol. 19, No 2

LUBLIN – RZESZÓW 2017

Linguistic consultant: Orest Hrekh

Typeset: Viktor Shevchuk, Adam Niezbecki

Cover design: Hanna Krasowska-Kołodziej

Photo on the cover: Janusz Laskowski

All the articles are available on the webpage:
http://www.pan-ol.lublin.pl/wydawnictwa/Teka-Motrol.html

All the scientific articles received positive evaluations by independent reviewers

ISSN 1730-8658

Editorial Office address
Polish Academy of Sciences Branch in Lublin
Pałac Czartoryskich, Plac Litewski 2, 20-080 Lublin, Poland
e-mail: eugeniusz.krasowski@up.lublin.pl

Publishing Office address
Lviv National Agrarian University
St. Vladimir the Great, 1, Dubliany, Ukraine, 80381
e-mail: motrol@ukr.net

Printing
Lviv National Agrarian University
St. Vladimir the Great, 1, Dubliany, Ukraine, 80381
phone: +38 032 22 42 954

Edition 150+16 vol.

MOTROL. Commission of Motorization and Energetics in Agriculture – 2017. Vol.19. No.2. 5-10

DEPENDENCE OF OIL CROPS YIELD ON WEATHER CONDITIONS IN EASTERN STEPPE OF UKRAINE

Nikolai Tsekhmeistruk[1], Victor Tymchuk[1], Oleksandr Glubokyi[2], Alla Fesenko[2], Oksana Pankova[2]

[1]The Plant Production Institute nd. a. V. Ya. Yuryev of NAAS Moskovskiy avenue, 142, Kharkiv, Ukraine. E-mail: laboplant@gmail.com

[2]Kharkiv Petro Vasylenko National Technical University of Agricultural St. Artema, 44, Kharkov, Ukraine. E-mail: agroecology265@gmail.com

Summary. Efficiency Improving of machine using in conditions of agricultural enterprises of Ukraine, the choice of the optimal timing of agricultural operations should be based on the peculiarities of development and needs of crops. And these conditions, the efficiency of nutrient absorption, growth and maturity crops depend on the weather conditions. The unpredictability of them increases in conditions of modern climate changing. Therefore, the establishment of climate change tendencies and the reaction of the cultivated varieties of crops on them are extremely important.

Analysis of weather influence on crop yield, crop features in an investigation area has been done. For 2004-2013 average daily temperatures have increased by + 1.3^0 C, the effective accumulated temperatures has been 1496.8^0 C, this is by 290.8^0 C, or 24.1% higher than before. Total precipitation has increased by 34.4 mm compared with long-term values. Large amount of rainfall in June has a negative impact on harvest value (the correlation coefficients for sunflower are -0.46 and -0.59; and for soybean are -0.47 and -0.60). The most positive impact, r = 0.33-0.36, has the May active temperatures. If mineral fertilizers have been used in June, positive influence occurs also, r = 0.32 and 0.34. In other months, this dependence is weak, with a negative value in July: r = -0.12-0.14 and positive one in August: r = 0.25-0.25.

Key words: accumulated active temperatures, precipitation, average daily temperature, oilseeds, crop, sunflower, soybean, correlation coefficient.

INTRODUCTION

Bioclimatic potential characterizing by a complex of climatic factors (for example, solar radiation, the duration of the growing period, temperature, amount and dynamics of precipitation, etc.) determines the potential biological productivity of crops, the economic purpose of land use, cropping mix and economic production efficiency.

The impact of climate on the plant growth and development, the processes of nutrients transformation in a soil and fertilizer efficiency is demonstrated mainly through the water and temperature regimes, the duration of the growing period, intensity of the spring warming and features of the autumn frosts.

Each of the factorial climate components has a multiple effect on the crop formation and on production quality. The highest fertilizer efficiency is manifested when the soil moisture content is equal to 65-80% of the total moisture capacity [1].

ANALYSIS OF RECENT RESEARCHES AND PUBLICATIONS

According to experts to the middle of the XXI century, the average air temperature will have increased by 1.8^{0}C in comparison with these days. Hence, the season duration change and the effective accumulated temperature increasing are expected. This might result in the change of the agroclimatic zoning and agricultural production strategy. Under the current dynamics, tendencies of air temperatures increase in March and April and them decrease in May are expected [2].

According to WWF data average temperature in Ukraine in the last 100 years has increased by 0.8^{0}C [3]. In areas that have a tendency to drought, rainfall is less and not always during the harvest formation period; these conditions hinder to generate the crops with high productivity

In crop production, yield increase by 50% or more occurs due to the optimization of the interaction in the system "a plant - environment". Growing techniques turn out efficient only when they ensure the optimal development of the crops in accordance with environmental conditions [4]. All the factors supporting the development of plants are closely linked. Changing one of them causes a change in the other ones [5, 6].

The weather conditions during crop season cause significant fluctuations in productivity not only in individual regions and countries, but also on the continents. They have increased from 2.26 to 3.36% in recent years. The instability of crop production happens in both developing and developed countries. [7, 8]. The greatest crop productivity decrease is observed during coincidence "critical" periods of development with abiotic stresses (young growth – a drought, drop of the air temperature; flowering – a drought, increase of air temperature) [9-12].

In the future, the dependence of crop productivity on the weather conditions will be even more [13, 14]. According to forecasts of IIASA (International Institute for Applied Systems Analysis), in Europe the temperature rise will have occurred from 1.0^0 to 4.0^{0}C until 2030. The main trend in precipitation is drier summers and wetted winters. The probability of droughts will increase during the growing period of crop [15]. Climate change will affect the agro-climatic characteristics, for instance: the growing season duration, the moisture availability for plants, the active and effective temperatures [16-18].

Crops production without taking into account the biological features of plants and climate change might cause decrease in the grain production by 1.0-60% in developing countries and by 9.0-11.0% in developed economies, and great difference between actual and potential yield. Reducing in crop output will be accompanied by food prices increase and increasing of famine in developing countries [19, 20].

Crops adaptation to climate change first and foremost will be determined by agronomic practices properly selected, for example, by tillage minimizing, change in terms and ways of sowing, plant density and crop range with more heat-loving plants [21-24]. The main way which does not allow to reduce crop productivity is increase of the photosynthesis efficiency, the pace and term of the leaf surface formation [25-28].

Temperature is one of the most important factors because there is a close relationship between potential yield and physiological processes that occur in plants [29]. This occurs because the ambient temperature conditions affect the sprouting, photosynthesis, growth and development of plants [30-32]. The optimal conditions for the growth and development of crops are in the range of 20-30^0 C [33].

Some authors believe the harvest formation does not depend on the sowing time, but it is determined by the ratio of the effective accumulated temperatures and the precipitation amount at critical stages of development. Especially important meaning has the meteorological conditions during the ripening periods [34-36].

OBJECTIVES

The purpose of the article is to analyze the weather influence on crop yield, crop features in an investigation area.

MATERIALS AND METHODS

The main field research had being conducted during 2004-2013 years in the stationary fallow-grain-row crop and temporary crop rotations at Crop and Cultivar laboratory of the Plant Production Institute nd. a. V. Ya. Yuryev of NAAS.

Soil of the experimental field is ordinary chernozem (black soil), deep, mean-humic, on loess. Agrochemical soil indexes: humus content (according to Tyurin) is 5.8%, pH_{KL} - 5.8, hydrolytic acidity is 3.29 mgEq/100 g of soil, the amount of alkalizes absorbed is 37.4 mgEq/100 g soil. In the soil the following deposit of nutrients has been accumulated during 40 years: nitrogen is 134 mg / kg, phosphorus is 97 mg / kg, potassium is 133 mg / kg.

Analysis of weather conditions during the years of study has shown that they were quite contrasting. The large amplitude of changes in the air humidity and temperature has a significant impact on the growth and development of the varieties tested within the years of cultivation. There is a warming trend in the period of sowing, and the resumption of the spring vegetation. Temperature instability in the autumn and the spring was observed too. For example, the average temperature in December can range from +4^0 to -8^0 C, and there is a similar pattern in January and February.

THE MAIN RESULTS OF THE RESEARCH

The effective accumulated temperatures (over than 10^{0}C) are very important for the growth and development of crops, because crops need a certain temperature amount passing through of the development phases. The faster accumulation of the temperature amount is shorter the growth stage and higher influence on the yield.

During the years of research, the effective accumulated temperatures in the autumn were significantly higher than long-term one. Thus, the average one for 2004-2013 in August was 383.6^{0}C compared to 282.0^{0}C; in September was 142.9 ^{0}C compared to 117.2^{0}C; in October was 34.2 compared to 0^{0}C. Also, a rapid temperature increase in the May – July is revealed.

Under the conditions of the research, the main limiting factors are precipitation and temperature regime during the growing season. Throughout research years, the weather conditions were quite contrasting during the growing season; it allows fully assessing cultivar and hybrid factors for oil crops.

On average, during the years of research (2004-2013) the deviation at an average daily temperature is equal to + 1.3^0 C (fig. 1). At the same time there is a significant difference in months and years. So, there is a significant warming during a period from August to November by 0.9-3.1^{0}C and a cooler period by 0.2^{0}C in April and June. March was warmer than historical averages by 0.9^{0}C, and May was warmer by 0.5^{0}C.

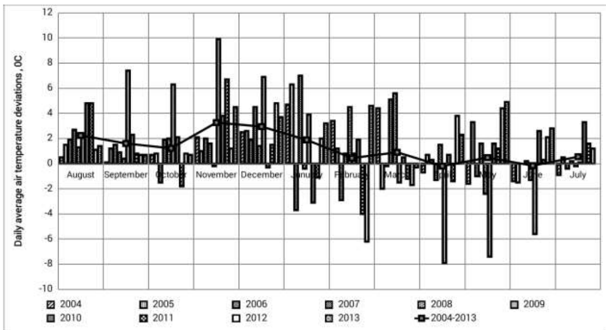

Fig. 1. Daily average air temperature deviations from the optimum value, 2004-2013 years

Over the years the diversity of research data was higher enough. For all the years of experience August - September were warmer in comparison with long-term data by 0.4-7.4^{0}C. The significant diversity of temperature is observed in spring and summer. So, Marchs were a cooler during 6 years from 10 (2005 – by 2.0^{0}C; 2006 – by 0.2^{0}C; 2009 – by 1.5^{0}C, 2011 - by 1.2^{0}C; 2012 - by 1.7^{0}C, and 2013 - 0.3^{0}C). For the spring crops, including oil crops, the highest value has the weather conditions in April. The April daily average temperatures for 4 years were below than the long-term indexes by 0.7-7.9^{0}C, one year had usual temperatures and 5 years exceeded it by 0.7-3.8^{0}C. May was cooler for 4 years and it was warmer for 6 years, on average by 0.9^{0}C. There was same situation for other summer months.

Fig. 2. The effective accumulated temperatures deviations from the optimum value, 2004-2013 years

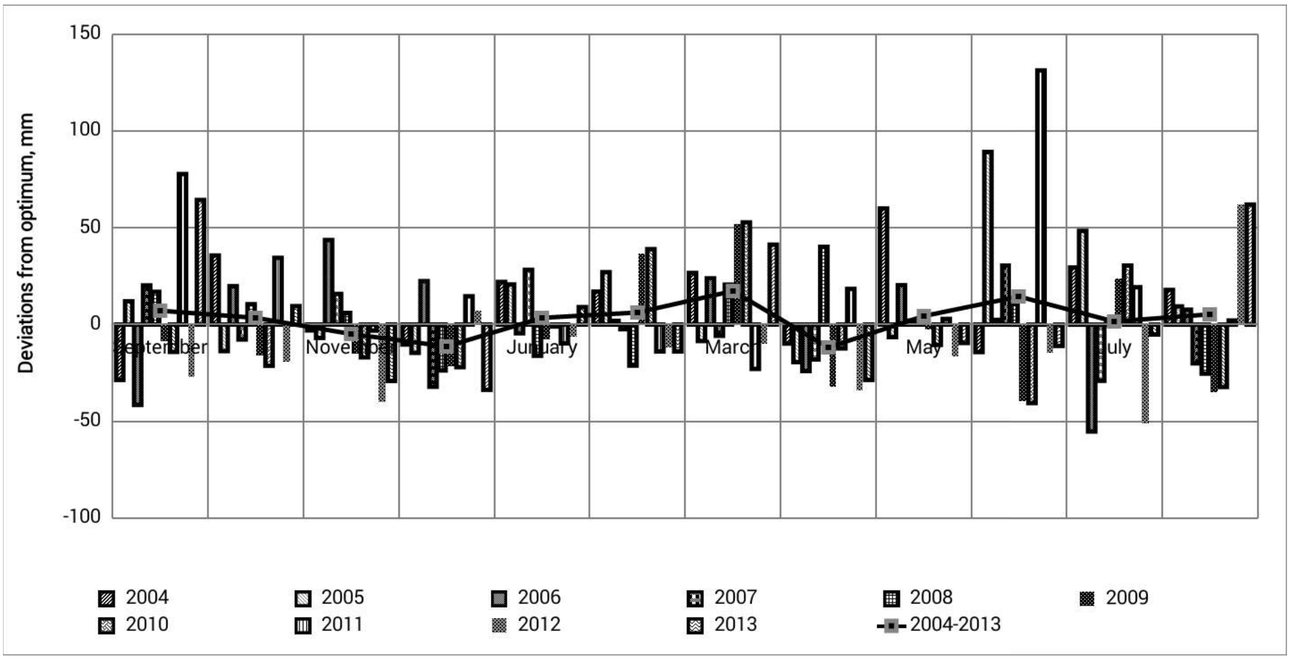

Fig. 3. Precipitation deviations from the optimal values, 2004-2013

In addition to a daily average temperature of air, the great importance for the growth and development of crops has the effective accumulated temperatures (over than 10^{0}C) for certain periods.

On average during 10 years of research, the effective accumulated temperatures were 1496.8^{0}C, which is by 290.8^{0}C, or 24.1% higher than the average long-term figures (fig. 2). All months this index increase was observed from 5.9 to 101.1^0 C. In the autumn months the largest increase in the effective accumulated temperatures was observed in the August - 101.1^0 C, in September - 31.3^0 C, in October - 39.3^0 C. Although for the last month there are no the effective accumulated temperatures according to long-term data. Same situation was in the spring and the summer. So, in April excess of the index above the optimal value is 5.9^0 C, and in May and June it is 64.6 and 34.4^0 C respectively.

Depending on the year of cultivation, the difference of the effective accumulated temperatures in comparison with long-term data were from minus 129.9^0 C in 2004 to plus 625.9^0 C in 2012.

In 2004, in almost all months except October and August the effective accumulated temperatures were below the optimal values by 3.7 and 57.7^0 C, respectively. In 2005, the decrease of this index was in April by 6.4^0 C; and in June and July it was by 49.2 and 23.5^0 C respectively.

Table 1. The correlation coefficients for yield of oil-bearing crops and meteorological factors, 2004-2013

Meteorological factors	Months	Sunflower		Soybean	
		Control	fertilized	Control	fertilized
Rainfall	May	-0.11	-0.13	-0.12	-0.13
	June	0.40	0.31	0.40	0.31
	July	-0.46	-0.59	-0.47	-0.60
	August	-0.06	-0.02	-0.07	0.00
	September	0.48	0.38	0.48	0.37
The accumulated active temperatures	May	0.36	0.33	0.36	0.34
	June	0.23	0.32	0.23	0.34
	July	-0.12	-0.14	-0.12	-0.14
	August	0.25	0.28	0.25	0.28
	September	0.53	0.60	0.52	0.61
Daily average air temperature	May	-0.05	-0.09	-0.05	-0.08
	June	-0.07	-0.03	-0.07	-0.02
	July	-0.27	-0.25	-0.27	-0.25
	August	0.16	0.16	0.16	0.15
	September	-0.03	0.00	-0.04	0.00

Analyzing the data by month, we can note that deviation towards reducing of the effective accumulated temperatures was observed in April almost all years: during 7 years from 10. For two years they were insignificant and in 2012 only they exceeded the optimum by 87.2^0 C.

In 2004 significant shortfall in the active temperatures were observed in May - 51.6, June - 57.7 and July - 40.8^0 C. In 2005 it was equal to: in June and July is 49.2 and 23.5^0 C, and in 2006 in June is minus 120.9^0 C. In 2004, the shortfall of the temperatures in the autumn and the spring-summer period was 129.9^0 C. In other years of studies their excess reached from 100.4 in 2005 to 625.9^0 C in 2012.

In addition to the air temperature, the amount of precipitation is very important for the growth and development of plants; it need for the timely passing phases and as a result for yield. Thus, in average during the investigation years the amount of precipitation increased by 34.4 mm compared to long-time indexes. There is a large variability in them, depending on the year of the study (Fig. 3). A significant shortage of moisture in the autumn caused problems with timely young growth and beginning development of crops. Rainfall deficiency in April - May and the high temperatures in the same time conduce to a more rapid passage of the development phases and poor yield.

According to the results of correlation analysis the greatest positive impact on the level of sunflower and soybean yields under the conditions of the Kharkiv region has a rainfall in June and September. June precipitation positively affects growth and development of crops, as well as the yield: if its amount is higher, the crops might form the higher yield. Precipitation in September creates, above all, the deposit of moisture for the next year yield. At the same time, a significant amount of rainfall in June has a negative impact on the plants; the correlation coefficients are equal to -0.46 and -0.59 for sunflower and -0.47 and -0.60 for soybean.

The effective accumulated temperatures act on yield by slightly different pattern. The greatest positive impact, r = 0.33-0.36, has a temperature in May. With using of fertilizers the effective accumulated temperatures in June affect positively too, r = 0.32 and 0.34. Maximum values of the dependence are in September, r = 0.52-0.61. Temperatures of May allow for plants to form a vegetative mass quickly. In September they accelerate the maturation and reduce the harvesting humidity. In other months this dependence is weak with a negative value in July, r = -0.12-1-0.14 and positive one in August, r = 0.25-0.25.

For the last 10 years, the daily average temperature increasing was +1.3^0 C, the effective accumulated temperatures are higher by 290.8^0 C, or 24.1%, and the amount of precipitation is by 34.4 mm higher, than the long-time data. The correlation coefficients of June rainfall and yields are equal to -0.46 and -0.59 for sunflower and -0.47 and -0.60 for soybean.

CONCLUSION

In average for 2003-2013 daily average temperature increasing is equal to +1.3 ^{0}C. There is significant difference of this index for months and years. For instance, warming during August-November by 0.9-3.1^{0}C and cooling in April and June by 0.2^{0}C were revealed. March was warmer than long-term indexes by 0.9^{0}C; May was warmer by 0.5^{0}C. March was cooler during 6 years from 10 (2005 was by 2.0; 2006 was by 0.2, 2009 – 1.5; 2011 – 1.2; 2012 – 1.7; 2013 – 0.3^{0}C). May was cooler during 4 years and much warmer during 6 years. The effective accumulative temperatures were 1496.8 ^{0}C, this index is more by 290.8^{0}C or 24.1% than average values. Precipitation amount increased by 34.4 mm compared to long-term indexes. The significant amount of rainfall in June negatively affects the harvest. Correlation coefficients were equal to -0.45 and -0.59 for sunflower and – 0.47 and -0.6 for soybean. The most positive influence (r=0.33-0.36) has the effective accumulative temperatures of May. This regularity was revealed for effective accumulative temperatures of June if mineral fertilizers have been used (r=0.32-0.34). In other months, this dependence is weak, with a negative value in July: r = -0.12-0.14 and positive one in August: r = 0.25-0.25. These regularities should be used for chose of crop production techniques and terms.

REFERENCES

1. http://www.activestudy.info/vliyanie-klimaticheskix-i-ekologicheskix-uslovij-na-urozhajnost- i-effektivnost-udobrenij (in Russia).
2. **Adamenko T.** http://www.fruit-inform.com/ru/analytics/23108#.VLeQkmOhGa0.
3. http://wwf.panda.org/uk/wwf_ukraine_ukr/climate change/climate_impacts_ua/ (in Russia).
4. **Kylik V.A.** Influence of weather conditions and methods of main soil treatment on wheat vegration http://www.agropromyug.com/nauka-apk/rastenievodstvo/27-obshchie-tekhnologii-rastenievodstva/27-vliyanie-pogodnykh-uslovij-i-sposobov-osnovnoj-obrabotki-pochvy-na-urozhajnost-ozimoj-pshenitsy.html. (in Russia).
5. **Vavilov N.I. 1940.** New systematics of cultivated plants. - M.: Selhozgiz. 89 - 90. (in Russia).
6. **Kornilov A.A. 1981.** Rícinus Don Cossacks / Kornilov AA, Sirotkina PI, Kazmin N.M. // Oilseeds crops. 31-32. (in Russia).
7. **Kornilov A.A. 1976.** Influence of the leaf surface of ricinus on the ricinus yield / Kornilov A.A., Sirotkina P.I. // Bulletin of scientific and technical information on oilseeds. - Krasnodar: VNIIMK. 30-32. (in Russia).
8. **Islam Y. 1983.** Growth and equity in agricultural development. - Gower. 197-198. (in English).
9. **Kraft S.E. 1984.** Trans. Stst. Academy Science / Kraft S.E., Dharmadnikare P. № 3-4. 219-228. (in English).
10. **Skazkin F.D. 1971.** Critical period of plants in relation to lack of water in the soil. - Leningrad: Leningrad University Press, 71. (in Russia).
11. **Skazkin F.D. 1955.** Critical periods of ontogenetic development in various agricultural crops // Izvestiya Nauchnoi Nauka. Instituta im. P.F. Lesgaft. - T. 27, 83. (in Russia).
12. **Skazkin F.D. 1961.** Critical period to insufficient water supply. - Moscow: Publishing House of the USSR Academy of Sciences, 51. (in Russia).
13. **Skazkin F.D. 1938.** Towards the Physiology of the Critical Period to the Shortage of Moisture in the Soil // Reports of the Academy of Sciences of the USSR. - T.18. No. 45. 303-306. (in Russia).
14. **Zhuchenko A.A. 1988.** Adaptive potential of cultivated plants (ecological and genetic basis). - Chisinau: Shtiintsa, 32. (in Russia).
15. **Zhuchenko A.A. 1990.** Adaptive plant growing. - Chisinau: Shtiintsa, 432. (in Russia).
16. **Yisrael Yu. A. 1993.** Problems of socio-ecological monitoring. Global and Regional Consequences of Environmental and Climate Change: Proceedings of the VII Baikal School Workshop / Izrael Yu.A., Anokhin Yu.A., Andrianova GA - St. Petersburg: Gidrometeoizdat. 31-35. (in Russia).
17. **Morgun V.V. 2006.** Physiological and genetic selection problems due to global climate change / Morgun VV, Shadchina T.M., Kirizii D.A. // Physiology and biochemistry of cultivated plants. - T.38. No. 5. 371-383. (in Ukrainian)
18. **Waddell T.E. 1988.** Agriculture and anvironment: what do really mean? / Waddell T.E., Bowen B.T. // Journal soil and water conservation. - № 3. 241-242.
19. **Zhykovsky E.E., Belchenko G.G., Brunova T.M. 1993.** Principles of estimating climate variation effect on productivity. - St.- Peterburg, 5.
20. **Fischer G. 1992.** Climate change and world food tade // American Society Agronomical Annual Meeting. - Minneapolis, 15. (in English).
21. **Zhuchenko A.A, King A.B. 1985.** Recombination in evolution and selection. - Moscow: Kolos. 27-37. (in Russia).
22. **Dwyer M. 1982.** Tyres: The most important factor // Power farming. - № 7. 16-23. (in English).
23. **Elenon P. 1988.** Reduced tillage research in Finland // Swedish University of agricultural sciences Upsala. -V. 77. 17-23. (in English).
24. **Perly J. 1994.** Crops and climate change // Nature. - № 6459. 118. (in English).
25. **Gonzalez J.L. 1992.** Yield component elasticity in hybrid and open pollinated safflower at several plant population / Gonzalez J.L., Gonson B.L., Schneiter A.A. and oth. // American Society Agronomy Annual Meeting. Minneapolis. - Minneapolis, 144. (in English).
26. **Alekseev A.P., Rodin V.F. 1981.** On the leaf surface of a short-form sunflower // Scientific and Technical Bulletin of VNIIMK. - Issue. 1 (76). 26-30. (in Russia).
27. **Matthes J. 1981.** The mechanical farm of 2030 / Contribution to British Association 150 Anniversary Meeting. York, 23 - 24 april, York, 5. (in English).
28. **McKenney M.S., Easterling W.E., Rosenberg N.J. 1992.** Sumula of crops productivity and responses to climate change in the year 2030: the role of future technologies abjustments and and aptations // Agronomy and forest meteorology. - № 1-2. 103-127. (in English).
29. **Merrien A., Champoliweer L., Raimbault J. 1993.** Tournesol oleijue: Premiers factoeurs de variation de la composition // Oleoscope. - № 15. 17-19. (in English).
30. **Leopold A. 1968.** Growth and development of plants. - Moscow: Kolos, 16. (in Russia).
31. **Demolon A. 1970.** Growth and development of cultivated plants. - M .: Nauka, 25. (in Russia).
32. **Lyubimenko V.N. 1921.** Analysis of adaptive activity of plants. - Petrograd: Society of Naturalists, 44. (in Russia).

33. **Lyubimenko V.N. 1924.** Plant biology. - Leningrad, 34. (in Russia).
34. **Lavrukhin P.V. 2002.** Extension of the concept of precision of sowing // Bulletin of the Russian Academy of Agricultural Sciences. - № 5. 17-19. (in Russia).
35. **Silchenok Z.T. 1967.** Influence of weather conditions and methods of agricultural technology on the yield and quality of sunflower seeds in the forest-steppe zone of the Voronezh Region: Abstract of Cand. Dis. For scientific research. Degree of Cand. S.-. Sciences: 06.01.09 "Plant growing" / Z.T. Sylvanok. - Voronezh, 19. (in Russia).
36. **Kraevsky A.N. 1993.** Influence of soil cultivation and watering methods on sunflower yield / A.N. Krayevsky, G.N. Poluektov, N.E.Bogatyrev // Agriculture.- №5. 29-30. (in Russia).
37. **Stotchenko V.E. 1982.** Minimization of soil cultivation during sunflower growing in the northern steppe of the Ukrainian SSR: dis. Candidate of agricultural sciences. Sciences: 06.01.01 / V.E. Stotchenko. - Voroshilovgrad, 205. (in Russia).
38. **Pankova O. 2015.** Prolonged effect of optical radiation of a red range during the germination of seeds/ O. Pankova , A. Fesenko, V. Bezpalko, N. Lysychenko L. Golovan, T. Romanova // MOTROL. Commission of Motorization and Energetics in Agriculture Vol.17. No.7. 29-34. (in Poland).
39. **Fesenko A.** Application of No-till growing sunflowers: technical, environmental and economic aspects. / Fesenko A., Pankova O., Bezpalko V., Gutyanskyi R. // MOTROL. Commission of Motorization and Energetics in Agriculture. Vol. 19. No. 1. 15-20 (in Poland).
40. **Gutyanskyi R. F**ormation soybean yields in the meteorological conditions of eastern-steppe of Ukraine / Gutyanskyi R., Pankova O., Fesenko A., Bezpalko V. // MOTROL. Commission of Motorization and Energetics in Agriculture – 2016. Vol. 18. No. 7. 43-47 (in Poland).

MOTROL. Commission of Motorization and Energetics in Agriculture – 2017. Vol.19. No.2. 11-14

TRIBO-ACOUSTIC ANALYSIS OF THE PROCESSES OF DYNAMIC FRICTION

Aleksandr Dykha, Yury Zaspa, Anatoly Vychavka
Khmelnytskyi National University
Instytutska Str.,11, Khmelnytskyi, Ukraine. E-mail: tribosenator@gmail.com

Summary. The experimental results of the tribo-acoustic control in the integrity of real time of nominally stationary friction joints under conditions of fretting are presented. Violation of the integrity due to the wear of tribofrictions are securely fixed both by the general change in the acoustogram shape of the operating noise, and by the spectrum of noise – the emergence of strong mid-range modes of the contact gap. The emergence of two oppositely directed wave energy cascades in the fretting regimes has been noted: a direct cascade from the mod pumping in the direction of high frequencies and the reverse – toward the low infrasonic frequencies. The first one is related to microplastic deformations in the zones of actual contact, the second one is related to dynamic pointing the slow angular motions in the system of friction. For research, the installation for testing the fretting, which doesn't contain rotating elements, creating high level of contact noise was used. It is shown that the use of a publicly available sound recording equipment and standard computer software allows to carry out (for low noise experimental units) contactless acoustic control of the integrity of nominally stationary friction joints under conditions of fretting. Established that low frequency auto-modulation of the friction process, which is manifested in the spectrum of the acoustic emission is a consequence of the dynamic targeting slow angular motion in the system of friction.

Key words: fretting, tribo-acoustics, contact, spectrum, energy cascade.

INTRODUCTION

The fretting processes in nominally-fixed joints, at first glance, are hard to hear in the general operating noise of the system, mechanism, or machine. However, because of the interrelatedness of dynamic processes in complex technical system, violation of integrity of any such connection will inevitably be reflected at the amplitude level and the spectral composition of the working noise. Due to the relatively low speeds slippage in modes of fretting the characteristic frequency of acoustic emission get exactly in the sound and nearby infrasonic spectrum range, which allows the use of normal sound recording equipment and computer software.

ANALYSIS OF RECENT RESEARCHES AND PUBLICATIONS

Acoustic methods for analysis and control of friction processes are widely used in tribology [1-20]. Methods of acoustic emission of ultrasonic frequency range with application of special contact-type sensors became most widespread [4-11]. Contactless acoustic control of sound and nearby infrasonic frequency ranges based on the standard (or special) computer software is much easier in technical implementation, however, it requires a separate analysis to separate the useful signal on the background of noise. Before tribo-acoustic methods were used mainly to movable functional compounds [13, 14, 18, 19].

OBJECTIVES

The paper aims at the task of performing the contactless tribo-acoustic control of integrity of nominally stationary friction joints under conditions of fretting, as well as determining the nature and direction of the leading wave processes of energy and momentum transfer in real time.

THE MAIN RESULTS OF THE RESEARCH

For research, the installation [16] for testing the fretting, which doesn't contain rotating elements, creating high level of contact noise was used fig. 1, 2. Fretting was carried out according to the scheme plane-the ball in contact with unhardened steel 30 HGSA (leading top sample 1 in the diagram fig. 1) and ball steel bearing LH-15 with a diameter of 12 mm (the lower driven counterbody 14 in the diagram fig.1). The surface of the sample was pre-processed by grinding and subsequent polishing on the 9-th class of roughness (Ra=0,2…0,3 μm).

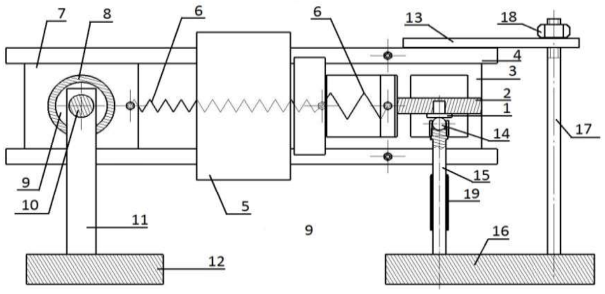

Fig. 1. The scheme of experimental unit: 1 – the leading sample of friction pair; 2 – sample holder; 3 – carriage; 4 – guidance; 5 – electromagnet; 6 – springs; 7 – plates; 8 – hub; 9 – angular contact bearings; 10 – shaft; 11 – tree stand; 12 – base; 13 – strap; 14 – driven counterbody (ball); 15 – strain gauge beam; 16 – base; 17 – pin; 18 – nut; 19 – the strain gages

Reciprocating motion of the driven sample was provided by an electromagnet and a spring system. The amplitude of vibration was 20 μm. The driven counterbody (the ball) was clamped in the rim strain of the beam (fig. 2). The normal contact load in the coupling (≈50 N) was provided to two-thirds by the weight of the drive and a one third by torque wrench force (fig. 1), gradually attenuated in the process of fretting. The basic operating frequency of vibration was 100 Hz.

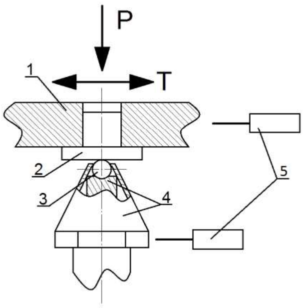

Fig. 2. Contact scheme: 1 – sample holder; 2 – sample; 3 – counterbody (ball); 4 – the fixation system of the counterbody; 5 –the inductive sensors of micromovements; P – downforce; T – tangential force

For recording the acoustic signal the remote microphone brand Media-tech SFX microfone MT 383 installed at a distance of several decimeters from the node friction was used. Computer processing of data was carried out by the program Audasity 2.0.4. As an additional informative channel the automated computer-based construction of loop contact hysteresis in coordinates: the displacement of the driven counterbody – tangential force was used. The latter was measured respectively by means of an inductive sensor of micromovements and the bridge of strain gages on the beam.

Acoustography were pre-recorded in the idle operation mode of unit – with an almost vertical position of the guides of the actuator. Then, in their horizontal position the starting clamp of connections were installed and the test in the mode of fretting was carried out: from initial ageing process to the violation of the integrity of the connection, expressed in the qualitative change of the amplitude level and the spectral composition of the acoustic signal.

Fig. 3 shows acoustography recorded for one minute each in the development of the testing process. They give a general idea about the process of fretting. Low-frequency instability typical for the initial stage of ageing (fig. 3, a) is significantly reduced to approximately $1{\cdot}10^5$ cycles of the oscillations (fig. 3, b), being replaced by a longer period of optimal operation of the connection ($\approx 5{\cdot}10^5$ cycles fig. 3, b).

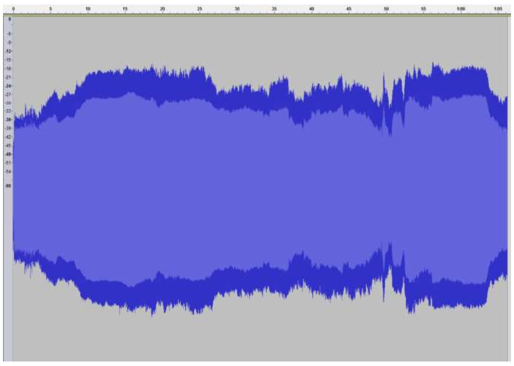

a)

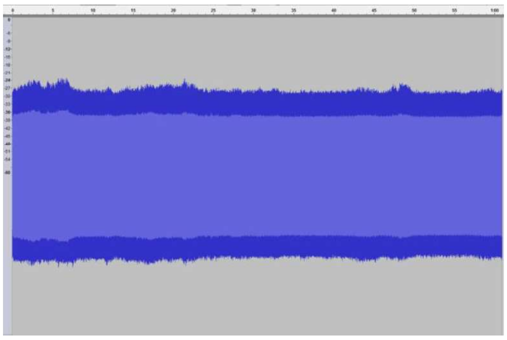

b)

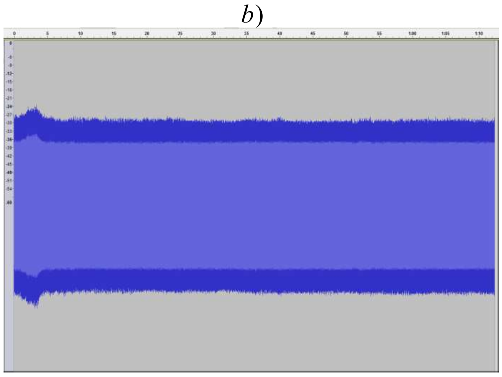

c)

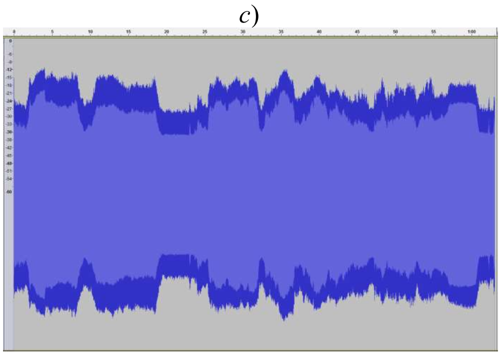

d)

Fig. 3. Acoustography of operating noise recorded on 1-st (a), 15-th (b), 55-th (c) and 88-th minutes (d) of testing. The horizontal axis shows time in minutes and seconds, vertical axis is the signal level in decibels

Severe violation of the integrity of the connection occurs in around the 88th minute of the test ($\approx 5{,}3{\cdot}10^5$ cycles – fig. 3, c). The corresponding hysteresis loop (fig. 4) are more similar and less informative. However, at the final stage (fig. 4, c) the enhancement of high frequency component signals, followed by the reduction of tangential effort on the driven counterbody, and decrease in the amplitude of its oscillations, indicating the slippage in the contact is noticeable.

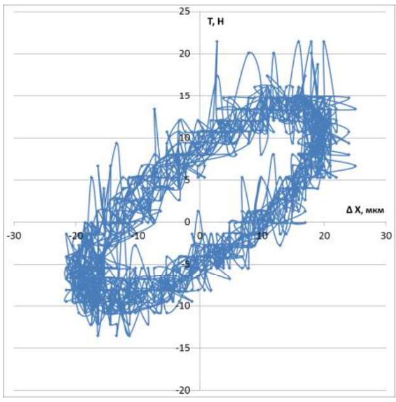

a)

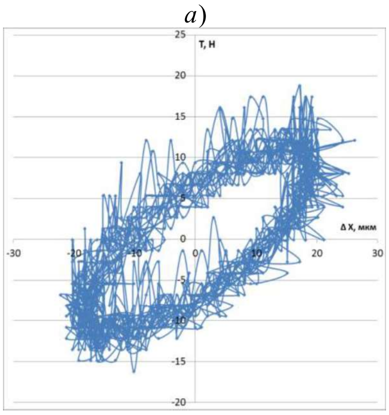

b)

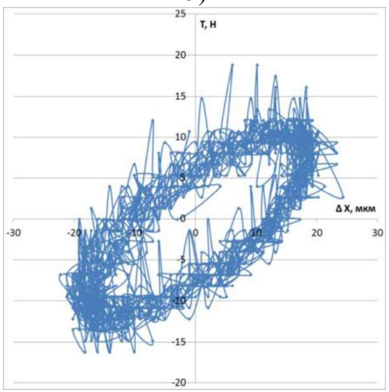

c)

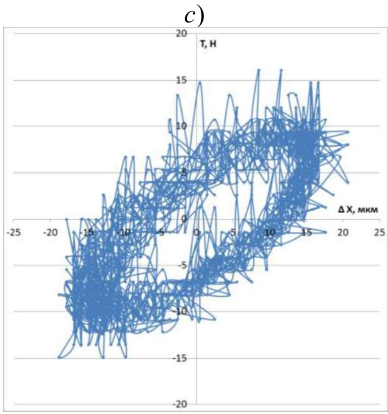

d)

Fig. 4. The contact hysteresis loop, built for the 1st (a), 15th (b), 55th (c) and 88th minutes (d) of testing

Of greatest interest in this case, are the Fourier spectra of the above acoustography – fig. 5. They are dominated by two main pump frequency disturbances, 50 Hz and 100 Hz and their harmonics arising from the nonlinearity in a dynamic system and a corresponding disharmony of vibrations. These harmonics at the initial stage of ageing (fig. 5, a) form a well-defined direct energy cascade towards high frequencies with the maximum at frequencies of 1-5 kHz.

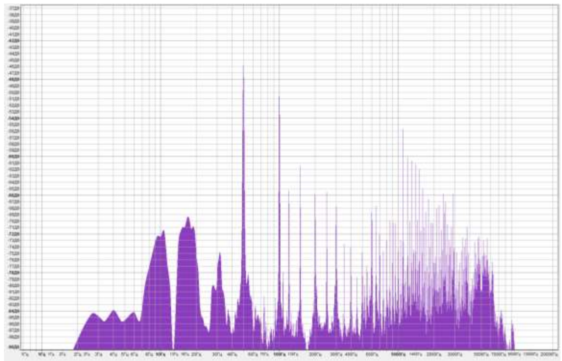

a)

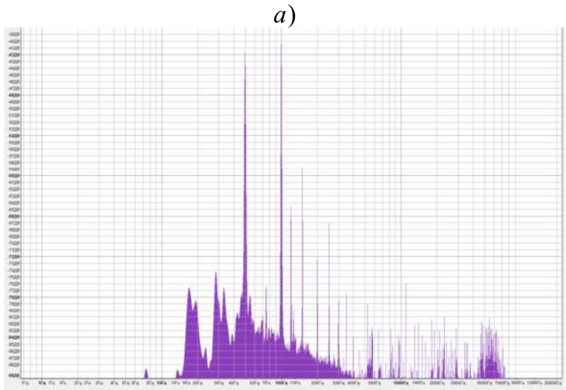

b)

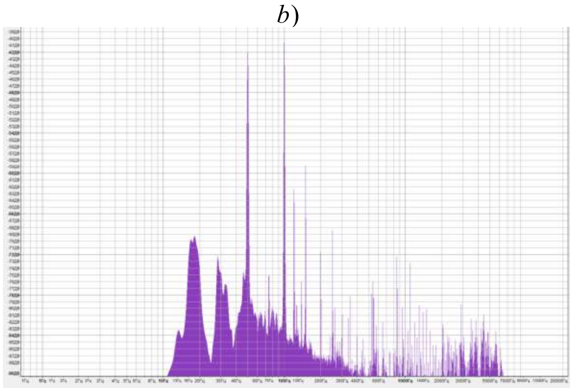

c)

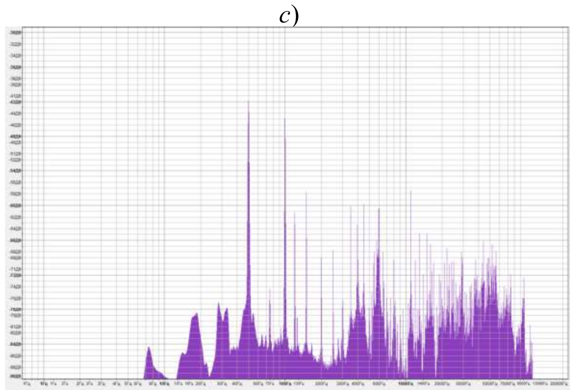

d)

Fig. 5. Fourier spectra of acoustic emission signals recorded on the 1st (a), 15th (b), 55th (c) and 88th (d) minutes of testing

The occurrence of this maximum is due to quasi-normal contact vibrations induced by the processes of microplastic deformations at the stage of ageing. The other – the reverse energy cascade is directed from the pumping modes in the low frequency nearby infrasound region of the spectrum (fig. 5, a). Its origin is connected with guided slow angular movements of the guides of the actuator, which has a direct impact on the rapid vibromovements of the leading sample of friction and, consequently, on the processes of contact interaction in the zone of fretting.

This kind of low-frequency auto-modulation of the friction process is often at the expense of cyclical damage accumulation and separation of wear particles [6]. In this case, such cyclicity is a consequence, not the cause of auto-modulation arising from the activation of the available degrees of freedom and backward linkages in the overall dynamic system of friction. Thus, the friction acts as a global (system-wide) but not just local (mesophysical) process.

CONCLUSIONS

Thus, the use of a publicly available sound recording equipment and standard computer software allows, at least with respect to low-noise experimental units, to carry out contactless acoustic control of the integrity of nominally stationary friction joints under conditions of fretting. Violation of the integrity of such joints is recorded both as a change in the overall shape of acoustogram of operating noise, and (more reliably) as typical changes in the spectrum of sound, with a strong mid-frequency components of the spectrum caused by arising from the contact gaps.

Low frequency auto-modulation of the friction process, which is manifested in the spectrum of the acoustic emission is a consequence of the dynamic targeting slow angular motion in the system of friction. It is mistakable to ascribe such auto-modulation directly to cyclical damage accumulation and separation of wear particles.

REFERENCES

1. **Zaspa Y.P. 2012.** Coherent tribodynamics // Journal of Friction and Wear. T. 33. № 6. 490-503.
2. **Svirideniuk A.I., Myshkin N.K., Kalmykova T.F., Kholodilov O.V. 1987.** Acoustic and electric methods in tribotechnics. Minsk: "Science and engineering", 280.
3. **Akay A. 2002.** Acoustics of Friction // J.Acoust. Soc. Am. – (111), №4, 1525-1548.
4. **Vlasov V.M., Melnichenko N.V., Reiser E.S. 1989.** Diagnostics by the method of acoustic emission of processes of destruction of bridges seizure in friction steels with no grease // Friction and Wear. (10), №2, 257-261.
5. **Fadin Yu. A., Leksovskii A. M., Ginzburg B. M., Bulatov V. P. 1993.** The frequency of the acoustic emission under dry friction pair of steel-brass // Technical Physics Letters. (19), Issue 5. 10-13.
6. **Fadin Yu.A., Kozyrev Y.P., Bulatov V.P. 1999.** Evaluation of mass loss in abrasive wear by acoustic emission data // Journal of Friction and Wear. T. 20. № 2. 74-77.
7. **Baranov V.M., Kudryavtsev E.M., Sarychev G.A. 1999**. On interrelation between the amplitude distribution of acoustic emission signals and the statistical parameters of rubbing surfaces // Journal of Friction and Wear. T. 20. № 2. 70-73.
8. **Asamene K., Sundaresan M. 2012.** Analysis of experimentally generated friction related acoustic emission signals // Wear. T. 296. 607-618.
9. **Fan Y., Gu F., Ball A. 2010.** Modelling acoustic emissions generated by sliding friction // Wear. T. 268. № 5-6. 811-815.
10. **Löhr M., Spaltmann D., Binkowski S., Santner E., Woydt M. 2006.** n situ acoustic emission for wear life detection of dlc coatings during slip-rolling friction // Wear. T. 260. № 4-5. 469-478.
11. **Sun J., Wood R.J.K., Wang L., Care I., Powrie H.E.G. 2005.** Wear monitoring of bearing steel using electrostatic and acoustic emission techniques // Wear. T. 259. № 7-12. 1482-1489.
12. **Gritsenko B.P. 2005.** Role of acoustic vibrations generated by friction, in the destruction of materials of tribosystem // Friction and Wear. (26), №5, 481-488.
13. **Kolubaev A.V., Kolubaev Ye.A., Vagin I.N., Sizova O.V. 2005.** Sound generation during sliding friction // Technical Physics Letters. – Volume 31, Issue 10, 813–816.
14. **Rubtsov V.Ye., Kolubaev Ye.A., Kolubaev A.V., Popov V.L. 2013.** Using acoustic emission for the analysis of wear processes during sliding friction // Technical Physics Letters. – Volume 39, Issue 2, 223–225.
15. **Zaporozhets V.V. Stadnichenko V.N. 2015.** Automated systems of tribodiagnostics of contact interactions // Friction and Wear. - (36), №2, 315-324.
16. **Kurskoi V.S., Slaschuk V.A. Slaschuk A.A. 2014.** Patent of Ukraine № 94006. Device for testing of materials under conditions of dynamic contact loading / / Appl. 05.05.2014, publ. 27.10.2014, Bull. №20.
17. **Popov A.P., Butakov B.I., Marchenko D.D., 2011.** Determination of stress-strain state of bodies in their contact interaction. Contact problem. [Text] / Alexey Popov, Boris Butakov, Dmitry Marchenko // Lublin (Poland). Publishing house Motrol, Volume 13A. 13 - 24.
18. **Aulin V. 2013.** Selective wear of cuttings elements of working organs of tillage machines with realization of self-sharpening effect / V. Aulin, T. Zamota // TEKA, Commission of Motorization and Energetics in Agriculture. Vol. 13., N4. Lublin-Rzezow. 9-17.
19. **Aulin V.V. 2013.** Improving the efficiency of tribological restoration tehnologies by control of running in processes of pairing. V.Aulin, T.Zamota Motrol. Commission of Motorization and power Industry in Agriculture. Vol. XV. Lublin. 12-19.
20. **Belodedov V., Nosko P., Boyko G., Fil P., Mazneva M., 2013.** Parameter optization of dosator for technique cultures on the quantity intervals, close by to calculation. MOTROL. Commission of Motorization and Power Industry in Agriculture. Vol.13, №4, Lublin, 18-24.

MOTROL. Commission of Motorization and Energetics in Agriculture – 2017. Vol.19. No.2. 15-19

TRIBOCORROSION OF STEEL – STEEL COUPLES IN THE PRESENCE OF SILVER NANOPARTICLES

Andriy Kytsya[1], Vasyl Vynar[2], Chrystyna Vasyliv[3], Liliya Bazylyak[1], Roman Gushchak[3]

[1]Lytvynenko Institute of Physical Organic Chemistry and Coal Chemistry of the NAS of Ukraine
Naukova Str. 3[a], Lviv, Ukraine. E-mail: andriy_kytsya@yahoo.com
[2]Karpenko Physico-Mechanical Institute of the NAS of Ukraine
Naukova Str. 5, Lviv, Ukraine. E-mail: vynar@ipm.lviv.ua
[3]Lviv National Agricultural University
V. Velykogo Str. 1, Dubliany, Ukraine. E-mail:chrystyna.vasyliv@gmail.com

Summary. At present different methods of AgNPs synthesis and their use as oil additives are well-described but the impact of silver nanoparticles and their antifrictional properties in the conductive media (particularly in water) are studied insufficiently. The idea of our work was to study the effect of additives of AgNPs of different concentrations in distilled water on tribological characteristics of friction pair C1020 steel - 52100 steel. 20 nm silver nanoparticles were synthesized and separated as a water-redispersible dry powder. The effect of low concentrations of silver nanoparticles on the tribocorrosion behavior of the friction couple "C1020 steel – 52100 steel" in water was studied. The nonmonotonic dependence of friction coefficient reduction and material losses on the concentration of silver nanoparticles in the reactive medium was observed. The steel surface after friction tests was investigated using scanning electron microscopy. The optimal concentration of silver nanoparticles in water was established to prevent wear of C1020 steel surface and to minimize the friction coefficient. It was founded that silver nanoparticles at the concentration of 0.01 % mass. uniformly deposited on the steel surface and reduced the wear track by 40 % as well as friction coefficient twice. The assumption that such uniform depositions of silver nanoparticles caused by appearance of Fe^{2+} ions in the zones of tribocorrosive dissolution of steel surface was done. A possible mechanism of the influence of silver nanoparticles on the tribocorrosion characteristics and the formation of a protective layer on the steel surface was proposed.

Key words: silver nanoparticles, tribocorrosion, wear, friction coefficient.

INTRODUCTION

At present different methods of AgNPs synthesis and their use as oil additives are well-described but the impact of silver nanoparticles and their antifrictional properties in the conductive media (particularly in water) are studied insufficiently. The idea of our work was to study the effect of additives of AgNPs of different concentrations in distilled water on tribological characteristics of friction pair C1020 steel - 52100 steel.

ANALYSIS OF RECENT RESEARCHES AND PUBLICATIONS

The substance fundamental properties, including mechanical, electrical, optical, etc. under transition from the macro-state to the state with a particle size of <100 nm undergo significant changes [1-3]. Nanoparticles, as compared to the conventional powders, possess a large excess of surface energy, which is manifested by a number of unique properties that have been used in diffusion bonding technology, for developing the protective and anti-friction coatings, for restoring worn parts of mechanisms, in magnetic, ceramic, composite materials, in medicine, agriculture etc. [4-12].

At present a large number of lubricants modified with nanoparticles, that prevent wear of units and mechanisms surfaces in operation, are proposed [13-15]. Different nanoparticles and nanocomponents, including molybdenum disulfide – copper composites [6,13], different oxides [14], phosphates [15], etc are widely used for production of lubricants.

However the characteristics of friction pairs depend on many parameters including size, shape and concentration of nanoparticles in suspension. The size of most nanoparticles as oil additives is within 2 ... 120 nm. For example, lubricants with additions of 5 and 20 nm silver nanoparticles (AgNPs) were investigated [16]. It was shown that 0.05 % mass. AgNPs concentration is sufficient for improving the tribological properties of the friction pairs and 1 % mass. is the optimal one. Moreover it was established that 20 nm AgNPs are more effective than 5 nm due to higher reactivity of smaller particles which promote the interaction of microirregularities of the friction surfaces.

EXPERIMENTAL PROCEDURES

Silver nitrate (Aldrich, 99 %), hydrazine hydrate (Aldrich, 99 %), sodium hydroxide (titrant, Kharkovreachem, Ukraine) and sodium citrate (Systema Optimum, Ukraine, 98 %) were used for silver sols preparation. Methanol (System Optimum, Ukraine, 98 %) was used for the precipitation of AgNPs as a dry powder.

Transmission electron microscopy (TEM) (Zeiss Libra 120 Transmission Electron Microscope), X–ray diffraction (XRD) analysis (DRON–3.0, Cu-K_α radiation), as well as UV/visible spectroscopy of the aqueous sols (Shimadzu UV–mini 1240 UV/visible spectrophotometer) were used for quantification of the obtained AgNPs.

Tribocorrosion investigations of steel couples have been done using bidirectional sliding tests by "ball-on-plate" scheme [17] (fig. 1) at 1 N load. C1020 steel plates (size 50×40×5 mm) were polished up to a roughness of 2.5 μm and were used as samples. The 9 mm diameter 52100 steel ball was used as a counterbody. Sliding tests have been done in distilled water, concentrations of AgNPs were equal to 0.004, 0.01 and 0.04 % mass. Kinetics of friction was fixed using a 0.25 s step measurement analog-to-digital converter.

Steel plate surface after friction tests was investigated using a scanning electron microscope (SEM) EVO-40XVP (Carl Zeiss) equipped with an energy dispersive microanalyzer INCA Energy 350.

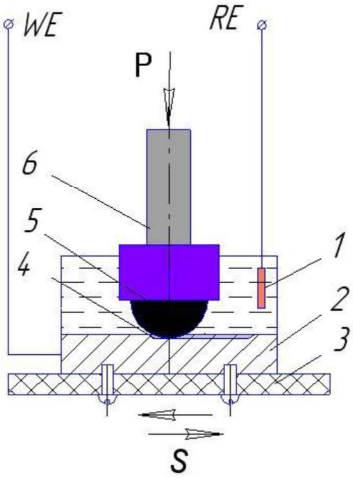

Fig. 1. The scheme of "ball-on-plate" sliding tests plant: *1* – reference electrode key; *2* –C1020 steel sample; *3* – moving base; *4* – contact zone; *5* –52100 steel counterbody; *6* – lever equipped with a strain sensor; *WE* – work electrode; *RE* – reference electrode; *P* – load

THE MAIN RESULTS OF THE RESEARCH

Silver sol was obtained by the reduction of 1 mM $AgNO_3$ solution by hydrazine (0.4 mM) in the presence of 1.25 mM NaOH and 0.5 mM sodium citrate at 25 ºC [12]:

$$4\ AgNO_3 + 4\ NaOH + N_2H_4 = 4\ Ag^0 + 4\ NaNO_3 + 4\ H_2O + N_2\uparrow.$$

The UV/visible spectrum of the obtained sol is presented in fig. 2 (a). It is known [19, 20] that the form and position of sol absorbance maximum can be used for characterizing the size and size distribution of AgNPs. As we can see, the obtained spectrum has only one maximum, so we can assume that AgNPs are of a sphere-like shape.

The calculated size of AgNPs is equal to 18±6 nm. TEM analysis of the obtained AgNPs has been done in order to confirm our calculations (fig. 2 b). It was found that the mean diameter of obtained AgNPs is 17±9 nm. Silver sol was evaporated up to 1/5 volume and precipitated using methanol and then dried at 70 ºC for obtaining the powder-like AgNPs. RD analysis of the obtained powder (fig. 2 c) confirmed the formation of metallic silver.

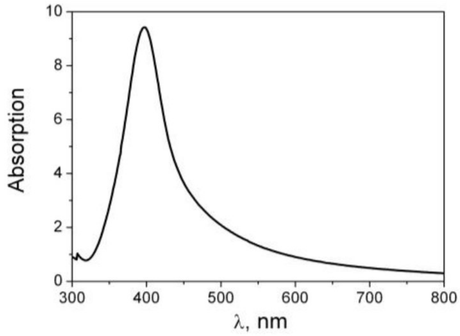

a)

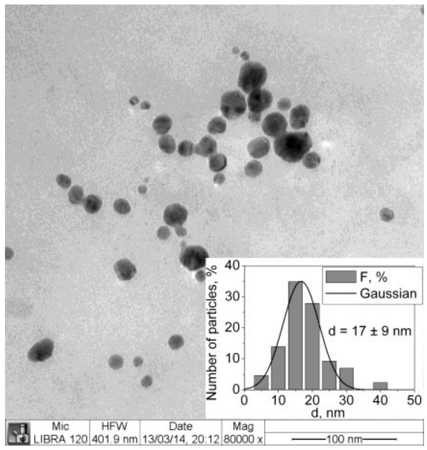

b)

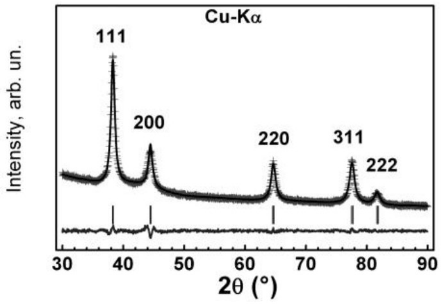

c)

Fig. 2. UV/visible spectrum (*a*), TEM image (*b*) and XRD pattern (*c*) of synthesized AgNPs

The influence of AgNPs concentration on the friction kinetic of steel couples in water was investigated. It was found (fig. 3) that addition of 0.004 % of AgNPs leads to about 15 %. reduction of friction coefficient and wear track width.

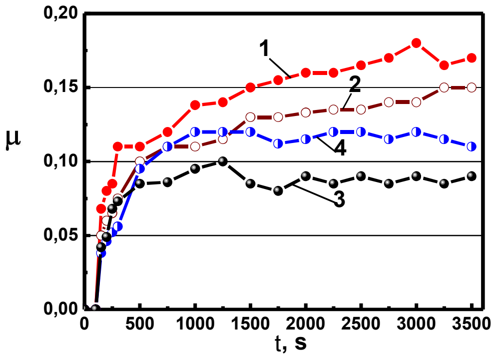

a)

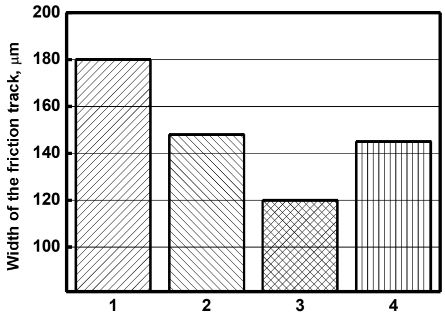

b)

Fig. 3. The average values of friction coefficient (*a*) and wear track widths (*b*) after friction in distilled water (*1*) and in water with addition of 0.004 (*2*), 0.01 (*3*) and 0.04 % mass. (*4*) AgNPs

When the concentration of AgNPs was equal to 0.01 % the friction coefficient was reduced almost twice and the wear track width was reduced by 35 – 40% and vice versa, if AgNPs concentration was equal to 0.04 %, the friction coefficient and the wear track width increased.

The local changes of the friction coefficient are in good correlation with the Ag nanoparticles concentration macro-changes in the solution. Thus, oscillations of friction coefficient in the presence of 0.004 % AgNPs are almost the same as in pure water. Such oscillation in the presence of 0.01 % AgNPs are by 40 % lower and oscillation of friction coefficient increased for the concentration of 0.04 % (fig. 4).

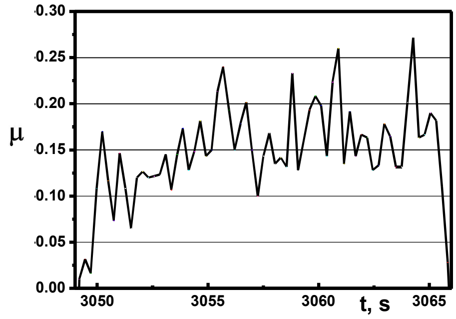

a)

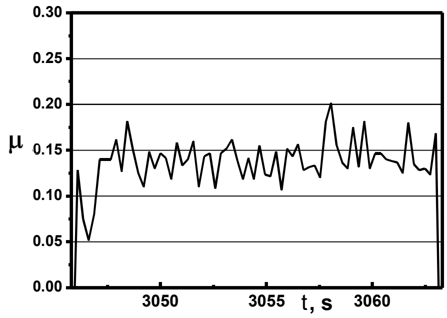

b)

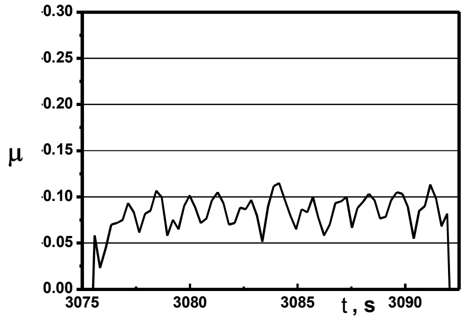

c)

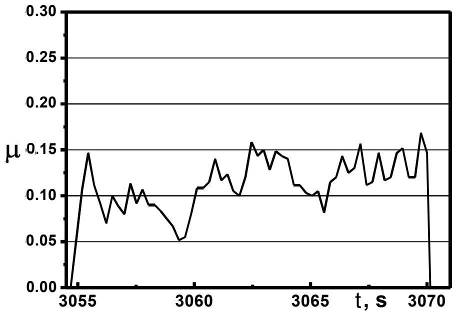

d)

Fig. 4. Local changes of the friction coefficient of steel couples in distilled water (*a*) and in water with addition of 0.004 (*b*), 0.01 (*c*) and 0.04 % mass. (*d*) AgNPs

SEM-analysis of the wear tracks topography (fig. 5) indicates that in pure water micro-cutting of the surface and local scoring are present. Surface topography in the presence of 0.004 % AgNPs is similar to the fracture in water, but the amount of damages of the surface is considerably lower. Surfaces of samples after friction in the presence of 0.01 and 0.04 % AgNPs are not damaged significantly. Thus, the destruction is almost absent at the AgNPs concentration of 0.01 %. Main friction interaction of surfaces proceeds in the zone of plastic deformation with a width of 15-20 μm only. Friction occurs on the surfaces containing agglomerates of silver and thus facilitating the interaction of the couple.

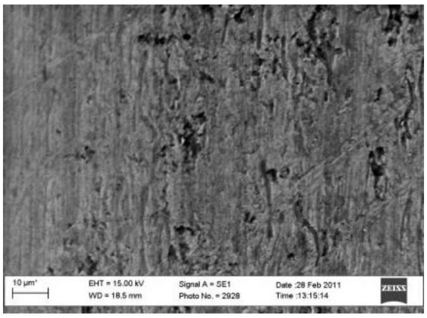

a)

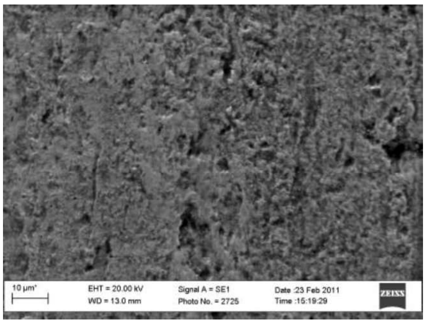

b)

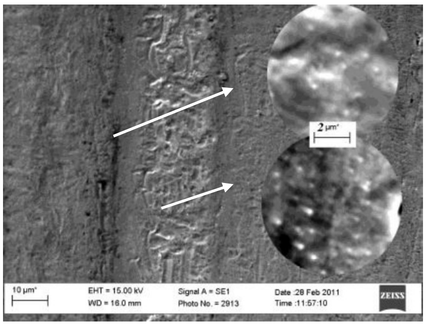

c)

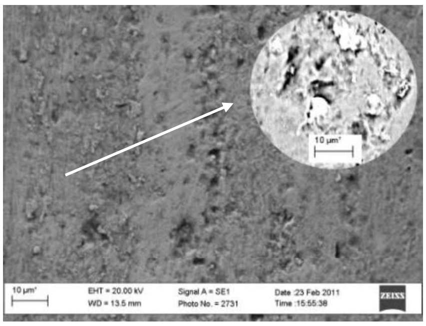

d)

Fig. 5. Surface topology of steel samples after friction in distilled water (*a*) and in water with addition of 0.004 (*b*), 0.01 (*c*) and 0.04 % mass. (*d*) AgNPs.

Formation of large silver agglomerates was observed at high concentrations of AgNPs. Such precipitated agglomerates reduce the wear resistance due to their deformation by an indenter and formation of micro-wedges. Moreover, big silver agglomerates form cathode areas that intensify the corrosion process.

Nonmonotonic changes of tribocorrosion characteristics of the friction pairs with the increasing AgNPs concentration are probably caused by the reduction of silver sol stability at high concentrations. Presumably, the deposition of AgNPs on the friction surface is caused by their agglomeration with Fe^{2+} ions. Ions are released under corrosion-mechanical dissolution of the anode region of the friction track and local changing of the ionic strength of the solution. It is means that at the AgNPs concentration equal to 0.01 % coagulation occurs only in the zones of maximum corrosive dissolution of steel and, respectively, most intense release of Fe^{2+} ions. This results in a uniform deposition of AgNPs on the wear track surface and formation of some protective composite layer. At AgNPs concentration of 0.04 % deposition of silver agglomerates is more intense and chaotic and causes occasional mechanical interaction between the indenter and the surface of friction.

CONCLUSIONS

Tribocorrosion characteristics of the couple "C1020 steel – 52100 steel" during friction in water in the presence of ~20 nm silver nanoparticles were investigated. The nonmonotonic changes of tribocorrosion characteristics of the friction pair with the increasing silver nanoparticles concentration were observed. The optimal concentration of silver nanoparticles in water was established to prevent wear of C1020 steel surface and to minimize the friction coefficient. A possible mechanism of the influence of silver nanoparticles on the tribocorrosion characteristics and the formation of a protective layer on the steel surface was proposed.

REFERENCES

1. **Rao C.N.R., Müller A., Cheetham, A.K. 2007.** Nanomaterials chemistry: recent developments and new directions. Darmstadt: WILEY, 405.
2. **Kelly L., Coronado E., Zhao L.L., Schatz G.C. 2003.** The optical properties of metal nanoparticles the influence of size, shape and dielectric environment. J. Phys. chem. B. V.107. 668-677.
3. **Korchagin A.I., Kuksanov N.K., Lavrukhin A.V. 2005.** Production of silver nanopowders by electron beam evaporation. Vacuum. 77(4). 485-491.
4. **Wu S.H., Chen D. H. 2003.** Synthesis and characterization of nickel nanoparticles by hydrazine reduction in ethylene glycol. J. Colloid. Interface Sci. V. 259. 282-286.
5. **Krutyakov Y.A., Kudrinskiy A.A., Olenin A.Y., Lisichkin, G.V. 2008.** Synthesis and properties of silver nanoparticles: advances and prospects. Russ. Chem. Rev. V. 77(3). 233-257.
6. **Tarasov S., Kolubaev A., Belyaev S., Lerner M., Tepper F. 2002.** Study of friction by nanocopper additives to motor oil. Wear. 252. 63-69.

7. **Ratska N. 2015.** Improvement tribological properties of the alloy Nb-Ti system by thermodiffusion oxidation / Ratska N., Vasyliv Ch., Kovalyshyn S. // MOTROL. Commission of Motorization and Energetics in Agriculture. – Vol. 17(4). 3-6.
8. **Vasyliv Ch., Vynar V., Ratska N. 2011**. Features of wear α-titanium alloys under the influence of hydrogen / Vasyliv Ch., Vynar V., Ratska N. // MOTROL Motorization and power indusrty in agriculture – Vol. 13D. 98-202.
9. **Guang-bin YANG, Shan-tao CHAI, Xiu-juan XIONG, Sheng-mao ZHANG, Lai-gui YU, Ping-yu ZHANG. 2012.** Preparation and tribological properties of surface modified Cu nanoparticles. Transactions of Nonferrous Metals Society of China. 22(2). 366-372.
10. **Sunil Mohan, Anita Mohan. 2015.** Wear, friction and prevention of tribo-surfaces by coatings/nanocoatings. Anti-Abrasive Nanocoatings, 3-22.
11. **Farid Bensebaa. 2013.** Nanoparticle Fundamentals. Interface Science and Technology. 19, 1-84.
12. **Fehim Findik. 2014.** Latest progress on tribological properties of industrial materials. Materials & Design, 57, 218-244
13. **Zhang Bao–Sen, Xu Bin-Shi, Xu Yi, Gao Fei, Shi Pei–Jing, Wu Yi–Xiong. 2011.** Cu nanoparticles effect on the tribological properties of hydrosilicate powders as lubricant additive for steel–steel contacts // Tribology International. 44. 878-886.
14. **Hernandez Battez A, Gonzalez R. L., Viesca, J., et al. 2008.** ZrO_2 and ZnO nanoparticles as antiwear additive in oil lubricants. Wear. 265(3–4). 422-428.
15. **Pokhmurskii V.I., Zin I.M., Vynar V.A., Khlopyk O.P., Bily L.M. 2012.** Corrosive wear of aluminium alloy in presence of phosphate.Corr. Eng. Sci. Tech. 47(3). 182-187.
16. **Sun L., Tao X., Zhang P., Zhang Z. 2008**. Synthesis and Tribology Properties of Stearate Coated Ag Nanoparticles. Technical Sessions. Proceedings of CIST2008 & ITS-IFToMM2008 Beijing, China.
17. **Vynar V. A., Dovhunyk V. M., Student M. M. 2011**. Methodical specific features of tribocorrosion investigations. Mater. Sci. 46(5). 633-639.
18. **Kytsya A., Basyliak L., Hrynda Y., Horechnyy A., Medvedevkikh Y. 2015.** The Kinetic Rate Law for the Autocatalytic Growth of Citrate-Stabilized Silver Nanoparticles. Int. J.Chem.Kin. 47(6). 351-360
19. **Slistan-Grijalva, A., Herrera-Urbina R., Rivas-Silva J.F., Avalos-Borja M., Castillon-Barraza F.F., Posada-Amarillas A. 2005.** Classical theoretical characterization of the surface plasmon absorption band for silver spherical nanoparticles suspended in water and ethylene glycol. Physica E. 27. 104-112.
20. **Kytsya A.R., Reshetnyak O.V., Bazylyak L.I., Hrynda Yu.M. 2013.** Extinction spectra of aqueous sols of silver nanoparticles as characteristics of their size and size distribution. J. Nano-Electron Phys. 4. 04064-1 - 04064-4 (Ukrainian).

MOTROL. Commission of Motorization and Energetics in Agriculture – 2017. Vol.19. No.2. 21-27

ANALYSIS OF THE MATHEMATICAL MODEL OF VIBRATING MILLING OF ANGULAR OSCILLATIONS

Yanovich Vitaliy, Tsurkan Oleg
Vinnytsia National Agrarian University,
Soniachna Srt. 3, Vinnytsia, Ukraine. E-mail: yanovichvitaliy@i.ua

Summary. The paper presents a schematic diagram and an example of the constructive realization of a vibration mill for angular oscillations that implements the idea of a complex technological impact on the material being processed, by providing an intensive shock-erasing effect, which is realized as a result of the angular motion of the grinding chambers of the vibrator.

On the basis of theoretical studies of the dynamic model of the vibrating mill, a series of analytical and graphical dependencies was obtained and optimal design parameters of its operation were established under the condition of the maximum dynamic state of the technological filler, and as a consequence of the effective realization of the process of fine grinding of free-flowing substances.

Key words: vibration drive, dynamics of motion, grinding, vibrating mill, angular oscillations.

INTRODUCTION

Among the main technological processes of primary processing of agricultural raw materials, the processes of grinding loose materials have become widespread. Thus, with the realization of the fine grinding process, the vibrational action makes it possible; on the one hand, to increase the fatigue damage of the material particles under the action of cyclic loads, and on the other hand, as a result of the dynamic interaction among themselves, ensures their ability to actively wear out [1-4].

At the same time, to the main shortcomings of traditional machines for the production of fine and highly disperse material, it is necessary to attribute significant specific energy inputs to the processing of raw materials, low performance characteristics of the executive bodies as a result of active wear of their working surfaces and a decrease in technological efficiency due to adhesion of products with high humidity [5, 6].

In order to eliminate the above-mentioned drawbacks in the intensification of grinding processes of agricultural raw materials and increase the operational and technological parameters of machines for their implementation, it is proposed to apply a complex vibromechanical action.

FORMULATION OF THE TASK

On the basis of the analysis of technological processes and constructive schemes of existing equipment for the realization of the process of fine grinding of loose raw materials, we proposed the design of a vibratory mill in which the introduction of the drive mechanism of the angular vibrations of the grinding chambers would significantly increase the impact-abrasive effect, and as a result intensify the process of grinding materials. The conditions for reducing the specific energy cost for this treatment.

However, in order to achieve high performance indicators of the process, it is necessary to perform a theoretical study of the dynamics of the executive body of the developed machine, and to justify the optimal parameters for an effective operating mode.

SUMMARY OF THE MAIN MATERIAL

In fig. 1, 2 is a schematic diagram and an external view of a vibrating mill for angular oscillations for fine grinding of loose raw materials [8-10].

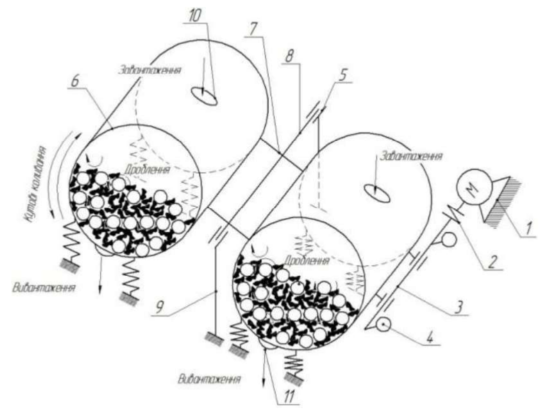

Fig. 1. The fundamental scheme of the vibrational millinar of angular vibrations: 1 – electric motor, 2 – elastic coupling, 3 – drive shaft, 4 – unbalance, 5 – bearing unit, 6 – grinding; chambers, 7 – traverses;8 – central axis, 9 – frame 10, 11 – respectively, pipes for supplying and unloading crushed raw materials

The principle of operation of this machine is that when the electric motor 1 is turned on, the torque through the elastic coupling 2 is transferred to the drive shaft 3 with the unbalances 4 placed on it, the rotation of which provides generation of a combined force and moment imbalance oppositely located relative to the central axis 8 of the grinding chambers 6 , which in turn are interconnected by traverses 9. These design features of the machine make it possible to provide the effect of angular oscillations providing a significant dynamic The state of the technological filler and, as a consequence, the high efficiency of grinding the bulk raw material continuously entering through the feed pipe 10 and crushing due to the force action of the crushing elements, is discharged through the pipe 11 from the mill.

The purpose of theoretical studies of the developed machines is to establish the regularities of the movement of their executive bodies and to determine on this basis the technological parameters of the processes being studied that ensure the most efficient processing of bulk raw materials.

To achieve this goal, it is proposed approach that involves the disclosure of internal structure of the dynamic system under investigation, search for linear and nonlinear effects and on on this basis, to formulate a mathematical model vibrating systems.

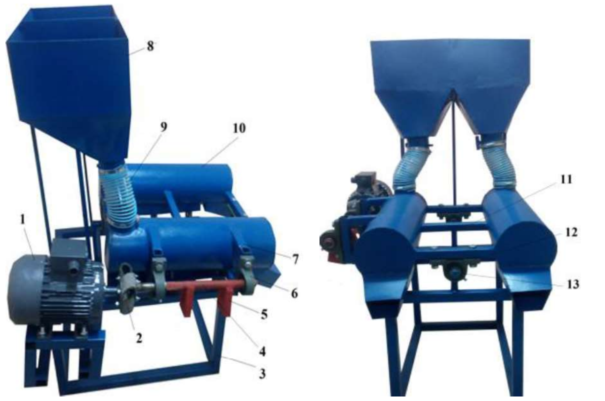

Fig. 2. Appearance of the vibratory mill of angular vibrations: 1 – electric motor, 2 – elastic coupling, 3 – bed 4 – drive shaft, 5 – unbalance, 6 – bearing units, vibrating drives,7 – racks, 8 – loading hopper, 9 – nutritional pipes, 10 – grinding chambers, 11 – traverses, 12 – bearing unit of the central axis, 13 – axis

The concept of mathematical analysis provides for optimization of amplitude-frequency parameters and trajectory the grinding chamber of a vibrating mill the optimal ratio of vertical and horizontal components of the amplitude of oscillations.

To determine the optimum operating mode, in particular, the strengthening of the vertical component vibrations of working chambers, it is necessary to carry out mathematical analysis of force and kinematics parameters of the investigated vibration system.

Taking into account the peculiarity of the movement of grinding chambers of the vibration mill of angular oscillations, mathematical interpretation of the system under study we construct in the polar coordinate system (fig. 3) [11, 12]

The investigated vibration system can be represented mathematical model with five degrees of freedom.

We accept degrees of freedom of the system: z, x – linear movements of the working container along the selected axes of coordinates *OZ, OX*; φ_1 – is the angle rotation of the container; α – is the deflection angle from vertical diameter, axis of rotation of the unbalance; φ_3 – angle of variable disbalance placement relative to the grinding chamber.

The investigated system is characterized by following masses: m_k – weight of the container; m_g – is the mass of the unbalance.

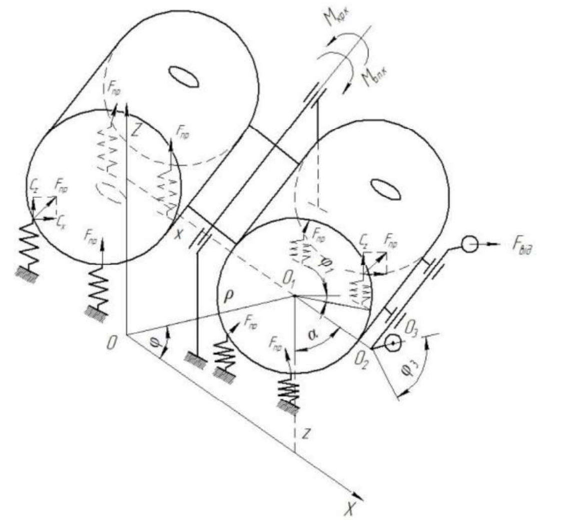

Fig. 3. Scheme for the theoretical study of the motion of the grinding chamber of the millennium

Legend: O_{xz} – fixed coordinate system; O_1 – is the center of mass of the container;

ρ and φ – are the coordinates of the center of mass of the container(Polar); I_k – is the moment of inertia of the container relative to the center of mass (the axis running along centers of mass of sections); I_g – is the moment of inertia unbalance relative to the center of mass; $l_2 = O_1O_2$,

$l_3 = O_2O_3$ – distance from the axis of rotation of the unbalance to its center of mass.

To determine the total kinetic energy system, we divide the mechanism into structural components and implement them kinetic analysis [13-15].

Container performs a flat movement $T_k = 0{,}5(m_k V_{O_1}{}^2) + 0{,}5(I_k \omega_1)$. The velocity of point O_1 in the polar coordinate system $V_{O_1}{}^2 = \dot{\rho}^2 + (\rho \cdot \dot{\varphi})^2$; container angular velocity $\omega_1 = \dot{\varphi}_1$. So, the kinetic energy of the container will be further:

$$T_k = 0{,}5m_k(\dot{\rho}^2 + \rho^2 \cdot \dot{\varphi}^2) + 0{,}5I_k \cdot \dot{\varphi}_1{}^2, \tag{1}$$

the imbalance produces a flat movement, because:

$$T_g = \frac{m_g V_{O_3}{}^2}{2} + \frac{I_g \omega_3{}^2}{2}. \tag{2}$$

The velocity of the center of mass of the unbalance is determined by the formula $\overrightarrow{V_{O_3}} = \overrightarrow{V_{O_1}} + \overrightarrow{V_{O_2O_1}} + \overrightarrow{V_{O_3O_2}}$;

$$V_{O_2O_1} = \dot{\varphi}_1 \cdot O_1O_2 = \dot{\varphi}_1 l_2;\ V_{O_3O_2} = (\dot{\varphi}_1 + \dot{\varphi}_3)l_3.$$

Projecting the vector equality on the axis of the cartesian coordinate system, we obtain.

Thus, the expression of the kinetic energy of the unbalance takes the form:

$$\left.\begin{aligned}
&V_{O_3X} = \dot\rho\cos\varphi - \rho\,\dot\varphi\sin\varphi + \dot\varphi_1\, l_2\cos(\alpha_2+\varphi_1) - (\dot\varphi_1+\dot\varphi_3) l_3\cdot\sin(\varphi_1+\varphi_3)\\
&V_{O_3Z} = \dot\rho\sin\varphi + \rho\dot\varphi\cos\varphi + \dot\varphi_1 l_2\cdot\sin(\alpha_2+\varphi_1) + (\dot\varphi_1+\dot\varphi_3) l_3\cos(\varphi_1+\varphi_3)\\
&V_{O_3}{}^2 = \dot\rho^2\cos^2\varphi + \rho^2\dot\varphi^2\sin^2\varphi + \dot\varphi_1{}^2 l_2{}^2\cos^2(\alpha_2+\varphi_1) + (\dot\varphi+\dot\varphi_3)^2 l_3{}^2\cdot\sin^2(\varphi_1+\varphi_3) +\\
&+\dot\rho^2\sin^2\varphi + \rho^2\,\dot\varphi^2\cos^2\varphi + \dot\varphi_1{}^2 l_2{}^2\sin^2(\alpha_2+\varphi_1) + (\dot\varphi_1+\dot\varphi_3)^2 l_3{}^2\cos^2(\varphi_1+\varphi_3) -\\
&-2\dot\rho\cos\varphi\cdot\rho\cdot\dot\varphi\sin\varphi_1 + 2\dot\rho\cos\varphi\,\dot\varphi_1\, l_2\cos(\alpha_2+\varphi_1) - 2\dot\rho\cos\varphi(\dot\varphi_1+\dot\varphi_3) l_3\sin(\varphi_1+\varphi_3) -\\
&-2\rho\,\dot\varphi\sin\varphi\cdot\dot\varphi_1\, l_2\cos(\alpha_2+\varphi_1) + 2\rho\,\dot\varphi\sin\varphi(\dot\varphi_1+\dot\varphi_3) l_3\sin(\varphi_1+\varphi_3) -\\
&-2\dot\varphi_1\, l_2\cos(\alpha_2+\varphi_1)(\dot\varphi_1+\dot\varphi_3) l_3\sin(\varphi_1+\varphi_3) +\\
&+2\dot\rho\sin\varphi\,\dot\varphi\cos\varphi_1 + 2\dot\rho\sin\varphi\cdot\dot\varphi_1\, l_2\sin(\alpha_2+\varphi_1) + 2\dot\rho\sin\varphi(\dot\varphi_1+\dot\varphi_3) l_3\cos(\varphi_1+\varphi_3)\\
&+2\rho\,\dot\varphi\cos\varphi\cdot\dot\varphi_1\, l_2\sin(\alpha_2+\varphi_1) + 2\rho\,\dot\varphi\cos\varphi(\dot\varphi_1+\dot\varphi_3) l_3\cos(\varphi_1+\varphi_3) +\\
&+2\dot\varphi_1\, l_2\sin(\alpha_2+\varphi_1)(\dot\varphi_1+\dot\varphi_3) l_3\cos(\varphi_1+\varphi_3) = \dot\rho^2 + \rho^2\,\dot\varphi^2 + \dot\varphi_1{}^2\, l_2{}^2 + (\dot\varphi_1+\dot\varphi_3)^2 l_3{}^2 +\\
&+2\dot\rho\cdot\dot\varphi_1\, l_2\cos(\varphi-\varphi_1-\alpha_2) + 2\dot\rho\,(\dot\varphi_1+\dot\varphi_3) l_3\sin(\varphi-\varphi_1-\varphi_3) +\\
&+2\rho\,\dot\varphi\cdot\dot\varphi_1\, l_2\sin(\alpha_2+\varphi_1-\varphi) + 2\rho\,\dot\varphi\cdot(\dot\varphi_1+\dot\varphi_3) l_3\cos(\varphi-\varphi_1-\varphi_3) +\\
&+2\dot\varphi_1\, l_2\cdot(\dot\varphi_1+\dot\varphi_3) l_3\sin(\alpha_2-\varphi_3).
\end{aligned}\right\}$$

$$\begin{aligned}
T_g = \frac{m_g}{2}\big[&\dot\rho^2 + \rho^2\dot\varphi^2 + \dot\varphi_1{}^2 l_2{}^2 + (\dot\varphi_1+\dot\varphi_3)^2 l_3{}^2 +\\
&+2\dot\rho\dot\varphi_1 l_2\cos(\varphi-\varphi_1-\alpha_2) + 2\dot\rho(\dot\varphi_1+\dot\varphi_3) l_3\sin(\varphi-\varphi_1-\varphi_3) +\\
&+2\rho\dot\varphi\dot\varphi_1 l_2\sin(\alpha_2+\varphi_1-\varphi) + 2\rho\dot\varphi(\dot\varphi_1+\dot\varphi_3)\times\\
&\times l_3\cos(\varphi-\varphi_1-\varphi_3) + 2\dot\varphi_1 l_2(\dot\varphi_1+\dot\varphi_3) l_3\sin(\alpha_2-\varphi_3)\big] +\\
&+0{,}5 I_g(\dot\varphi_1+\dot\varphi_3)^2.
\end{aligned} \tag{4}$$

The general form of the kinetic mechanical system takes the form:

$$\begin{aligned}
T = &\frac{m_k}{2}\left(\dot\rho^2 + \rho^2\dot\varphi 2\right) + \frac{I_k}{2}\dot\varphi_1^2 +\\
&+\frac{m_g}{2}\Big[\dot\rho^2 + \rho^2\,\dot\varphi^2 + \dot\varphi_1{}^2\, l_2{}^2 +\\
&+(\dot\varphi_1+\dot\varphi_3)^2 l_3{}^2 + 2\dot\rho\,\dot\varphi_1\, l_2\cos(\varphi-\varphi_1-\alpha_2) +\\
&+2\dot\rho\,(\dot\varphi_1+\dot\varphi_3) l_3\sin(\varphi-\varphi_1-\varphi_3) +\\
&+2\rho\,\dot\varphi\,\dot\varphi_1\, l_2\sin(\alpha_2+\varphi_1-\varphi) + 2\rho\,\dot\varphi\,(\dot\varphi_1+\dot\varphi_3)\times\\
&l_3\cos(\varphi-\varphi_1-\varphi_3) + 2\dot\varphi_1 l_2(\dot\varphi_1+\dot\varphi_3) l_3\sin(\alpha_2-\varphi_3)\Big] +\\
&+0{,}5 I_g(\dot\varphi_1+\dot\varphi_3)^2
\end{aligned} \tag{5}$$

To evaluate the regularities of motion of the executive body of the equipment under study for each of the independent coordinates, we form the Lagrange equations of the second kind [16-19]. Substituting the derivatives of the generalizing forces of the system into a system of equations, and also taking into account the dissipative forces of resistance in the system under investigation, we obtain the expression:

Assumptio:

$M_{кр} = const$ тоді $\omega = \omega_3$, при $\omega_0 = const$ - $\omega_{кр} = const$. We are looking for approximate solutions, like $\rho(t) = \rho_0 + \rho_1(t)$;

where $\rho_0 = const$

$\varphi(t) = \omega\cdot t + \varphi_0(t) + \beta;\ \varphi_3(t) = \omega t$.

So:

$$\begin{aligned}
&(m_k + m_g)\ddot\rho_1 - (m_k + m_g)(\rho_0 + \rho_1(t))(\omega + \dot\varphi_0(t))^2 +\\
&+m_g[\ddot\varphi_1 l_2\cos(\omega t + \varphi_0(t) + \beta - \varphi_1 - \alpha_2) +\\
&+\ddot\varphi_1 l_3\sin(\omega t + \varphi_0(t) + \beta - \varphi_1 - \omega t) +\\
&+\dot\varphi_1{}^2 l_2\sin(\omega t + \varphi_0(t) + \beta - \varphi_1 - \alpha_2) -\\
&-(\dot\varphi_1 + \omega)^2 l_3\cos(\omega t + \varphi_0(t) + \beta - \varphi_1 - \omega t)] =\\
&= -\left(c_x\cos^2\varphi + c_z\sin^2\varphi\right)\rho.
\end{aligned} \tag{6}$$

By grouping the expressions, we get:

$$\begin{aligned}
&-(m_k + m_g)\rho_0\omega^2 - m_g\omega^2 l_3\cos(\varphi_0(t) - \varphi_1 + \beta) +\\
&+(m_k + m_g)\ddot\rho_1 - (m_k + m_g)(2\rho_0\omega\dot\varphi_0(t) + \rho_0\dot\varphi_0{}^2(t) +\\
&+\rho_1(t)(\omega + \dot\varphi_0(t))^2 + m_g[\ddot\varphi_1 l_2\cos(\omega t + \varphi_0(t) + \beta - \varphi_1 - \alpha_2) +\\
&+\ddot\varphi_1 l_3\sin(\varphi_0(t) - \varphi_1 + \beta) + \dot\varphi_1{}^2 l_2\sin(\omega t + \varphi_0(t) - \varphi_1 + \beta - \alpha_2) -\\
&-(2\omega\dot\varphi_1 + \dot\varphi_1{}^2) l_3\cos(\varphi_0(t) - \varphi_1 + \beta) = -(c_x\cos^2\varphi + c_z\sin^2\varphi)\rho;
\end{aligned} \tag{7}$$

Using the principle of smallness of quantities, we obtain:

$$-(m_k + m_g)\rho_0\omega^2 - m_g\omega^2 l_3\cos(\varphi_0(t) - \varphi_1 + \beta) = 0$$ or

$\rho_0 = \dfrac{-m_g l_3\cos\beta}{m_k + m_g}$, to $\rho_0>0$, то $\cos\rho<0$.

So:

$$\begin{aligned}
&(m_k + m_g)(\rho_0 + \rho_1(t))^2\ddot\varphi_0 + 2(m_k + m_g)\times\\
&\times(\rho_0 + \rho_1(t))\dot\rho_1(t)(\omega + \dot\varphi_0(t)) +\\
&+m_g[(\rho_0 + \rho_1(t))\ddot\varphi_1 l_2\sin(\alpha_2 + \varphi_1 - \varphi) +\\
&+\rho\dot\varphi_1{}^2 l_2\cos(\alpha_2 + \varphi_1 - \varphi) +\\
&+\rho\ddot\varphi_1 l_3\cos(\omega t + \dot\varphi_0(t) + \beta - \varphi_1 - \omega t) +\\
&+\rho(\dot\varphi_1 + \omega)^2 l_3\sin(\omega t + \varphi_0(t) + \beta - \varphi_1 - \varphi_3) =\\
&= (c_x - c_z)\rho^2\sin\varphi\cos\varphi.
\end{aligned} \tag{8}$$

Separating the largest value m_g:

$$\rho_0\omega^2 l_3\sin(\varphi_0(t) - \varphi_1 + \beta) = (c_x - c_z)\rho_0\sin\varphi\cos\varphi. \tag{9}$$

We integrate this dependence in the interval [0; T] and obtain:

$$m_g\cdot\omega^2 l_3\sin\beta\cdot T = (c_x - c_z)\int_0^{\frac{2\pi}{\omega}}\sin(\omega t + \varphi_0(t) + \beta)\cos\varphi d\varphi \tag{10}$$

$$m_g\cdot\omega^2 l_3\sin\beta\cdot T = (c_x - c_z)\frac{\sin^2\varphi}{2}\Bigg|_0^T = 0.$$

So, $\sin\beta = 0$.

as $\cos\beta < 0$, то $\beta = \pi$.

There fore: $\varphi(t)=\omega t+\pi+\varphi_0(t),\ \rho_0=\dfrac{m_g l_3}{m_k+m_g}.$

We are looking for the law of rotational motion of a container, we find with the equation:

$$\left.\begin{aligned}
&\left(I_k+I_g+m_g l_2^2+m_g l_3^2+2m_g l_2 l_3\sin(\alpha_2-\varphi_3)\right)\ddot{\varphi}_1+\\
&+m_g[-\rho_0\omega^2 l_2\cos(\alpha_2+\varphi_1-\varphi)-\rho_0\omega^2 l_3\sin(\pi+\varphi_0(t)-\varphi_1)-\\
&-2\dot{\varphi}_1\cdot\omega l_2 l_3\cos(\alpha_2-\varphi_3)-\omega^2 l_2 l_3\cos(\alpha_2-\varphi_3)]=\\
&=-c_{\varphi_1}\cdot\varphi_1-m_g\cdot g(l_2\sin(\alpha_2+\varphi_1)+l_3\cos(\varphi_1+\varphi_3));\\
&\left(I_k+I_g+m_g l_2^2+m_g l_3^2+2m_g l_2 l_3\sin(\alpha_2-\omega t)\right)\ddot{\varphi}_1-\\
&-2m_g\omega l_2 l_3\cos(\alpha_2-\omega t)\dot{\varphi}_1+c_{\varphi_1}\cdot\varphi_1=\\
&=m_g\cdot\omega^2\begin{pmatrix}+\rho_0 l_2\cos(\alpha_2+\varphi_1-\omega t-\pi-\varphi_0(t))+\\+\rho_0 l_3\sin(\pi+\varphi_0(t)-\varphi_1)+l_2 l_3\cos(\alpha_2-\omega t)\end{pmatrix}-\\
&-m_g\cdot g(l_2\sin(\alpha_2+\varphi_1)+l_3\cos(\varphi_1+\omega t));\\
&\ddot{\varphi}_1\cdot\left(I_k+I_g+m_g l_2^2+m_g l_3^2+2m_g l_2 l_3\sin(\alpha_2-\omega t)\right)-\\
&-2m_g\omega l_2 l_3\cos(\alpha_2-\omega t)\dot{\varphi}_1+c_{\varphi_1}\cdot\varphi_1=\\
&=m_g\cdot\omega^2(-\rho_0 l_2\cos(\omega t-\alpha_2)+\rho_0 l_3\sin\pi+l_2 l_3\cos(\omega t-\alpha_2))-\\
&-m_g\cdot g(l_2\sin\alpha_2+l_3\cos(\varphi_1+\omega t)).
\end{aligned}\right\}\quad(11)$$

Given that the movement of the container causes the movement of the unbalance, we get:

$$\begin{aligned}&\left(I_k+I_g+m_g l_2^2+m_g l_3^2+2m_g l_2 l_3\sin(\alpha_2-\omega t)\right)\ddot{\varphi}_1=\\&=m_g\cdot\omega^2 l_2(l_3-\rho_0)\cos(\omega t-\alpha_2).\end{aligned}\quad(12)$$

As:

$$\int_0^{\frac{2\pi}{\omega}}\sin(\alpha_2-\omega t)dt=\frac{1}{\omega}\cos(\alpha_2-\omega t)\Bigg|_0^{\frac{2\pi}{\omega}}=\frac{1}{\omega}(\cos(\alpha_2-2\pi)-\cos\alpha_2)=0,$$

so:

$$(I_k+I_g+m_g l_2^2+m_g l_3^2)\ddot{\varphi}_1=m_g\omega^2 l_2(l_3-\rho_0)\cos(\omega t-\alpha_2)$$

$$\ddot{\varphi}_1=\frac{m_g\omega^2 l_2(l_3-\rho_0)\cos(\omega t-\alpha_2)}{I_k+I_g+m_g l_2^2+m_g l_3^2};\quad(13)$$

$$\dot{\varphi}_1(t)=\frac{m_g\omega l_2(l_3-\rho_0)\sin(\omega t-\alpha_2)}{I_k+I_g+m_g(l_2^2+l_3^2)}+\dot{\varphi}_1(0)\quad(14)$$

$$\varphi_1(t)=-\frac{m_g l_2(l_3-\rho_0)\cos(\omega t-\alpha_2)}{I_k+I_g+m_g(l_2^2+l_3^2)}+\dot{\varphi}_1(0)\cdot t+\varphi_1(0).\quad(15)$$

Since the initial conditions with time do not affect the motion of the system, then:

$$\varphi_1(t)=-\frac{m_g l_2(l_3-\rho_0)\cos(\omega t-\alpha_2)}{I_k+I_g+m_g(l_2^2+l_3^2)}.\quad(16)$$

Thus, the movement of the container is approximately described by the equations:

$$\rho_0=\frac{m_g l_3}{m_k+m_g};\quad\varphi(t)=\omega t+\pi;$$

$$\varphi_1(t)=-\frac{m_g m_k l_2 l_3\cos(\omega t-\alpha_2)}{\left(I_k+I_g+m_g(l_2^2+l_3^2)\right)(m_k+m_g)}\Rightarrow\quad(17)$$

$$\Rightarrow-a\cos(\omega t-\alpha_2)$$

The law of motion of an arbitrary point M of θ container whose position is determined by an angle is described by parametric equations $O_1M=R$:

$$\left.\begin{aligned}x_M(t)&=\rho\cos\alpha+R\cos(\theta+\varphi_1);\\z_M(t)&=\rho\sin\alpha+R\sin(\theta+\varphi_1)\end{aligned}\right\},\quad(18)$$

that is

$$x_M(t)=\frac{m_g l_3}{m_k+m_g}\cos(\omega t+\pi)+R\cos(\theta-a\cos(\omega t-\alpha_2)).$$

The velocity of the point M takes the form:

$$\left.\begin{aligned}x_M(t)&=\frac{-m_g l_3}{m_k+m_g}\cos\omega t+R\cos(\theta-a\cos(\omega t-\alpha_2))\\z_M(t)&=\frac{-m_g l_3\sin\omega t}{m_k+m_g}+R\sin(\theta-a\cos(\omega t-\alpha_2))\end{aligned}\right\}\quad(19)$$

Speed of point M is equal to:

$$\left.\begin{aligned}&\dot{x}_M(t)=\frac{m_g l_3\omega\sin\omega t}{m_k+m_g}-R\sin(\theta-a\cos(\omega t-\alpha_2))\times\\&\times a\omega\sin(\omega t-\alpha_2)\\&\dot{z}_M(t)=\frac{-m_g l_3\omega\cos\omega t}{m_k+m_g}+R\cos(\theta-a\cos(\omega t-\alpha_2))\times\\&\times a\omega\sin(\omega t-\alpha_2\end{aligned}\right\}\quad(20)$$

Acceleration of point M is equal to:

$$\left.\begin{aligned}&\ddot{x}_M(t)=\frac{m_g l_3\omega^2\cos\omega t}{m_k+m_g}-R\cos(\theta-a\cos(\omega t-\alpha_2))\times\\&\times(a\omega\sin(\omega t-\alpha_2))^2-\\&-R\sin(\theta-a\cos(\omega t-\alpha_2))\cdot a\cdot\omega^2\cos(\omega t-\alpha_2)\\&\ddot{z}_M(t)=\frac{m_g l_3\omega^2\sin\omega t}{m_k+m_g}-R\sin(\theta-a\cos(\omega t-\alpha_2))\times\\&\times(a\omega\sin(\omega t-\alpha_2))^2+\\&+R\cos(\theta-a\cos(\omega t-\alpha_2))\cdot a\cdot\omega^2\cos(\omega t-\alpha_2)\end{aligned}\right\}\quad(21)$$

де $a=-\dfrac{m_g\cdot m_k\cdot l_2\cdot l_3}{\left(I_k+I_g+m_g(l_2^2+l_3^2)\right)(m_k+m_g)}$,

$0\le t\le\dfrac{2\pi}{\omega}$. The moment of resistance of rolling friction forces in bearing O_2 is approximately equal to:

$$\begin{aligned}M_{on}&=m_g\cdot r\cdot f[+\rho_0\omega^2\cos\pi+\omega^2 l_3]=m_g\cdot r\cdot f\cdot\omega^2(-\rho_0+l_3)=\\&=m_g\cdot r\cdot f\cdot\omega^2\left(\frac{-m_g l_3}{m_k+m_g}+l_3\right),\end{aligned}\quad(22)$$

$$M_{on}=\frac{m_g\cdot m_k\cdot r\cdot f\cdot\omega^2\cdot l_3}{m_k+m_g}.\quad(23)$$

We need the lowest point of the container to move in such an interval (limits) relative to the OZ axis upwards. We substitute values into equation (A) $\angle\theta=270°$. Then:

$$z_M(t)=-\frac{m_g l_3\sin\omega t}{m_k+m_g}+R\sin\left(\frac{3\pi}{2}-a\cos(\omega t-\alpha_2)\right),\quad(24)$$

$$z_M(t)=-\frac{m_g l_3\sin\omega t}{m_k+m_g}-R\cos(a\cos(\omega t-\alpha_2)).\quad(25)$$

Function $cos\alpha$ is a pair function then $z_M(t_x) = \frac{m_g l_3}{m_k + m_g} - R\cos(a\sin\alpha_2)$. So at the time tx, t_x, when $sin\,\omega t_x = -1$, to reduce the movement of the bottom of the container upward, it is necessary that: $cos(a\,sin\,\alpha_2) = 1$, and this is possible, if $a\,sin\,\alpha_2 = 0$. Function $sin\alpha_2 = 0$, optional $\alpha_2 = \theta$ або $\alpha_2 = \pi$.

So, to reduce the amount of movement of the bottom up (container) of the position of the unbalance is determined by the angle α, which should be equal to $\alpha_2 = 0°$ or $\alpha_2 = 180°$.

So, the moment of resistance will be small, if expression $r \cdot m_g \cdot f \cdot \omega^2 \cdot T[-\frac{al_2}{2} + l_3 + \frac{a^2 l_3}{2}]$ will take the slightest signification. From the angle α_2 the moment of resistance is independent.

Thus, in the first approximation, the moment of resistance is equal to:

$$M_{on} = r \cdot m_g \cdot f \cdot \omega^2 [\frac{a^2 l_3}{2} - \frac{al_2}{2} + l_3 - \rho] = \\ = r \cdot m_g \cdot f \cdot \omega^2 [\frac{a}{2}(al_3 - l_2) + \frac{m_k l_3}{m_k + m_g}], \quad (26)$$

where: $a = -\frac{m_g m_k l_2 l_3}{(I_k + I_g + m_g(l_2^2 + l_3^2))(m_k + m_g)}$.

$$M_{on} = r \cdot m_g \cdot f \cdot \omega^2 \left[\frac{a}{2} \left(-\frac{(I_k + I_g)(m_k + m_g)l_2 + m_g^2 (l_2^2 + l_3^2) l_2 + m_k m_g l_2^3}{(I_k + I_g + m_g(l_2^2 + l_3^2)) \times (m_k + m_g)} \right) + \frac{m_k l_3}{m_k + m_g} \right]. \quad (27)$$

In order to optimize the motion of the points of the grinding chamber, consider the case where it is necessary to achieve a result so that the lowest point of the container moves upwards about the axis Oz as high as possible.

Substituting the values $\angle\alpha = 270°$, then we get:

$$z_M(t) = -\frac{m_g l_3 \sin\omega t}{m_k + m_g} - R\cos(a\cos(\omega t - \alpha_2)). \quad (28)$$

For a significant energy-intensive process of vibratory grinding, it is necessary to achieve the maximum movement of the grinding chamber upward [20], which is possible, if $\sin\omega t_k = -1$ or $\omega t_k = \frac{3\pi}{2}$. At this point in time, the equation obtained will take the form:

$$z_M(t_k) = \frac{m_g l_3}{m_k + m_g} - R\cos\left(a\cos(\frac{3\pi}{2} - \alpha_2)\right),$$

or:

$$z_M(t_k) = \frac{m_g l_3}{m_k + m_g} - R\cos(-a\sin\alpha_2). \quad (29)$$

Function cosα is a pair function $z_M(t_k) = \frac{m_g l_3}{m_k + m_g} - R\cos(a\sin\alpha_2)$. So, at the moment of time, t_k, when $sin\,\omega t_k = -1$, to increase the value of the bottom movement of the container up, it is necessary that the function $cos(a\,sin\,\alpha_2)$ takes the minimum possible value, and this is possible $\sin\alpha_2 = \pm 1$, since the value $a < 1$. This equation is satisfied provided that $\alpha_2 = 90^0$ either $\alpha_2 = 270^0$. In order to increase the value of the bottom movement of the container, it is necessary that the position of the unbalance be determined by an angle equal to $\alpha_2 = 90°$ or $\alpha_2 = 270°$.

In studying the obtained functional dependencies in the MathCad software environment, taking into account the coefficient of the attached mass of the grinding chambers, the optimum position of the exciter was obtained by varying the angle α_2 (fig. 4) and the corresponding change in the trajectory of the motion of the material point on the bottom of the grinding chamber. The criterion of optimization was the maximum ratio of vertical and horizontal components of the amplitude, which corresponded to a value of angle α_2 =290 град.

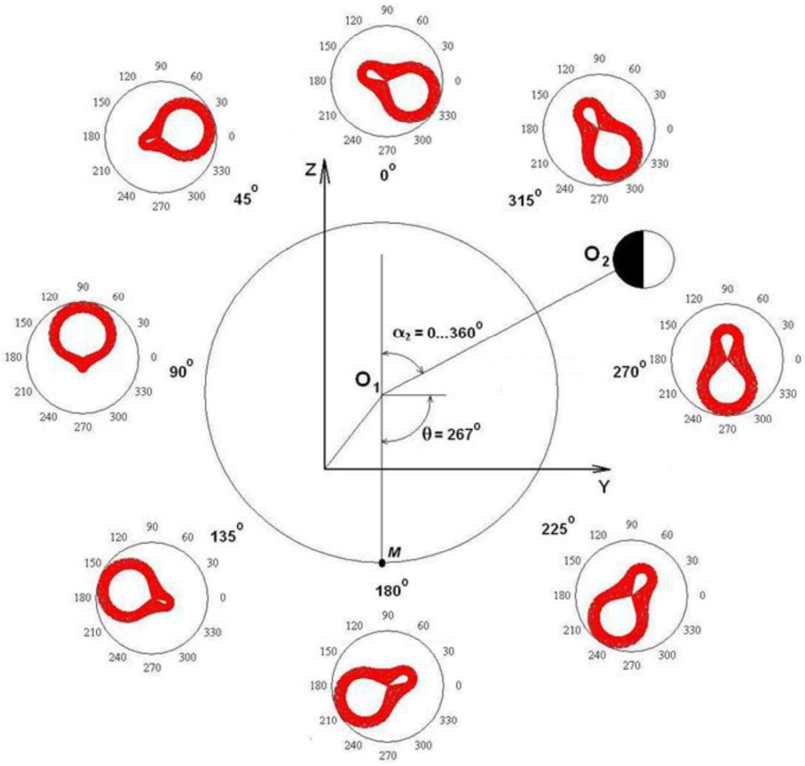

Fig. 4. Trajectories of movement of the lowest point of the grinding chamber bottom with variational values of the angle of position of the vibrator

Analyzing the graphical dependence in Fig. 3 it was found that the maximum ratio of the components of the amplitude of the oscillations is A_Z / A_X = 2,46 and is observed at angles α_2 = 290 degrees at the angular velocity of the drive shaft ω = 110 рад/с. In this case, the amplitude of the displacement of the grinding container along the axis OZ = 5,4 mm along the axis OX = 2,2 mm. The obtained data make it possible to provide the maximum dynamic state of the investigated vibration system, and as a consequence to increase the intensity of processing of bulk raw materials.

CONCLUSIONS

For the first time a new scientific direction of the development of high-performance vibrating machines has been formed on the basis of the development of the main provisions of the theory of the drive of angular oscillations for the realization of highly efficient complex machining of bulk raw materials.

As a result of an analytical study of the dynamics of the motion of the grinding chambers of a vibration mill of angular vibrations, it was found that the optimum position of the vibrator drive is 290 degrees, which makes it possible to obtain the maximum ratio of the vertical component of the vibration amplitude of 5.4 mm, and as a result, to provide a significant force effect on the material being processed, Specific energy consumption for said treatment.

REFERENCES

1. **Palamarchuk I.P., Lipovoy I.G., Yanovich V.P. 2009.** Razvitie konstruktivnyih shem vibrotsentrobezhnyih tehnologicheskih mashin dlya realizatsii protsessov mehanicheskoy obrabotki selskohozyaystvennogo syirya. Vibratsii v tehnike i tehnologiyah. №2(54). 105-115. (in Ukraina).
2. **Palamarchuk I.P. 2008**. Nauchno-tehnicheskie osnovyi razrabotki energosberegayuschih vibromashin mehanicheskogo vozdeystviya pischevyih i pererabatyivayuschih proizvodstv. Dissertatsiya na soiskanie uchenoy stepeni d.t.n. Kiev: NUPT, 479. (in Ukraina).
3. **Rilley R.V. 1996.** Theory and practice of grinding. Chemical and process engineering. № 4. 189-195.
4. **Bond F.C. 1998.** Some recent advances in grinding theory and practice. Brit. Fnang. № 9. 84-93.
5. **Gonzalez A.T.J. 1995.** Milling process of durum wheat. Options Mediterrancennes. №2, 43-51.
6. **Boldyrev V.V. 2002.** Powder Technol. Vol. 122. No. 2-3, 247.
7. **Nasir A. 2005.** Development and testing of hammer mill. Department of Mechanical Engineering. № 8(3). 124-130.
8. **Yanovich V.P., Kupchuk I.M., Bably G.R.** Vibratsionnaya dvokonteynernaya melnitsa. Pat. na poleznuyu model № 93366 UkraYina, MPK B02S19/16. Vladelets Yanovich Vitaliy Petrovich № 201404797 Byul. №18. (Ukraina).

9. **Yanovich V.P., Kupchuk I.M., Korlchuk V.S.** Sposob polucheniya melkodispersnyih poroshkov. Pat. na sposob № 101586 UkraYina, MPK B02S19/00. № 201501954. Vladelets Yanovich Vitaliy Petrovich № 201501954 Byul. №18. (Ukraina).
10. **Yanovich V.P., PolEvoda Yu.A., Nurmetov V.M.** Razrabotka vibratsionnoy melnitsyi uglovyih kolebaniy dlya proizvodstva entero- i imunnosorbtsionnyih pischevyih dobavok. Materialyi mezhdunarodnoy nauchno-prakticheskoy konferentsii /NUHT. Kiev, 2016. 197-199.
11. **Franchuk V.P., Chervonenko A.G., Tarasenko A.A., Korolev P.P. 1970.** Energeticheskaya i silovaya otsenka razlichnyih tipov privodov vibratsionnyih melnits. Sbornik nauchnyih trudov: Problemyi vibratsionnoy tehniki. K.: Naukova dumka, 202-210. (Ukraina).
12. **Yaroshevich N. 2011.** Double multiple synchronization of the mechanical vibroexciters connected wih linear oscillatory system. MOTROL. Commission of Motorization and Energetics in Agriculture. Lublin. Vol. 6. 294-302.
13. **Solonaya E.V., Lyubin V.S. 2013.** Trimassnaya vibratsionnaya melnitsa s chetyirmya vibrovozbuditelyami. MOTROL. Commission of Motorization and Energetics in Agriculture. Lublin. Vol.15. No.4. 219-224.
14. **Franchuk V.P., Tarasenko A.A., Korolev P.P. 1970.** K voprosu ucheta massyi tehnologicheskoy zagruzki vibratsionnoy melnitsyi. Sbornik nauchnyih trudov: Problemyi vibratsionnoy tehniki. K.: Naukova dumka, 193-197. (in Ukraina).
15. **Serdyuk L.I. 1994.** Metodika rascheta vibratsionnyih stankov. Poltavskiy selskohozyaystvennyiy institut. №3, 34-36. (Ukraina)
16. **John H., Stephens R.C. 1984.** Mechanic of Machines. London: Edward. 213-224.
17. **Maitra G.M., Prasad L.V. 1985.** Handbook of Mechanical Design. New Delhi: McGraw Hill. 89-108.
18. **Byihovskiy I.I. 1969.** Osnovyi teorii vibratsionnoy tehniki. M.: Mashinostroenie, 363.
19. **Bernik P.S., Velichko L.L., Palamarchuk I.P. 1994.** Analiticheskoe issledovanie kombinirovannogo sposoba vozbuzhdeniya kolebaniy. Materialyi II mezhdunar. NTK “Primenenie kolebaniy v tehnologiyah. Raschet i proektirovanie mashin dlya realizatsii tehnologiy.” Vinnitsa: VGSHI, 13-14. (Ukraina).
20. **Spivakovskiy A.O., Goncharevich I.F. 1983**. Vibratsionnyie mashinyi. M.: Nauka, 288. (Ukraina).

MOTROL. Commission of Motorization and Energetics in Agriculture – 2017. Vol.19. No.2. 29-32

PHYSICAL AND MECHANICAL PROPERTIES OF THE SURFACE LAYERS OF NB, TI AND NB-TI ALLOY AFTER ELECTROLYTICAL HYDROGENATION

Nadija Ratska[1], Chrystyna Vasyliv[1], Yurij Kovalchyk[2]
[1]Karpenko Physico-Mechanical Institute of the NAS of Ukraine
Naukova Str. 5, Lviv, Ukraine. E-mail: nadija.ratska@gmail.com
[2]Lviv National Agricultural University
V. Velykogo Str. 1, Dubliany, Ukraine. E-mail: yurij.kovalchyk@gmail.com

Summary. The article is devoted to studying the influence of electrolytic hydrogenation on microstrains features on the surface layers of niobium, α-titanium alloy BH-10 by nanoindentation method. Research by this method as a way of NDT; help us to predict performance properties, particularly tribological behavior. It is founded that physical and mechanical properties of the surface layers niobium, titanium and BH-10 have improved after hydrogenation for electrolytic current density 1.0 A / dm^2 and duration 1 hour. In particular, hardness, Young's modulus and internal stress increases, while ductility of materials decreases. Work of elastic component increased at 12%, for niobium alloy and reduced at 40% for titanium. This difference is caused by different solubility of hydrogen in materials. Crystal lattice volume of niobium increases after electrolytic hydrogenation and internal stresses appears. In particular stress increased by 15 ... 18% in comparison with the initial state. Micro hardness and elastic deformation of surface layers niobium increases after hydrogenation, which will positively affect to its tribological properties. Chemical and thermal threatment of the alloy by oxidation improves parameters of elastic-plastic deformation, increases microhardness to 5 ... 10%, which will improve the tribological properties of the material.

Effect of hydrogen on physical and mechanical properties of micro-and submikrovolumes oxidized alloy varies slightly. However, the stress state in the crystal lattice decreases in the surface layer and its ductility improves.

Key words: niobium, titanium, alloys of Nb-Ti system, electrolytic hydrogenation, oxidation, nanoindentation.

INTRODUCTION

Aim of the work – to investigate the influence of electrolytic hydrogenation to micro deformation of the surface layers of niobium, titanium, and alloys of Nb-Ti system in initial state and after thermodiffusion oxidation.

Recently, many papers have been devoted to studying the influence of oxidation on the physicochemical and mechanical properties of multi-alloyed alloys of niobium. Nature of oxide phases depends on the chemical composition and heat treatment conditions [22-28]. Development of the methods of checked oxidation allows us to improve the operation properties and to extend the application fields of titanium-niobium alloys. The influence of conditions of thermodiffusion oxidation of BH-10 alloy (32 mass.% Ti; 8 Al; 4 V; 1.8 Zr; 0.13 O; 0.05 C; remaining Nb) on its structure, physicomechanical and tribological properties has been investigated earlier [28].

Combined chemical-heat treatment of the BH-10 alloy was applied. It consists of preliminary oxidizing at 900°C for 3 h and subsequent vacuum annealing at 1200°C for 1 h. Oxygen concentration on the surface of the oxidized alloy after 3 h exposure reach to 22-24 mass %, the thickness of the gas-saturated layer is 50-70 mm.

High-temperature annealing in vacuum of the preliminary oxidized alloys is used in order to increase the thickness of the gas-saturated layer, to provide the homogeneity of its structural and phase composition and to stabilize the physical and mechanical properties [28]. As a result of such heat treatment the internal oxidation occurs. In the gas-saturated layer the disperse oxides are formed with higher thermodynamic stability to compare with the phases appearing from the over-saturated solid solutions. Parameters of thus formed gas-saturated layer are determined by the temperature-time conditions both of the previous oxidation and the following vacuum annealing.

After annealing the depth of the gas-saturated layer reaches 100…110 µm and homogeneity of its structure increases. Under these conditions distribution of the oxide inclusions is uniform and their content in the diffusion zone is 40…50%.

The chemical composition of inclusions and matrix indicates the formation of Ti(Nb,Al,V)O_2 oxides in solid solution of titanium in niobium (Fig. 1).

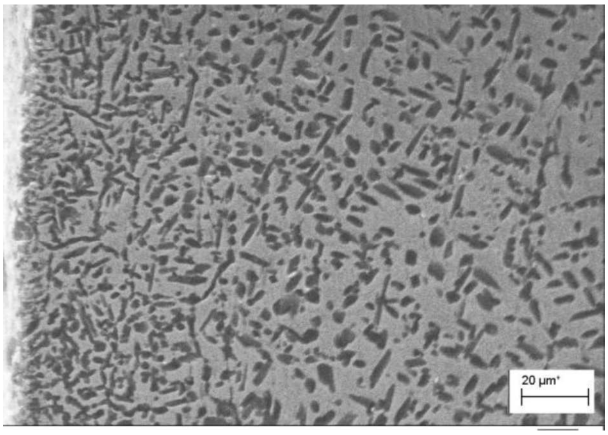

Fig.1. Microstructure of the BH-10 alloy after thermodiffusion oxidation

During vacuum annealing of the preliminary oxidized alloys decay and reconstruction of metastable oxides on the surface and at the near-surface layers of the alloy is observed. Released oxygen atoms diffuse into material depth and interact with the alloy components first along the grain boundaries. Besides, oxygen available in the alloy in solid solution Nb(Ti,Al,V,O) interacts with metal atoms under high-temperature annealing. It promotes the formation of thermo-resisting oxides Ti (Nb, Al, V)O_2 in the near-surface layer of the matrix both along the grain boundaries and in its volume.

ANALYSIS OF RECENT STUDIES AND PUBLICATIONS

Niobium has unique technological and anticorrosive properties, particularly refractoriness, resistance to corrosion in many hostile environments, satisfactory strength, good thermal conductivity, resistance to radiation and others and is used in the chemical industry and in various branches of engineering industry. However, gas absorption under relatively low temperatures (below 300ºC) increases the tendency to embrittlement of the metal. It is the result of formation of solid phases, such as oxides, hydrides, etc. [1-3]. Important disadvantage of niobium is low wear resistance [8, 9].

Alloying of niobium by titanium, aluminium, etc. and chemical-thermal treatment are used to improve the properties of material [8, 9, 13-18].

Oxidation can provide the near-surface hardening of material, to approve corrosion and tribological properties [5-7, 15-17]. Great contribution to the studying of physical, chemical and mechanical properties of niobium and its alloys have made Korotaev A.D., Maksimovic G., Zakharov A.V., Ivantsov V.I., T.Murakami, J. Benard, R. Kieffer et al. However, the nature of the oxide phases and the dependence of their properties on the composition and the environment are in some cases very limited.

Therefore, the studying of physical and mechanical properties of niobium-titanium alloy in a hydrogen exposure opens up new perspectives in the development of engineering of material surface. Operational properties, in particular tribological, depend on the state and properties of the thin surface layer (about 0.1 mm thickness). Mechanical properties of the thin surface layers can be determined by nanoindentation [4-7,11].

EXPERIMENTAL PROCEDURES

Reseach materials: niobium НбЦ, titanium ВТ1-0 and ВН-10 alloy (32 mass % Ti, 8 %Al, 4 %V;. 1,8% Zr; 0,13 %B; 0,05 % C, the remaining Nb). Chemical-thermal treatment was carried out in stages: in air for 3 hours at 900ºC (furnace type SNOL 1.6.2, 5.1 / 9-I3) and in vacuum for 1 hour at 1200 ºC (vacuum furnace СНВ -1.3.1 at a pressure of 10^{-2} Pa). Metallographic investigation of the surface layers was done by a scanning electron microscope EVO 40XVP with a system of micro X-ray spectral analysis on the energy-dispersive spectrometer INCA ENERGY 350 (Carl Zeiss).

To determine the mechanical properties of the surface layers the durometer ПМТ-3 and the method of dynamic indenting were used. It is based on the automated recording of the loading curve $P = f(h)$, where P is the load applied to the indenter, h is the depth of its introduction into the investigated material surface. The main advantage of the method is that the hardness is determined at the time of the tip maximum penetration (h_{max}), i.e to the beginning of elastic recovery of the material. The curve gives the information about the indenter work needed to overcome the material resistance A_{plast} (area under the loading branch) and the work spent by the material to restore its properties A_{elast} (area under the unloading branch). From these data, the degree of the surface plasticity ε is determined according to the formula $\varepsilon = (A_{plast} - A_{elast})/A_{plast}$. The value of microhardness by Meyer is found as a ratio of the maximum load P_{max} to the area of the projection dent A, Young's modulus is defined as $E = S/2\sqrt{\pi/A}$, where S is tangent of the initial unloading curve area.

Moreover, the scratch method was used. This method is based on continuous recording of the friction force at movement of the indenter over the surface. The applied load was 1 N and speed of movement – 0.2 mm/s. The method was combined with the determination of the, volume of the material displaced by the indenter and parameters of the roughness of the surface, which was formed at the scratch bottom.

Electrolytic hydrogenation was realized by cathodic polarization in 1N solution H_2SO_4 + 10 mg/l As_2O_3. Duration 1 h and current density 1.0 A/dm^2 was used [10].

RESULTS AND DISCUSSION

The effect of hydrogen on the mechanical properties of niobium, titanium, and their alloys in micro and submicro volumes has been evaluated by method of dynamic nanoindentation. The loading curves were obtained for the test materials in the initial state and after hydrogenation (Fig. 2). On the basis of these diagrams physical and mechanical characteristics of the surface layers were calculated (Table. 1).

After electrolytic hydrogenation the physical and mechanical properties of the alloy ВН-10 are better than those of niobium and titanium (Fig.2).

Table 1. Physical and mechanical properties of the surface layers of materials in initial state/after electrolytic hydrogenation*

Metals	Nb	Ti	Alloy ВН-10
H_{Mayer}, GPa	1,449/1,583	2,066/2,475	4,628/4,967
E, GPa	63,9/98,7	91,1/105,2	124,5/115,2
A_{plast}, J	75,43/71,38	62,52/58,88	43,73/43,93
A_{elast}, J	10,36/11,44	13,54/8,32	9,94/10,11
σ_n, GPa	0,863/0,379	0,783/0,567	0,981/1,018

*H_{Mayer} - Mayer microhardness; E - Young's modulus; A_{elast} and A_{plast}. - work of elastic and plastic deformations, σ_n - internal stresses.

In particular, the physical and mechanical properties of titanium surface layer change significantly (Table 1). Internal stresses in the crystal lattice increase by 19% in comparison with the initial state. At the same time microhardness (according to Mayer) increases by

20% and Young's modulus by 15%. The work of restoration the volume of material after deformation reduced significantly (by 40%) and surface plasticity degree (□ increases [4, 11]. Since titanium belongs to the group of exothermic metal occluders, it can be assumed that a significant loss of plasticity is associated with the formation of hydride phases.

After hydrogenation the volume of niobium crystal lattice increases and internal stresses appear. In particular, the stress σ_n increases by 15 ... 18% compared to the initial state (Table 1), the Meyer microhardness changes by 11%, while the Young's modulus changes from 63.9 to 98.7 GPa. The degree of the surface plasticity decreases from 0.863 to 0.840.

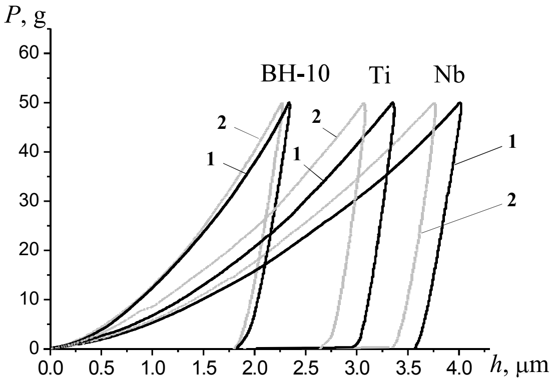

Fig. 2. Loading curves of niobium, titanium and BH-10 alloy in the initial state (1) and after electrolytic hydrogenation (2). Load 0.05 kg, loading rate of 5 g/s, temperature 20ºC

Work of the niobium surface destruction by the indenter changes under the influence of hydrogen. The work of plastic deformation (A_{plast}) decreases and the work of the elastic deformation A_{elast} grow by 9% (table 1).

The solubility of hydrogen in niobium (0.033 mass %) is significantly higher than in titanium (0.0008 mass %), so physical and mechanical properties of niobium and titanium under hydrogenation effect are different.

Thus, after hydrogenation of niobium, titanium and BH-10, microhardness, Young's modulus and internal stresses increase, while plasticity decreases. The difference is that work of the elastic deformation of the niobium and niobium-titanium alloy A_{elast} increases by ~12%, and A_{elast} of titanium decreases by 40%.

The influence of thermodiffusion oxidation to physical and mechanical properties of BH-10 alloy surface layer has been studied. The thermodiffusion oxidation of BH-10 alloy has been realized under conditions: oxidation at 900 ° C for 3 h followed by vacuum annealing at 1200 ° C for 1 h. Under these conditions the depth of the gas-saturated layer reaches 100…110 µm. A surface layer consists of the solid oxide inclusions, localized in relatively mild matrix of solid solution Nb(Ti,Al,V,O). It should positively affect the physical and mechanical properties of the alloy (Fig.3) [11].

Oxidation improves the parameters of elasto-plastic deformation of the alloy; in particular, microhardness and the work of elastic deformation of the surface layer increase by 5 ... 10%, which will obviously have a positive effect on the frictional properties of the material [11, 19, 20].

After hydrogenation of the oxidized BH-10 alloy, the stress state in the crystal lattice of the surface layer was reduced and its plasticity increased. In particular, the microhardness of the surface layer decreases by approximately 25%, and the degree of ductility increases by ~10% (fig. 3, table 2).

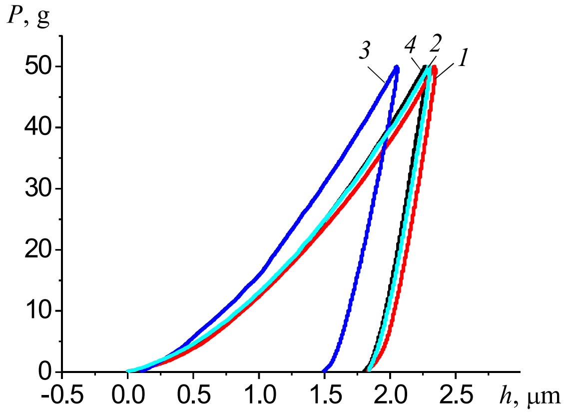

Fig. 3. Load diagrams for the BH-10 alloy in the initial state (1), after hydrogenation (2), after oxidation (3) and after hydrogenation of oxidized material (4). Load 0.05 kg, loading rate 5 g/s, temperature 20ºC

Table 2. Physical and mechanical properties of the surface layer of oxidized alloy BH-10 before and after the electrolytic hydrogenation.

Treatment	H_{Mayer}, GPa	E, GPa	$A_{plast.}$, J	$A_{elast.}$, J	σ_n, GPa
Before hydrogenation	6,899	127,1	42,03	12,55	1,351
After hydrogenation	5,126	123,3	44,48	10,09	1,060

The physical and mechanical properties of the oxidized niobium-titanium alloy are less sensitive to hydrogenation (Fig. 3).

CONCLUSIONS

The physical and mechanical properties of surface microlayers of niobium, titanium and niobium-titanium alloy BH-10 alloy has been studied with using of dynamic indenting method. The influence of thermodiffusion oxidation to physical and mechanical properties of BH-10 alloy surface layer has been studied too.

1. The work of elastic-plastic deformation of titanium is reduced after the hydrogenation due to hydride formation.

2. The microhardness and work of elastic deformation of the niobium surface layers insignificantly increases after hydrogenation at a current density of 1 A/dm^2.

3. Characteristics of elastic-plastic deformation of the alloy BH-10 are less sensitive to hydrogenation than niobium and titanium.

4. The physical and mechanical properties of the oxidized niobium-titanium alloy are less sensitive to hydrogenation.

REFERENCES

1. **Burkhanov G.S., Ufimov Yu.V.** 1986. Refractory metals and alloys. Moscow: Metallurgy, 251.
2. **Voitovich, R. F., Golovko, E.I.** 1984. High-temperature oxidation of metals and alloys: Ref. - K.: Nayk. Dumka, 255.
3. **Samsonov G.V., Borisova A.L., Zhidkova T.G.**1978. Physical and chemical properties of oxides: Ref. M.: Metallurgy, 472.
4. **Golovin Yu.I.** 2008. Nanoindentation and mechanical properties of solids in submicrovolumes, thin near-surface layers and films (review). - Solid State Physics, Vol. 50, Issue 12. 2116-2142.
5. **Shyrokov V.V., Ratska N.B**. 2008. Regularities of the oxidation of niobium with increased titanium content. - Material science.-Vol. 44, Issue 4. 581-588.
6. **Lyutyi Ye.M., Yeliseeva O.I., Stepanyshyn V.I.** 1995. Mechanism and regularities of oxidation of Nb-Ti and Nb-Ti-Si systems. Phys.-Chem. Mechanics of materials. No. 1, 107-115. (Ukraine).
7. **Shyrokov V.V., Ratska N.B.** 2007. Influence of titanium admixtures on the structure and physicomechanical properties of niobium. - Materials Science, Vol. 43, Issue 2. 215-221.
8. **Murakami T., Mano H., Kaneda K. et al.** 2010. Friction and wear properties of zirconium and niobium in a hydrogen environment. Wear. 268. 721-729.
9. **Vasyliv Kh., Vynar V., Rastka N., Panasyuk P**. 2013. Influence of the oxidation temperature on the micromechanical and tribological properties of the alloy of the Nb-Ti-Al system. Motorization and power industry in agriculture. MOTROL. -Lublin. No. 4. 186-192.
10. **Vasyliv Kh., Vynar V., Ratska N.** 2011. Peculiarities of wear of α-titanium alloys under hydrogen influence. Motorization and power industry in agriculture MOTROL. - Lublin. V.13D. 198-202.
11. **Rats'ka N., Vasyliv Kh., Kovalyshyn S.** 2015. Application of thermodiffusion oxidation to improve the tribological properties of the niobium-titanium alloy system. Motorization and power industry in agriculture MOTROL. -Lublin. No. 4. 3-6.
12. **Kopeckiy Ch.V.** 1974. Structure and properties of refractory metals. - Moscow: Metallurgy, 187.
13. **Semenov A.P.** 1972. Friction and adhesion interaction of refractory metals at high temperatures. M.: Science. 160.
14. **Makarkin AN, Nazarenko P.V.** 1983. Investigation of the influence of hydrogen on the change in the microstructure of near-surface layers under external friction. Friction and wear. №1, 120.
15. **I.I. Fierger.** 1982. Heat treatment of alloys: Ref. L.: Mechanical Engineering, 304.
16. **Ruksk R. J. Sheip L.V.** 1956. High-Temperature Technology. John Wiley and Sons, Inc., New York, 114-130.
17. **Tcvikilevitch O.S., Vasyliv C.B.** 2002. Stability of strengthened niobium alloys in long-term high-temperature loading conditions. Z. Metallkunde 11. 1123-1131.
18. **Vasilyeva E.V. Gorbova AS, Prokoshkin DA 1975.** Structure and Elastic Characteristics of Alloys of the Nb-Ti System. Metallurgy and heat treatment of metals. №3. 73-74.
19. **Hensley C.F. Male A.T., Rowe C.W.** 1968. Friction properties of metal oxide at high temperatures. Wear. №3. 233-235.
20. **Mathieu S., Knittel S., Berthod P., Mathieu S., Vilasi M**. 2012. On the oxidation mechanism of niobium-base situ. Corrosion. No. 60. 181-192.
21. **Aniołek K., Kupka M., Łuczuk M., Barylski A.** 2015. Isothermal oxidation of Ti-6Al-7Nb alloy. Vacuum 114, 114-118.
22. **W.Q. Wei, H.W. Wang, C.M. Zou, Z.J. Zhu, Z.J. Wei**. 2013. Microstructure and oxidation behavior of Nb-based multi-phase alloys, Mater. Des. 46. 1-7.
23. **Jiten Das, G.Appa Rao, S.K.Pabi, M. Sankaranarayana, T.K.Nandy**. 2014. Oxidation studies onW–Nb alloy. Int. Journal of Refractory Metals and Hard Materials 47. 25-37.
24. **Vazquez, S.K. Varma.** 2011. High-temperature oxidation behavior of Nb–Si–Cr alloys with Hf additions, J. Alloys Compd. 509. 7027-7033.
25. **Jianshu Zheng, Xinmei Hou, Xiangbin Wang, Ye Meng, Xin Zheng, Lei Zheng**. 2016. Isothermal oxidation mechanism of a newly developed Nb–Ti–V–Cr–Al–W–Mo–Hf alloy at 800–1200°C. Int. Journal of Refractory Metals and Hard Materials 54. 322-329.
26. **E. M. Lyutyi, O. I. Eliseeva, V. I. Stepanyshyn**. Mechanism and regularities of oxidation in Nb–Ti and Nb–Ti–Si systems. 1995. Materials Science. V. 29, Issue 1. P. 56-60.
27. **M. Sankar, R.G. Baligidad, A.A. Gokhale.** 2013. Effect of oxygen on microstructure and mechanical properties of niobium, Mater. Sci. Eng. A569. 132-136.
28. **Nadiya Ratska, Vasyl Pokhmurskii, Chrystyna Vasyliv, Vasyl Vynar.** 2017. Improvement of the reciprocating sliding wear resistance of a Nb-based alloy using thermal oxidation. Tribology Letters 65. 90-99.

MOTROL. Commission of Motorization and Energetics in Agriculture – 2017. Vol.19. No.2. 33-39

OPTIMIZATION OF ROUGHNESS PARAMETERS AND THE DEGREE OF HARDNESS AFTER ROLLING WITH ROLLS WITH THE STABILIZATION OF WORKING EFFORT

Boris Butakov, Vitaliy Artyukh, Olena Baranova, Maxim Shatohin
Nikolaev National Agrarian University
Georgiia Gongadze Str., 9, Nikolaev, Ukraine. E-mail: vitaliy5555555555@rambler.ru

Summary. Surface plastic deformation (SPD) by rolling with rolls or coining by strikers is used to harden the surface layer of metal parts of critical use. Finish SPD is applied to improve the presentation and to increase the wear resistance of the surface layer, and hardening is used to increase the wear resistance of parts.

Modern equipment for hardening surface layers which mostly defines the performance characteristics of the machine parts includes a number of methods: heat treatment, hardening with the HFP, laser processing, etc. Rolling with rolls is widely used for hardening the surface layers of the machine parts.

Spherical or toroidal rolls are mostly used in the technological process of rolling, and the surface becomes wavy with the step other than the feed rate, when the roll is pressed at a high angle.

A lot of researchers believe that the major reason for waviness appearing is the presence of runout roller resulting in a variable rolling feed rate. To avoid the appearing of waviness in finish rolling it is advisable to take the indentation angle valued 2 - 3^0, which limits the roughness of the rolled surface measured $40 < R_z < 80$ mcm, and to decrease the waviness it is advisable to use the rolls with a precise profile and to re-grind them as often as possible. At the reinforcement rolling the thin surface layer is whittled away and this decreases greatly the efficiency of the reinforcement.

The constituents of the effort P of the rolling of shafts made of steel 40 (200 HB) with a diameter of 100-200mm on a lathe with a toroidal roll using a device for stabilization of the working effort were measured with the universal UDM dynamometer.

The way of rolling the parts with rolls with the stabilization of the working effort allows to get a reinforced layer of various thickness with a fairly high and homogeneous hardness and increased wear resistance.

Key word: rolling, a roll, average angle of indentation, hardness, response surface, surface roughness.

INTRODUCTION

An effort, transmission, roller diameter are the major components of rolling. The transmission of rolling in multiseries and mass production is determined experimentally by a trial lot of details [5-18]. It is necessary to optimize the parameters influencing the wear resistance of bodies of rotation after rolling them with rolls in order to reduce the cost of the experiment.

It is necessary to develop modes for rolling the bodies of rotation with rolls to prevent waviness on the workpiece surface.

ANALYSIS OF RECENT RESEARCHES AND PUBLICATIONS

Yu. G. Proskuryakov, L. M. Shkolnik [20] suggested a method for calculating the effort of rolling shafts and holes with Ball and roller with rectilinear generatrix based on the experiments. The effort is defined depending on geometrical sizes of the roll and the detail, the modulus of elasticity of the material being rolled and maximum contact pressure during rolling.

V. M. Braslavskiy [1-7] also developed a technique for selecting the rolling modes and introduced a hardness coefficient.

The works[19, 23, 25, 26, 27] present a technology of rolling the details with rolls with a little effort.

OBJECTIVES

To find the optimal modes of rolling which ensure the details' maximum wear resistance after processing with the help of multifactorial experiment.

In order to determine an objective assessment of the device's functioning we solved the following tasks:

- the main factors that have the greatest impact on the quality of the process were identified;

- the possibilities of changing the parameters of the identified main factors are determined through appropriate adjustments.

THE MAIN RESULTS OF THE RESEARCH

Determination of factors influencing the course of the technological process was carried out by the method of peer review ("psychological experiment"), [21, 22, 24, 28] the following analyzes of the factor ranging diagrams. The major factors influencing the course of the technological process are presented in table 1.

Table 1. The main factors influencing the process

№	Factors	Code marks	Range of variation	Factor levels		
				Top+1	Basic 0	Bottom -1
1	Roll diameter, mm	X_1	10	60	50	40
2	Rolling effort, кН	X_2	1,12	2,99	1,87	0,75
3	Roller feed, S mm/rot	X_3	0,02	0,09	0,07	0,05

4	Initial surface roughness Ra, mcm	X_4	0,1	0,40	0,30	0,20
5	Number of the roller passes	X_5	1	3	2	1
6	Average angle of indentation φ, gr.	X_6	1	5	4	3
7	Detail diameter , mm	X_7	10	60	50	40
8	Radius of the roller profile rp, mm	X_8	1	6	5	4

For each factor, we find the sum of the ranks $\sum_{j=1}^{m} a_{ij}$,

where: m – number of specialists interviewed; a_{ji} – rank of factor I appropriated by the researcher j .

Next, we determine the deviations Δ of the sum of the ranks from the average sum of ranks for each of the factors:

$$\Delta_i = \sum_{j=1}^{m} a_{ij} - \frac{1}{k}\sum_{i=1}^{k}\sum_{j=1}^{m} a_{ij}, \quad (1)$$

where: Δ_i – the deviations od the sum of the ranks of factor i from the average sum of ranks; k – the number of factors; $\frac{1}{k}\sum_{i=1}^{k}\sum_{j=1}^{m} a_{ij}$ – the average sum of ranks.

We estimate the degree of consistency of experts' interviewed opinions. To do this, we use the concordance coefficient, which is determined by formula:

$$W = \frac{12S}{m^2(k^3 - k)}, \quad (2)$$

where: $S = \sum_{i=1}^{k} \Delta_i^2$.

In this case, the concordance coefficient will be $W = 0,93$.

It was estimated, that at k>7 value $m(k-1)W$ obeys the χ^2 – distribution with the number of degrees of freedom $f = k\text{-}1$.

The significance of the concordance coefficient W is established using the Pearson criterion.

Having convinced of the consistency of specialists' opinions, it is possible to construct a diagram of ranks (fig.1).

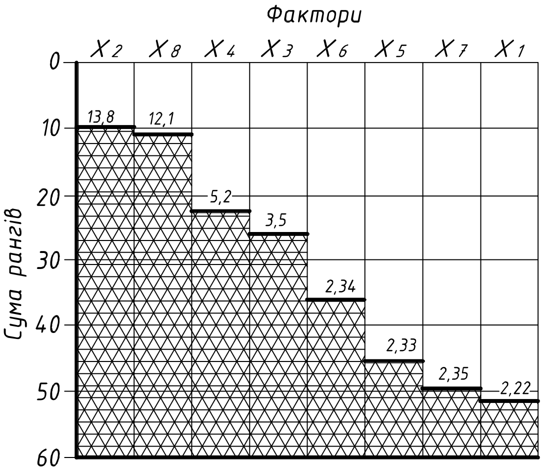

Fig. 1. A diagram of ranks X_1 – the roller diameter; X_2 – the rolling effort; X_3 – roller feed; X_4 – the initial surface roughness; X_5 – number of roller passes; X_6 – the average angle of indentation; X_7 – the diameter of the details; X_8 – the radius of the roller profile

By using the obtained diagram, the significance of the factors was evaluated. To determine the factors that do not affect the technological process, the Student's test was used.

Comparing their values with tabular values for the significance level 0,05 at the number of degrees of freedom $f = 7$, it was estimated that factors X_1, X_5, X_6, X_7 X_1, X_5, X_6, X_7 can be excluded from the following research, and it can be stated that the hypothesis about the significance of the above factors is not accepted. Really, the roller diameter (X_1) doesn't influence the technological process, as the roll has the profile radius in contact with the detail. The number of the roller passes (X_5) slightly influences the quality of the process, and the average angle of indentation (X_6) cannot be changed in the process of experimental research. Similarly, the detail diameter (X7) practically does not affect the technological process.

The analysis of the expert evaluation and their statistical processing made it possible to conclude that the following four factors have the greatest effect on the course and quality of the technological process: rolling effort X_2; roller feed X_3; initial surface roughness X_4; radius of the roller profile X_8.

In order to reduce the volume of experimental studies and to reduce the number of readjustments of the device, as well as to obtain objectively necessary information on the dependence of the degree of cold hardening and surface roughness on the one-time variation of several kinematic regimes, we used a three-level D-optimal second-order planning for four independent factors.

After statistic processing of the experimental data of the process of rolling the details with rolls, mathematical models of cold hardening(CH) and surface roughness (SR) were obtained with the help of PC. They describe the technological process of rolling with rolls with stabilization of working effort [3]:

$$CH = 18{,}93207 - 2{,}99185\,X_1 + 1{,}252594\,X_2 - 0{,}06056\,X_3 - 0{,}04519\,X_4 + \\ + 0{,}558542\,X_{12} - 0{,}06812\,X_{13} + 0{,}114792\,X_{14} - 0{,}10562\,X_{23} + 0{,}135625\,X_{24} - \\ - 0{,}17104\,X_{34} + 0{,}474089\,X_1^2 + 0{,}527422\,X_2^2 + 1{,}555756\,X_3^2 - 1{,}07924\,X_4^2. \quad (3)$$

$$SR = 0{,}165438 - 0{,}01254\,X_1 + 0{,}012037X_2 + 0{,}002352\,X_3 - 0{,}00019\,X_4 + \\ + 0{,}001188\,X_{12} + 0{,}002646\,X_{13} + 0{,}001646X_{14} + 0{,}002521\,X_{23} + 0{,}000354\,X_{24} \\ - 0{,}00027X_{34} + 0{,}00865X_1^2 + 0{,}00815\,X_2^2 - 0{,}01185X_3^2 - 0{,}01652X_4^2. \quad (4)$$

After statistic processing the analyzes the obtained regression equations were carried out with encoded values of the factors. Investigation of optimization criteria depending on changes in independent factors was carried out using the two-dimensional cross-section method.

The analyzes of mathematical models were carried out for rolling the detail by a roller. In accordance with the experimental design, an assessment was made of the dependence of the technological process performance indicators of the on the rolling effort, *кН* (X_1), radius of the roller profile, *mm* (X_2), initial surface roughness, *mm* (X_3), and roller feed *mm/rot* (X_4), which have the greatest effect on the quality of the technological process. The repetition of the experiments on each of the optimization criteria was three times.

For each row of the plan the average value of CH and SR were calculated. In turn, two factors were equated to zero, leaving the other two unequal to zero. The regression equations for the degree of cold hardening and the surface roughness of the steel experimental sample with possible combinations of factors were obtained.

The combination of such factors of the technological process, as the radius of the roller profile, (X_2), and initial surface roughness, (X_3) at $X_1 = 0$ (the rolling effort = 1,87 *кН*) and $X_4 = 0$ (the roller feed = 0,07 *об/мм*) allowed to get the regression equation in the form:

$$CH = 18{,}93207 + 1{,}252594\,X_2 - 0{,}06056\,X_3 - \\ - 0{,}10562\,X_{23} + 0{,}527422\,X_2^2 + 1{,}555756\,X_3^2, \quad (5).$$

$$ШП = 0{,}165438 + 0{,}012037X_2 + 0{,}002352\,X_3 + \\ + 0{,}002521\,X_{23} + 0{,}00815\,X_2^2 - 0{,}01185X_3^2. \quad (6)$$

We take partial derivatives with respect to X2 and X3 and obtain the system of equations for each of the optimization criteria:

$$\begin{cases} \dfrac{\partial CH}{\partial X_2} = -0{,}10562 \cdot X_3 + 1{,}054844 \cdot X_2 + 0{,}25259 = 0, \\ \dfrac{\partial CH}{\partial X_3} = 3{,}111512 \cdot X_3 - 0{,}10562 \cdot X_2 - 0{,}0606 = 0. \end{cases} \quad (7)$$

$$\begin{cases} \dfrac{\partial ЗШ}{\partial X_2} = 0{,}002521 \cdot X_3 + 0{,}0163 \cdot X_2 + 0{,}01204 = 0, \\ \dfrac{\partial ЗШ}{\partial X_3} = -0{,}0237 \cdot X_3 + 0{,}002521 \cdot X_2 + 0{,}00235 = 0. \end{cases} \quad (8)$$

After solving the system of equations for each of the mathematical models, the coordinates of the response surface centers were determined for both optimization criteria and the value of the objective function in the found center of Y_S.

The angle of rotation of the axes in the center of coordinates of the mathematical model in the canonical form was determined by the formula:

$$artg2\alpha = \frac{B_{23}}{B_{22} - B_{33}}. \quad (9)$$

The calculated coordinates of the centers of the response surfaces:

for the degree of cold hardening X_2 = - 1,1896, X_3 = - 0,0209164, α = 2,93213777 °, Y_S = 18,18768;

for the surface roughness X_2 = - 0,7416, X_3 = 0,02035403, α'= 3,59212185 °, Y_S = 0,16100.

The coefficients of the regression equations in the canonical form were determined from the characteristic equations for each of the optimization criteria:

$$f(\lambda) = \begin{vmatrix} B_{22} - \lambda & B_{23}/2 \\ B_{32}/2 & B_{33} - \lambda \end{vmatrix} = 0, \quad (10)$$

after which the equation was reduced to the form:

$$\lambda^2 - I \cdot \lambda + D = 0. \quad (11)$$

The roots of this equation are the coefficients of the mathematical model in canonical form. After the calculations, the regression equations in canonical form will have the form:

$$CH - 18{,}18768 = 1{,}55846 \cdot X_2^2 + 0{,}524717 \cdot X_3^2, \quad (12)$$

$$SR - 0{,}16100 = 0{,}00823 \cdot X_2^2 - 0{,}011929 \cdot X_3^2. \quad (13)$$

The results obtained by combining the factors X2 and X3 are shown in Fig. 2. If we consider the constructed graphs, we can conclude that the zone of optimal alignment of factors is limited by the curves of *CH* and *SR* at the points A, B, C, D and E, F, G, H. In this case, the surface roughness in both zones is within 0,15 *mcm* < *SR* < 0,16 *mcm*, the degree of work hardening 20,5 *%* < *CH* < 21 *%*.

With these indicators of optimization criteria, the radius of the roller profile is limited to 4,62…4,89 *mm*, and also the initial surface roughness has two diapasons 0,23…0,28 *mm* and 0,33…0,38 *mm*.

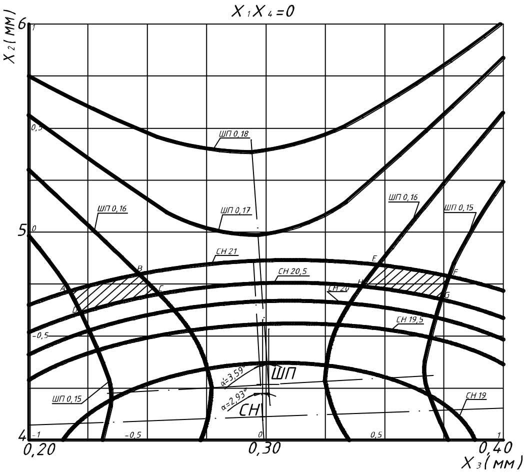

Fig. 2. The two-dimensional surfaces at the intersection of the response factors combining with X_2 and X_3 if $X_1 = 0$ and $X_4 = 0$

Successively changing the combination of factors, two-dimensional intersections of response surfaces are obtained with all possible combinations of factors.

So, when combining the factors of the rolling effort

(X_1) and the radius of the roller profile (X_2) at X_3=0 (the initial surface roughness equals 0,30*мм*) и X_4 = 0 (the roller feed equals 0,07 *мм/об*) regression equations were obtained in the form:

$$CH = 18{,}93207 - 2{,}99185X_1 + 1{,}252594X_2 + ; \quad (14)$$
$$+ 0{,}558542X_{12} + 0{,}474089X_1^2 + 0{,}527422X_2^2$$
$$ШП = 0{,}165438 - 0{,}01254X_1 + 0{,}012037X_2 + . \quad (15)$$
$$+ 0{,}001188X_{12} + 0{,}00865X_1^2 + 0{,}00815X_2^2$$

The coordinates of the centers of the response surfaces are calculated:

For wear of a bronze sample X_1 = 5,6023, X_2 = – 4,1539, α = – 42,2728°, Y_S = 7,9499.

For the surface roughness X_1 = 0,7795, X_2= – 0,7953, α' = 33,5875°, Y_S = 0,15576.

Fig. 3 shows the graph constructed for equations (14) and (15).

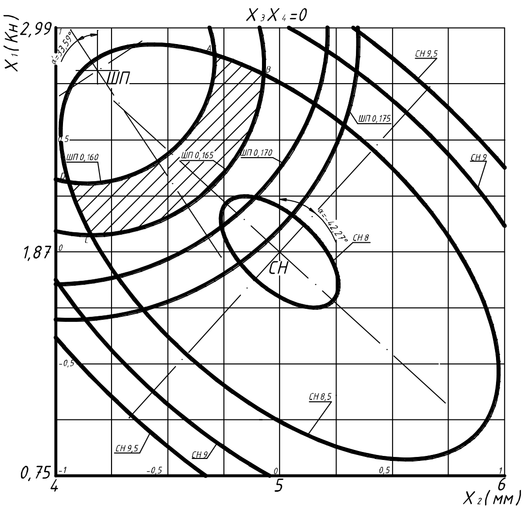

Fig. 3. The two-dimensional response surface section when combining factors when X_1 and X_2 if X_3=0 and X_4 = 0

If we consider the constructed graphs, we can conclude that the zone of the optimal combination of factors is limited by the curves *CH* и *SR* at the points A, B, C, D. In these conditions the surface roughness is within 0,16 *mm* <*SR* <0,165 *mm*, the degree of work hardening makes 8,5%.

With these indicators of optimization criteria, the rolling efforts are within 2...2,4 *кН*, and the profile radius of the roller is 4,1...4,8 *mm*. At combining the factors, the initial surface roughness (X_3) and roller feed (X_4) at X_1 = 0 (rolling effort equals 1,87 *кН*) and X_2 = 0 (the radius of the roller profile equals 5 *mm*.) The regression equations were obtained:

$$CH = 18{,}93207 - 0{,}06056X_3 - 0{,}04519X_4 - , \quad (16)$$
$$- 0{,}17104X_{34} + 1{,}555756X_3^2 - 1{,}07924X_4^2$$
$$ШП = 0{,}165438 + 0{,}002352X_3 - 0{,}00019X_4 - . \quad (17)$$
$$- 0{,}00027X_{34} - 0{,}01185X_3^2 - 0{,}01652X_4^2$$

The coordinates of the centers of the response surfaces were calculated:

For the degree of work hardening X_3 = 0,02, X_4 = -0,022, α = 1,86 °, Y_S = 18,93;

For the surface roughness X_3 = 0,099, X_4 = -0,0065, α'= 1,65 °, Y_S = 0,17.

Fig. 4 shows the graph constructed for equations (16) and (17).

If we consider the constructed graphs, we can conclude that the zone of the optimal combination of factors is limited by the curves *CH* and *SR* at the points A, B, C, D. In these conditions the surface roughness is within 0,14 *mm* <*SR*<0,13 *mm*, the degree of work hardening makes is within 21% <*SR* <20%.

With these indicators of optimization criteria, the initial surface roughness is within 0,37...0,40 mm, and the roller feed is 0,053...0,059 *mm/rot*.

When combining the forces of the rolling efforts (X_1) and the roller feed (X_4) at X_2 = 0 (the radius of the roller profile equals 5 *mm*.) и X_3 = 0 (initial surface roughness is 0,30 *mm*.).

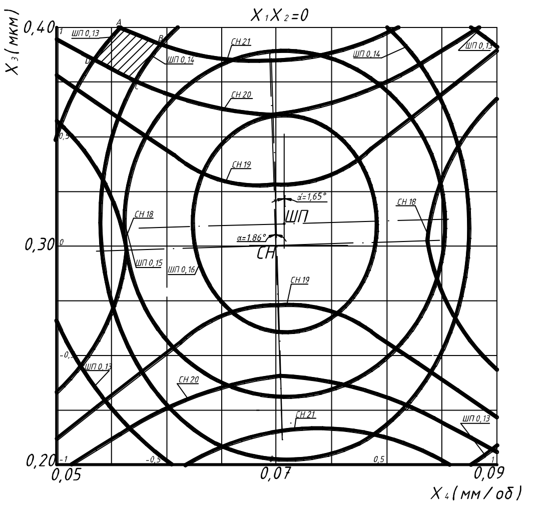

Fig. 4 Two-dimensional response surfaces crossing the combination X_3 and X_4 factors in the X_1 = 0 and X_2 = 0

The regression equations were obtained:

$$CH = 18{,}93207 - 2{,}99185X_1 - 0{,}04519X_4 + 0{,}114792X_{14} + 0{,}474089X_1^2 - 1{,}07924X_4^2; \quad (18)$$

$$ШП = 0{,}165438 - 0{,}01254X_1 - 0{,}00019X_4 + 0{,}001646X_{14} + 0{,}00865X_1^2 - 0{,}01652X_4^2. \quad (19)$$

The coordinates of the centers of the response surfaces were calculated:

For the degree of work hardening X_1 = 3,14, X_4 = 0,15, α = 2,11°, Y_S = 14,23;

For the surface roughness X_1 = 0,72, X_4 = 0,030, α'= 1,87 °, Y_S = 0,16.

Fig. 5 shows the graph constructed for equations (18) and (19).

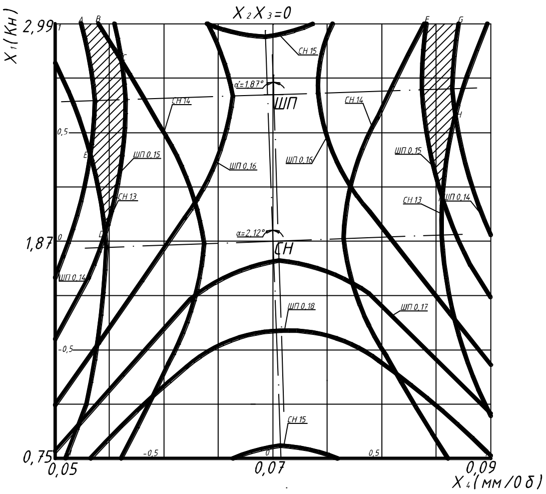

Fig. 5 Two-dimensional response surface section with a combination of factors X_1 and X_4 if X_2 = 0 and X_3= 0

When combining the factors of the rolling effort (X_2) anf the roller feed (X_4) at X_1 = 0 (the rolling effort equals1,87 *кН*) and X_3 = 0 (initial surface roughness equals 0,30 *mm*.) The regression equations were obtained in such forms:

$$CH = 18{,}93207 + 1{,}252594X_2 - 0{,}04519X_4 + 0{,}135625X_{24} + 0{,}527422X_2^2 - 1{,}07924X_4^2, \quad (19)$$

$$ШП = 0{,}165438 + 0{,}012037X_2 - 0{,}00019X_4 + 0{,}000354X_{24} + 0{,}00815X_2^2 - 0{,}01652X_4^2. \quad (20)$$

The coordinates of the centers of the response surfaces were calculated:

For the degree of work hardening X_2 = -1,18, X_4 = - 0,095, α=2,41°, Y_S = 18,20;

For the surface roughness X_2 = - 0,74, X_4 = - 0,0085, α'= 0,41°, Y_S = 0,16.

Fig. 6 shows the graph constructed for equations (19) and (20).

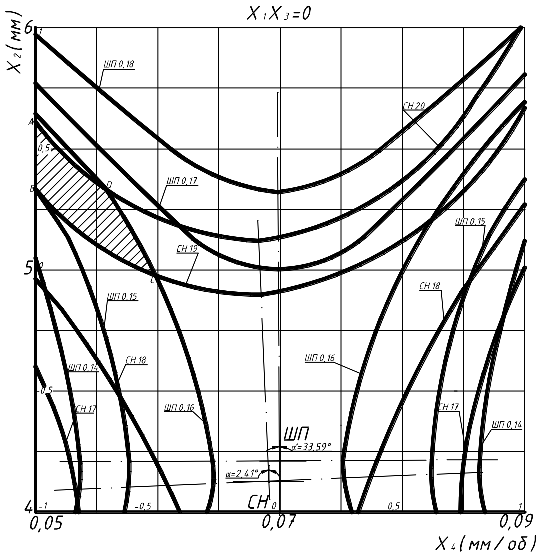

Fig. 6 Two-dimensional cross-section of response surfaces with a combination of factors X_2 and X_4 at the X_1= 0 and *X3* = 0

If we consider the constructed graphs, we can conclude that the zone of optimal alignment of factors is limited by curves *CH* and *RS* at the points A, B, C, D. In these conditions the surface roughness is within 0,16 *mm*, and the degree of work hardening makes is within 19% < *CH* <20%.

With these parameters of optimization criteria, the radius of the profile of the roller fluctuates within 5,3...5,5 *mm*, and the roller feed will be equal 0,05...0,061 *mm/rot*.

When combining the factors of the rolling efforts (X_1) and initial surface roughness (X_3) at X_2 = 0 (the radius of the roller profile equals 5 *мм*.) and X_4 = 0 (the roller feed equals 0,07 *mm/rot*.) The regression equations were obtained in such forms:

$$CH = 18{,}93207 - 2{,}99185X_1 - 0{,}06056X_3 - 0{,}06812X_{13} + 0{,}474089X_1^2 + 1{,}555756X_3^2, \quad (21)$$

$$ШП = 0{,}165438 - 0{,}01254X_1 + 0{,}002352X_3 + 0{,}002646X_{13} + 0{,}00865X_1^2 - 0{,}01185X_3^2. \quad (22)$$

The coordinates of the centers of the response surfaces were calculated:

For the degree of work hardening X_1 = 3,16, X_3 = 0,089, α=1,80°, Y_S = 14,20;

For the surface roughness X_1 = 0,70, X_3=0,18, α'= 3,68°, Y_S = 0,16.

Fig. 6 shows the graph constructed for equations (21) and (22).

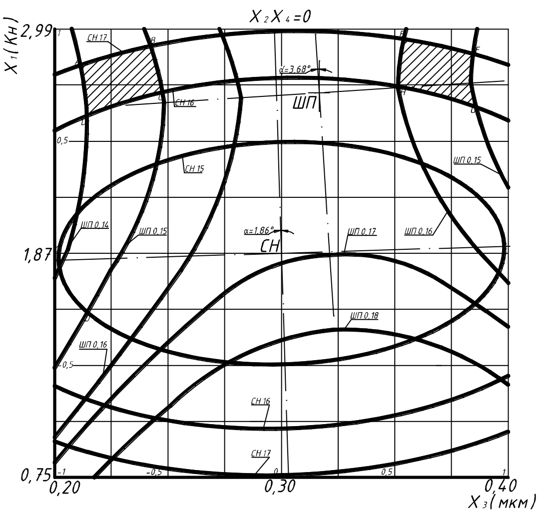

Fig. 7 Two-dimensional cross-section of response surfaces with a combination of factors X_1 and X_3 with X_2 = 0 and X_4 = 0

If we consider the constructed graphs, we can conclude that the zone of optimal alignment of factors is limited by curves CH and RS at the points A, B, C, D and E, F, G, H. In these conditions the surface roughness is within 0,15*mm*<*SR*<0,14*mm*, and the degree of work hardening makes is within 17%<*SR*<16%.

With these indicators of the optimization criteria, the rolling effort fluctuates within 2,6...2,89 *кH*, and the initial roughness is 0,21...0,24 *mm* и 0,35...0,38 *mm*.

CONCLUSION

With the help of experiment planning during the optimization of the technological process of rolling of the bodies of rotation with rolls with stabilization of the rolling efforts, the following optimum processing regimes were obtained: The optimal rolling effort at a clean mode is 0,75 *кH*, at a hardening mode is 3 *кH*, the radius of the roller profile is 6 *mm*, the roller feed is 0,07 *rot/min,* the initial surface roughness is 0,18...0,15 *mm*.

REFERENCES

1. **Braslavskiy V.M. 1975.** Tehnologiya obkatki krupnyih detaley rolikami 2-e izd. M.: Mashinostroenie, 160.
2. **Butakov B.I. 1984.** Usovershenstvovanie protsessa chistovogo obkatyivaniya detaley rolikami. Vestnik mashinostroeniya. № 7. 50 – 53.
3. **Babey Yu.I., Butakov B.I., Syisoev V.G. 1995.** Poverhnostnoe uprochnenie metallov. K.: Naukova dumka, 256.
4. **Azarevich G.M., Bershteyn G.Sh. 1963.** Chistovaya obrabotka tsilindricheskih poverhnostey plasticheskim deformirovaniem. M.: ONTI NII Traktorselhozmasha, 43.
5. **Braslavskiy V.M., Topyichkanov V.V. 1989.** Obkatka detaley rolikami kak sredstvo povyisheniya iznosostoykosti. Pr-vo krupnyih mashin, NIIT-YaZhMASh Uralmashztszoda Vyip. XIX. 136-144.
6. **Braslavskiy V.M. 1975.** Tehnologiya obkatki krupnyih detaley rolikami. M.: Mashinostroenie, 160.
7. **Braslavskiy V.M., Butakov B.I., Shilkov Yu.Ya. 1985.** Povyishenie iznosostoykosti vintovyih par obkatyivaniem rolikami Tehnologiya, organizatsiya i mehanizatsiya mehanosborochnogo proizvodstva. M.: NIIformTYaZhMASh. 15-17.
8. **Butakov B.I. 1984.** Usovershenstvovanie protsessa chistovogo obkatyivaniya detaleyrolikami Vestn. mashinostroeniya. № 7. 50-53.
9. **Ivanov V.V. 1980.** Iznosostoykost stalnyih detaley, uprochnennyih obkatkoy rolikom. Tr. TsNIITMASha, kn. 2.M. 67-75.
10. **Kascheev V.N. 1985.** Predvaritelnyiy naklep i abrazivnoe razrushenie metallicheskoy poverhnosti. Selhozmashina. № 1. 20 - 26.
11. **Kragelskiy I.V., Dobyichin M.N., Kombalov V.S. 1985.** Osnovyi raschetov na trenie i iznos. M.: Mashinostroenie, 526.
12. **Kudryavtsev I.V., Grudskaya R.E. 1984.** Novyie sposobyi poverhnostnogo plasticheskogo deformirovaniya. Mashinostroitel, № 7. 28-29.
13. **Markov A.I. 1980.** Ultrazvukovaya obrabotka materialov. M.: Mashinostroenie, 238.
14. **Fridman Ya.B. 1987.** Mehanicheskie svoystva metallov. M.: Oborongiz, 556.
15. **Odintsov L. G. 1981.** Finishnaya obrabotka detaley almaznyim vyiglazhivaniem i vibrovyiglazhivaniem. M.: Mashinostroenie, 160.
16. **Papshev D.D. 1983.** Otdelochno-uprochnyayuschaya obrabotka poverhnostnyim plasticheskim deformirovaniem. M.: Mashinostroenie, 152.
17. **Ryizhov E.V., Suslov A.G., Fedorov V.P. 1979.** Tehnologicheskoe obespechenie ekspluatatsionnyih svoystv detaley mashin. M.: Mashinostroenie, 176.
18. **Stepnov M.N. 1980.** Statisticheskaya obrabotka rezultatov mehanicheskih ispyitaniy. M.: Mashinostroenie, 232.
19. **Hruschov M.M., Babichev M.A. 1984.** Eksperimentalnyie osnovyi teorii abrazivnogo iznashivaniya Vesti, mashinostroeniya. № 6. 56 - 62.
20. **Shkolnik L.M., Shahov V.I. 1964.** Tehnologiya i prisposobleniya dlya uprochneniya i otdelki detaley nakatyivaniem. M.: Mashinostroenie, 184.
21. **Popov A. 2010.** Novaya teoriya kontaktnoy prochnosti uprugo szhatyih tel / Motrol, Motoryzacja I energetyka rolnictwa. Lublin. Tom12A. 223-232.
22. **Holoptsev A. W. 2011.** Osobennosti primeneniya mnozhestvenno-regresionnyih modeley dinamiki aktivnosti Sr-90 v tashlyikskom vodohranilischnom vodoeme Yuzhnoukrainskoy AES pri ee prognozirovanii / Zhebet L.S. // Motrol, Motoryzacja I energetyka rolnictwa. Lublin. Tom13. 137-149.
23. **Popov A. 2015**. Analiz harakteristik kontakta poverhnostey s pervonachalnyim lineynyim i tochechnyim kasaniem / Motrol, Motoryzacja I energetyka rolnictwa. Lublin. VOL 17. No.2. 9-16.
24. **Aulin V. 2015.** issledovanie izmeneniya moschnosti dizelya avtomobiley, rabotayuschih v nestatsionarnyih usloviyah / Motrol, Motoryzacja I energetyka rolnictwa. Lublin. VOL 17,. No.2. 103-108.

25. **Butakov B. 2013** Volnistost poverhnosti pri obkatyivanii tel vrascheniya rolikami / Motrol, Motoryzacja I energetyka rolnictwa. Lublin. – Vol 15, No2. 15-22.
26. **Butakov B. 2012** Issledovaniya tochnosti valov obkatannyih ustroystvom so stabilizatsiey rabochego usiliya obkatyivaniya / Motrol, Motoryzacja I energetyka rolnictwa. Lublin. – Tom14A. 15-22.
27. **Butakov B.I., Artyuh V. A. 2013** Opredelenie optimalnogo usiliya obkatyivaniya valov rolikami. Sankt – Peterburg, Ch. 2. 58-64.
28. **Pastushenko S. I., Gorbenko O. A., Ogiyenko M.M.** Prognozuvannya ta vy`probuvannya texniky` i texnologij dlya sil`s`kogospodars`kogo vy`robny`cztva : zb. nauk. pracz` UkrNDI. – Doslidny`cz`ke, 2008. – Vy`p. 11 (25). 349-356.

MOTROL. Commission of Motorization and Energetics in Agriculture – 2017. Vol.19. No.2. 41-45

FEATURES OF MATHEMATICAL MODELING OF MECHANIZED OPERATIONS FOR CORN HARVESTING

Dmytro Kuzenko, Oleg Krupych, Jaroslav Semen
Lviv National Agrarian University
V. Velykogo Str. 1, Dubliany, Ukraine. E-mail: kuzenko-dv@meta.ua

Summary. The article deals with the basics of mathematical modelling of separate technological operations of corn-for-grain harvesting process, which is one of the most complex and energy intensive technological processes. This process involves a significant number of individual operations: cutting and pulling stems, cobs separation, husks peeling, collecting and grinding stems and husks, loading cobs and crushed mass on vehicles.

It is also noted that mentioned technological operations are characterized by complexity and inhomogeneity, there are no linear specifically identified connections that could link these technological operations. Therefore, when studying such processes in order to improve them, it is necessary to have a transition from empirical engineering methods to analytical computer based methods with wide use of mathematical support. Application of mathematical modelling and optimization of technological parameters and operating modes are particularly effective. The attention is drawn to the expediency of using a new method of cobs separation, which is based on the creation of a multi-factor effect on the system "stem-peduncle-cob".

Based on this it is offered a method for modelling dynamic features of cobs as complex bodies that have one axis of symmetry and a very wide range of shape variations, on the basis of the approximation method.

It is offered a mathematical model for the process of cobs re-orientation in the working area of cob-separating machine in order to provide conditions of multi-factorial cobs separation. Special attention is paid to the choice of rational kinematic parameters of the device that prevent unilateral separation of cobs.

The conditions of effective use of vibrational forces on cobs are considered. Motion regularities of the mathematical pendulum are used as the main model for cobs movement in the working area under the action of vibrational forces. For the theoretical substantiation of the husks destruction under vibrational forces the model of the physical pendulum is the most appropriate. Here the cob is featured as a combination of two bodies with corresponding elastic properties and inertial characteristics.

Ensuring the process of husks loosening while separating cobs opens new possibilities for radical change in design and quality improvement of work of the cob-separating machines. Based on this, a new design scheme of cob-separating machine is proposed. Its technological process is based on the interaction of a cob with a peeling roll and an anti-cutting plate, which creates the cutting force directed tangentially to the core of the cob. Mathematical model of the process of its operation is obtained.

It is made conclusions on the expediency of using mathematical modelling in designing cob-separating machines for solving a specific technological problem.

Key words: cob-separating mechanism, cob husk, vibrational force, husk destruction, differential equation, moment of cob inertia, mathematical modelling.

INTRODUCTION

Corn harvesting is an intensive process, which requires an expenditure of much labour and energy in a limited by agrotechnical requirements period. This technological process is also characterized by complication and heterogeneity of technological operations, which it consists of, - by absence of linear separately determined connection which would link these technological operations. Therefore a search of new technical means for corn harvesting and a modernization of separate working organs of already existing harvesting aggregates is the issue of the day of modern agricultural production.

Therefore, when studying such processes in order to improve them, it is necessary to have a transition from empirical engineering methods to analytical computer based methods with wide use of mathematical support. Application of mathematical modelling and optimization of technological parameters and operating modes are particularly effective in this case.

ANALYSIS OF RECENT RESEARCHES AND PUBLICATIONS

Mathematical models of processes of working bodies interaction with processed material are widely used to predict the development and to design new machines of various technological application, including agricultural production. The scientific basis for the modelling of agricultural machinery processes was developed by well-known scientist in the field of agricultural mechanics, P. Vasylenko [1].

A number of scientists have devoted their research to the development of mathematical models of movement and operation of machines in unpredictable conditions of agricultural production [1-9]. At present, most fully theoretically developed and experimentally studied are the models of movement of self-propelled harvesting machines [2-4], provision of variable norms for application of fertilizers and technological materials [5], separation of grain mixtures [7-8].

D. Voytyuk has generalized experience in his work [6] and has grounded perspectives for the further use of modelling methods in researches of processes of agricultural machines.

However, it should be noted that it is given not enough attention to the question of modelling the technological processes of corn harvesters. It is given some elements of the modelling of process of corn-separating machines of the old type in the paper [9-12], which today are not used as morally outdated and low-efficient.

These issues are more fully elaborated in papers [13-17], but there is a need for a generalization of the tasks that are solved while researching corn harvesters by means of modelling.

OBJECTIVES

The aim of the paper is to analyse the modern tasks that are solved during research of corn harvesters by means of modelling, as well as to determine the prospects for further application of this method in order to increase the effectiveness of technical support for corn harvesting.

THE MAIN RESULTS OF THE RESEARCH

When choosing areas of research of the process of cob-separation during mechanized corn for grain harvesting, which we have been carrying out for the last 10 - 15 years, the preference was given to mathematical modelling rather than physical. This is explained by the fact that the physical models of cob separators are labour-intensive in manufacturing, complicated in organizing and conducting experiments, limited in capabilities, because they do not allow to vary the parameters in a wide range during research. Studies of physical models are also limited in time due to the seasonal nature of agricultural production.

Instead, when replacing real objects with idealized mathematical models, it is much easier to find rational values of variable engineering parameters, although mathematical modelling was preceded by the research of this process on physical models (experimental installations). This made it possible to study the characteristics of the behaviour of the complex system "stem-cob-working body" at different stages of the interaction of corn plants with the working elements of cob separating machines (i.e. in the context of separate stages of the process of cobs separation).

The conducted researches have given an opportunity to propose a new method of cobs separation [20], which is based on the creation of a multi-factor effect on the system of "stem-peduncle-cob". Depending on wide ranged physical and mechanical properties of corn plant elements, the proposed method provides a flexible technological process for different types of forces (stretching, bending, cutting, vibrational motion, torsion), effecting the destruction of the peduncle.

Given the above, particular attention should be paid to research of physical and mechanical properties of corn plants, which have not been studied until now. In particular, generally accepted indicators of the physical properties of corn plants - the size-mass characteristics and the forces of the destruction of certain elements, which are widely researched and listed in the reference literature, - do not allow to fully solve the tasks of efficient separation of cobs that are moving unpredictably in space until they are reoriented to the working area, and that acquire oscillatory movements under vibration.

Therefore, it is needed to identify properties that characterize the specific behaviour of stems and cobs under external influences that occur during this technological process. The most important is the study of the dynamic characteristics of corncobs (complicated bodies that have one symmetry axis and a very wide range of form variations) we use the method of approximation [14]. Thus component elements, to which a corncob (complicated body of rotation) is divided, depending on their configurations and necessary exactness we approximate by bodies of simple geometric shapes:

- cylinder elements of identical height, taken with a larger radius;
- cylinder elements of identical height, taken with a middle radius;
- truncated cones and finite cone of identical height.

By the first method of approximation, when a corncob is divided by planes, that are perpendicular to the symmetry axis, into simple geometrical bodies of rotation with the identical height h_i. Each element we present as a solid cylinder (fig. 1, a), the radius of it R_i is equal to the radius of larger basis of element. In this case we get a bit overrated results, but comparing experimentally got data to the analytical calculations the rejection is less than 4,0%, i.e. this method can be used for determination of inertia characteristics of corncobs.

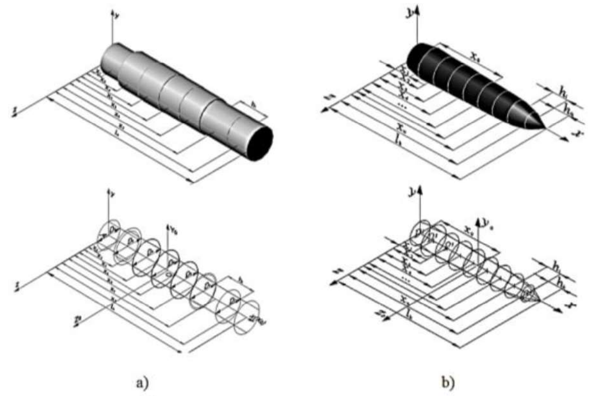

Fig. 1. Approximation of a corncob by elementary bodies of simple geometric shape: a – cilindric; b – conical

In order to get more exact results it is more reasonable to use the 3rd method of approximation, by which a corncob is approximated by the truncated cones (fig. 1, b).

On the basis of «Microsoft Excel» a program, with the help of which main inertia characteristics of corncobs are determined, was created: volumes of *i*–section (cylinder) and the whole corncob (V_i, V); a centre of gravity of *i*–section in relation to the fixing point (A) of a corncob (x_{0i}); static moments of *i*–section and the whole body in relation to the plane of *YAZ* (S_{xi}, S_x); moments of inertia of *i*-element by the body volume in relation to the major central planes Z_0OX_0 and X_0OY_0 and the main central axes and the points of their intersection. With this the moment of volume inertia is defined as follows:

- in relation to major central planes Z_0OX_0 and X_0OY_0:

$$I^V_{Z_0OX_0} = I^V_{X_0OY_0} = \sum_{i=1}^{n} I^V_{(Z_0OX_0)_i} = \sum_{i=1}^{n} I^V_{(X_0OY_0)_i} = \sum_{i=1}^{n} \frac{1}{4} \cdot R_i^2 \cdot V_i; \quad (1)$$

– relative to X_0X_0 (taking into account, that the axis X_0X_0 is simultaneously a symmetry axis):

$$I^V_{X_0X_0} = \sum_{i=1}^{n} I^V_{(Z_0OX_0)_i} + I^V_{(X_0OY_0)_i} = 2\sum_{i=1}^{n} I^V_{(Z_0OX_0)_i} = \frac{1}{2} \cdot \sum_{i=1}^{n} \cdot R_i^2 \cdot V_i; \quad (2)$$

– relative to Y_0Y_0 (besides $I^V_{Y_0Y_0} = I^V_{Z_0Z_0}$):

$$I^V_{Y_0Y_0} = I^V_{Z_0Z_0} = \frac{1}{12} \cdot \sum_{i=1}^{n} V_i \cdot h_i + \sum_{i=1}^{n} \left[V_i \cdot x_{0_i}^2 + \frac{1}{4} \cdot R_i^2 \cdot V_i \right] - V \cdot \frac{\sum_{i=1}^{n} V_i \cdot x_{Oi}}{\sum_{i=1}^{n} V_i}; \quad (3)$$

– relative to the point A (centre-of-mass):

$$I^V_A = \frac{1}{12} \cdot \sum_{i=1}^{n} V_i \cdot h_i + \sum_{i=1}^{n} \left[V_i \cdot x_{0_i}^2 + \frac{1}{2} \cdot R_i^2 \cdot V_i \right] - V \cdot \frac{\sum_{i=1}^{n} V_i \cdot x_{Oi}}{\sum_{i=1}^{n} V_i}. \quad (4)$$

According to [15, 20], the most important condition for ensuring the process of multifactorial cob separation is the mandatory reorientation of them in the working area of cob separator (fig. 2) and the full incline to the stripper plate 2 in order to stabilize the separation angle [15, 20]. However, in the process of stem stretching, cob tearing is possible as a result of their excessive swinging in space and when encountered with a horizontal stripper plate. It is called a one-sided separation, that is the source of excessive loss of cobs as a result of their "shooting".

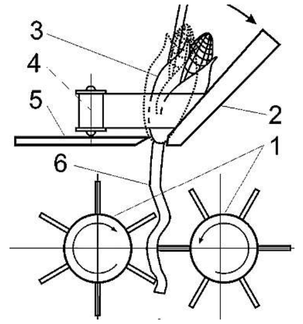

Fig. 2. Scheme of the device: 1 – stretching rollers; 2 – inclined stripper plate; 3 – cob; 4 – transporter; 5 – horizontal plate; 6 – stem

As the main model in research of the conditions for the emergence of a one-sided separation of cobs, a whipping of a flexible thread was taken. The obtained mathematical model in the form of nonlinear differential equation of the second order in relation to the angle of rotation of the cob φ (1) fully describes the speed parameters of the process of cob movement in the working area:

$$\ddot{\varphi} = \frac{A(\varphi, \dot{\varphi})}{B(\varphi, \dot{\varphi})}. \quad (5)$$

In equation (5) the following abbreviations are taken:

$$\begin{cases} A(\varphi,\dot{\varphi}) = h \cdot \sin\varphi \; m \cdot h \cdot \dot{\varphi}^2 \cdot \sin\varphi - mg - m \cdot h \cdot \dot{\varphi}^2 \cdot \sin\varphi \cdot C + \\ \qquad + m \cdot h \cdot \dot{\varphi}^2 \cdot \sin\varphi \cdot D, \\ B(\varphi,\dot{\varphi}) = I_c + m \cdot h^2 \cdot \sin^2\varphi + m \cdot h^2 \cdot \sin\varphi \cdot \cos\varphi \cdot C - m \cdot h \cdot \cos\varphi \cdot D. \end{cases} \quad (6)$$

where: φ - an angle of cob rotation; f - the coefficient of cob friction on the working surface of the stripper plates; m – cob weight; h – parameter of the working area of the cob separator.

Parameters C and D are being found as follows:

$$C = \frac{\cos\psi + f \cdot \sin\psi}{\sin\psi - f \cdot \cos\psi}; \quad D = \frac{\frac{-V \cdot \cos\psi}{\dot{\psi}} + f \cdot h}{\sin\psi - f \cdot \cos\psi}. \quad (7)$$

During solving the equation (5) by the numerical Runge-Kutta method one can find an angle acceleration $\xi(t) = \ddot{\varphi}(t)$, angular velocity $\omega(t) = \dot{\varphi}(t)$ and an angle of rotation $\dot{\varphi}(t)$. Further, the value of the marginal velocity of the stretching V is determined, depending on the inertial forces that arise at the same time, under the action of which occurs a one-sided cob separation.

As the main model of movement of a cob in the working area under vibrational forces, the laws of the motion of the mathematical pendulum are taken (Fig. 3). In contrast to the mathematical pendulum, which has a free hinge, a stubble has a certain rigidity, meaning it possesses not a free and elastic hinge (at the point of clamping in rollers) with constant angular rigidity C, and in the balanced position is inclined from the vertical at a certain angle [18, 19]. The mathematical equation describing this model is as follows:

$$\psi = \psi_0 \cos\omega_0 t + \frac{\dot{\psi}_0}{\omega_0} \sin\omega_0 t - \frac{F_a}{J(\omega_0^2 - \omega^2)}(\cos\omega t - \sin\omega t). \quad (8)$$

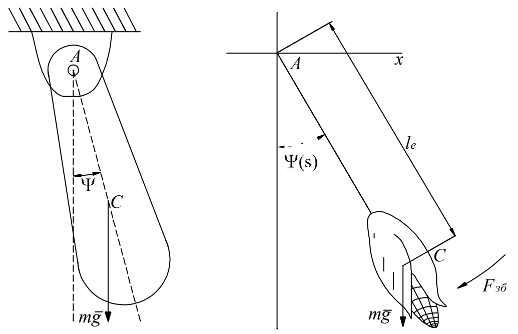

Fig.3. The oscillatory system

In the result of the theoretical researches, and with the help of PC, an oscillogram of the trajectory of the cob movement was constructed, which gives the opportunity to select the optimal parameters of the mode of operation of the vibration mechanism.

Exposing the nature of the influence of vibration on the system of stem-cob-husk (SCH), it should be noted that there are two types of motion occurring in this system:

– a general motion of the whole system as a body; (thus, in direct interaction with a vibrational stimulator, the SCH system can be detached from the working part and move as a body;

– a relative movement of the components of the system (subsystems: cob-stem (CS), corb-husk (CH)), which makes it possible for the system to acquire new physical and mechanical properties - to change the forces of friction and adhesion between the components of the system, and therefore the shape, volume and their location.

On this basis, we can conclude that in this technological process, the vibrational action performs the following functions:

- as an additional factor that intensifies the process of separation by active force as a result of reducing the frictional forces and adhesion between the components of the system of CS, the destruction of the system′s shape, and among the vibrational motions of the system only relative motion is considered (the process of husk loosening in the CH system);

- as the primer factor that solves the main technical task, in this case, both types of vibrational motions play a major role (the destruction of the connections between stem and cob and between cob and husk).

For the theoretical substantiation of the husk destruction under vibrational force on a cob, the most appropriate is the model of the physical pendulum [7,10], in which a cob is modelled as a set of two bodies with corresponding elastic properties and inertial characteristics. In particular, a husk can be represented as a cylindrical shell with weight m_1, with a stem as a cylinder with weight m_2. Both the husk and the stem have one fixed end (elastic hinge) at the place of attachment of the cob to the peduncle. These elastic hinges have corresponding stiffness C_1 and C_2. It is a significant difference in the weights of components (husks and stems) of this vibrational system, as well as various values of the stiffness of elastic hinges, that explain the nature of the forces of husks destruction.

Taking into account that we are studying the dynamics of the cob, which is securely fixed in the cob separator, is considered, the model of the "husk-stem" oscillation system has one degree of freedom corresponding to the angular deviation of the axis cob. In this case, the full period of oscillation must be divided into two phases, which are fundamentally different from each other: the first phase is the period of forced oscillations under the action of the perturbing force of the vibrator, and the second is the period of free slowing oscillations of the cob. It is obvious that the process of destruction of husks will occur during the second phase, when there is no action of perturbing force.

The free movement of the cob depends primarily on the properties of the elements of the oscillatory system, in particular, the weight m, the distance between the centre of gravity of the cob to the fastening point - l, the moment of inertia of the cob - I, stiffness of the fastening point (elastic hinge) – C:

$$\upsilon_{max} = \sqrt{\left(\frac{C}{2 \cdot m \cdot g \cdot l}\right)^2 + \frac{S^2 \cdot b^2}{m \cdot g \cdot l^3 \cdot I}} - \frac{C}{2 \cdot m \cdot g \cdot l}. \qquad (9)$$

where: S – value of shock pulse; b – the distance between the point of application of the pulse to the point of clamping of the peduncle.

In the equation (6) the value $\frac{C}{2 \cdot m \cdot g \cdot l}$ - shows the impact on free motion of stiffness the oscillatory system, and the value $\frac{S^2 \cdot b^2}{m \cdot g \cdot l^3 \cdot I}$ - the impact of the inertial properties.

When studying the components of the equation (1), in particular, the values of S, b, l for the husk and the stem can be considered as equal. And when substituting values C_1, m_1, I_1 i C_2, m_2, I_2, we can determine possible virtual moves φ_1 assuming that the husk performs oscillation without the stem of the cob, and φ_2 assuming that the stem performs oscillations without the husk. Obviously, the difference between the values of possible virtual movements will represent the way of husk destruction.

Ensuring the process of husks loosening during separation, opens new possibilities for radical change of design and improvement of the quality of work of corn husker machines. Fig. 4 shows the scheme of a corn husker machine, the basis of the technological process of which is interaction of the cob with a cleaning roller and a knife, which creates a cutting force directed at the tangent to the core of the cob [11]. Thus, it differs significantly from the technological process of the corn huskers with two rollers. In addition, such a design allows to combine the operation of cobs separation with their husking in a single structural and technological unit, which greatly simplifies the design and reduces the energy intensity of a corn harvester.

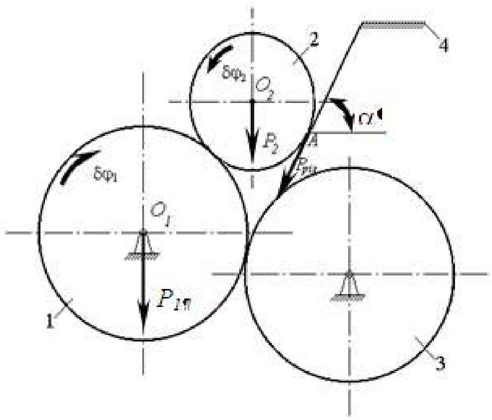

Fig. 4. The scheme of the corn husker machine: 1 – cleansing roller; 2 – cob; 3 – helping roller; 4 – counter-plate

For simulation of the process we consider the cleansing roller and a cob as solid round cylinders. At some point, the system "roller-cob-counter-plate" is a system with one degree of freedom, since the position of the main roller 1 determines the position of all material points of the system. Therefore, the angle of rotation φ_1 of the cleaning roller is chosen as a generalized coordinate. A mathematical model can be represented by the differential equation (7) of the cob moving under the force of a cleaning roller and a counter-plate. As can be seen from the obtained equation, depending on the ratio of values $P_{\text{різ}} \cdot r_1 \cdot н$ and M_1, it is possible to obtain different modes of cob′s movement:

$$\ddot{u}_2 = 2g \cdot \frac{P_{\text{різ}} \cdot r_1 \cdot н - M_1 \cdot r_1 \cdot н}{\left[P_1 \cdot r_1^2 + P_2 + P_{\text{різ}} \cdot sin б \cdot r_1 \cdot н^2\right] \cdot r_2}, \qquad (10)$$

where: $P_{\text{різ}}$ – cutting force directed at the tangent to the core of the cob; r_1, r_2 – radius of the main roller and the cob, acordingly; M_1 – moment of pair of forces applied at cleansing roller; v – coefficient of the cob slipping on the surface of the roller; P_1, P_2 – weight of the roller and weight of the cob, ccordingly.

The use of the obtained differential equation (7) makes it possible to determine the basic parameters of a cob husker machine under certain initial conditions. In particular, the length of the cleansing rollers is required, provided that the husk is cleared during the turning of the cob at an angle of 2π, determined from the following dependence:

$$l_{min} = V_{mp} \cdot \sqrt{\frac{p \cdot r_2 \left[P_1 \cdot r_1^2 + \ P_2 + P_{pi з} \cdot sin б \ \cdot \ r_1 \cdot н^{\ 2} \right]}{g \cdot r_1 \cdot н \cdot \ P_{pi з} \cdot sin б \cdot r_1 \cdot н - M_1}}. \quad (11)$$

As can be seen from expression (8), the length of the rollers and hence the dimensions of the husker depend primarily on the dimensions of the cob r_2 and the rollers r_1; efforts to destroy the husk $P_{piз}$; power intensity of the cleansing roller M_1.

CONCLUSIONS

1. The developed mathematical models of processes occurring during performance of cob-separating systems of multi-factor action, were repeatedly experimentally tested. It was confirmed not only the qualitative, but also the quantitative conformity of technological parameters that were determined theoretically and experimentally [8, 10, 11].

2. The use of mathematical modelling and obtained mathematical models in the design of cob-separating machines in order to solve a specific technological task is proved to be expedient and can open up new opportunities in improving the design and technological parameters of the working bodies of harvesting machines.

REFERENCES

1. **Vasilenko P.M., Vasilenko V.P. 1980.** The method of construction of calculation models of functioning of technical systems (machines and machine units). – K.: RIO USKHA, 137. (in Russia).
2. **BulgakovV.M. 1980.** The method of constructing a calculation model for the functioning of a self-propelled root harvester. M.: “Doklady VASKHNIL”. 39-41. (in Russia).
3. **Podurayev YU.V., Kuleshov V.S. 2000.** Principles of construction and modern trends in the development of mechanical systems // Mekhatronika. №1. 5–10. (in Russia).
4. **Pankratova N.D. 2001.** System optimization of complex constructive elements of modern technology // Kibernetika i sistemnyy analiz. №3. 119-131. (in Russia).
5. **Adamchuk V.V. 2002.** Justification of the model of making mineral fertilizers // Mekhanizatsiya ta elektryfikatsiya sil's'koho hospodarstva. Vyp. 86. Hlevakha. 90-99. (in Ukrainian).
6. **Voytyuk D.H. 2008.** Prospects for the use of modeling in research of machines and processes of agricultural production // Visnyk L'vivs'koho derzhavnoho ahrarnoho universytetu: Ahroinzhenerni doslidzhennya. №12, T.2. L'viv. 326-332. (in Ukrainian).
7. **Zaika P.M. 1992.** Selected tasks of agricultural mechanics. – K.: Izd-vo USKHA, 507. (in Russia).
8. **Lukianenko V. 2013.** Mathematikal model of motion of interactive seed on sloping vibrating surface and numeral methods of decision of sistems of kivtmatics equalizations. MOTROL. Commission of Motorization and Energetics in Agriculture –Vol.15. No 7. 135-143.
9. **Karpusha P.P., Konopel'tsev N.I. 1972.** Justification of the parameters and operating modes of the comb-separating device of the combing type. Tr. Melitopol'sko-go SKHI, T KHVÍÍ. Voprosy mekhanizatsii sel'skogo khozyaystva. 42 – 55. (in Russia).
10. **Rodionov L.V. 1983.** Substantiation of the basic parameters of the slit element of a dynamically active stripping device. ZH. "Traktory i sel'khozma-shiny", №8. 16-18. (in Russia).
11. **Karpusha P.P., Konopel'tsev M.Í. 1970.** Optimum parameters of the ductwork separators of the forcing type. Vísnik síl's'kogospodars'koї nauki, №6, Kiïv. 48-59. (in Ukrainian).
12. **Karpusha P.P. 1970.** Substantiation of the operating mode of the corn-picking machine of corn-harvesting machines from the cob-strength condition. Sbornik – Tekhnicheskiy progress i perspektivy razvitiya sel's-kogo khozyaystva. "Urozhay", Kiyev. (in Russia).
13. **Kuzenko D.V., Pastushenko S.I. 2003.** Theory of the vibrational method of separating the cobs of maize. MOTROL. Commission of Motorization and energetics in agriculture. Vol.6. 275-284.
14. **Kuzenko D.V., Kucheruk D.V. 2005.** Results of study of inertia characteristics of maize dumplings // Vísnik agrarnoї nauki Prichornomor'ya. Vip.4. - Mikolaïv. 178-187. (in Ukrainian).
15. **Kuzenko D. V. 2008.** Modeling of the process of moving the cocoon for one-sided separation // Visnyk L'vivs'koho derzhavnoho ahrarnoho universytetu: Ahroinzhenerni doslidzhennya. №12, T.1. L'viv. 124-129. (in Ukrainian).
16. **Kuzenko D. V. 2008.** Experimental studies of vibration ducts separating mechanism.. Mizhvidomchyy tematychnyy naukovyy zbirnyk: Mekhanizatsiya ta elektryfikatsiya sil's'koho hospodarstva. Vypusk 92. Hlevakha. 164-171. (in Ukrainian).
17. **Kuzenko D.V., Kuzenko L.M. 2005.** Investigation of the interaction dynamics of the cockpit with the working elements of the cathodic cleaning mechanism // Visnyk Kharkivs'koho DTUS·H. Vyp. 20. – Kharkiv. 168-173. (in Ukrainian).
18. **Bulgakov V., Adamchuk V., Golovach I. 2008.** Investigation of impact on the interaction of a vibration dipping working body with the body of the root. Motrol, - Motoryzacja I energetyka rolnictva. - Lublin. Tom 10. 31 - 44.
19. **Babiy A., Babiy M., Rybak T. 2014.** Mathemftical model of loading of mower cutting apparatus. MOTROL. Commission of Motorization and energetics in agriculture. Vol.16. No.4. 275-284.
20. Patent Ukraïni 69417, MPK A 01 D 65/02. Method for harvesting corn / M. Trostyaniy, D. Kuzenko, O. Bondarenko, V. Timoshchuk. - Zayavl. 14.02.2001; Opubl. 15.09. 2004, Byul.

MOTROL. Commission of Motorization and Energetics in Agriculture – 2017. Vol.19. No.2. 47-51

THEORETICAL BACKGROUNDS OF SCREW LOADERS OPERATION WITH POURING INTO ANOTHER CONTAINER

Andrii Diachun[1], Ihor Hevko[1], Dmytro Shmatko[2], Olena Skyba[1], Liubomyr Slobodian[1] Olexandr Marunych[3]

[1]Ternopil Ivan Pul'uj National Technical University
Tekstulna Str., 28, Ternopil, Ukraine. E-mail: kaf_am@tu.edu.te.ua
[2]Dneprodzerzhinsk State Technical University
Dniprobudivska Str., 2, Dneprodzerzhinsk, Ukraine, E-mail: zombik@gmail.com
[3]National University of Water and Environmetal Engineering
Soborna Str., 11, Rivne, Ukraine, E-mail: zombik@gmail.com

Summary. Based on the equation of motion in a screw conveyor-mixer, the kinematics of bulk material is researched. The motion of bulk material in medium speed operation mode of screw conveyor-mixer is analyzed in details. The technique of determining the nature of loading the screw conveyor elements is developed. The analytical dependences for determining the speed change of the given bulk material volume in relation to a casing in medium speed mode of conveyor while mixing the bulk material are developed. This technique can be widely used for designing the screw transport and technological systems

Theoretical backgrounds of screw loaders performance for unloading bulk materials from the horizontal truss on the vertical one are substantiated. The analytical dependences for determining the value of axial force of feeding bulk materials by means of horizontal branch from an inclination angle of the vertical truss are developed. The graphic dependences of the change of minimum axial force of feeding bulk material from the inclination angle of a conveyor vertical branch are developed as well.

Key words: screw feeders, bulk material, feeding force.

INTRODUCTION

Nowadays screw conveyors are widely used for technological transporting and mixing the bulk materials. These conveyors are characterized by simplicity of their design. They are highly reliable, easy to use and easy to adapt when used in automated systems, and they are ecologically friendly as well [2, 4, 7-8, 12-20]. To cut down power consumption and to increase the quality of mixing the bulk materials, a number of screw mixers' original designs are developed. The use of the working body depends on the peculiarities of bulk material loading the auger as well as on the peculiarities of the nature of bulk material motion, and the practicability of using the auger working body.

ANALYSIS OF RECENT RESEARCHES AND PUBLICATIONS

The advantages of using such augers include the increase of load coefficient in the area of transporting the bulk material from a tanker into auger that leads to the increase of conveyor's productivity.

Analysis of recent research and publications. The works of Grygoryev A.M. [1], Hewko B.M., Rohatynskyi R.M. [3, 10-11], Hewko I.B. [3, 9] and others are dedicated to the issue of transporting and mixing different materials. However, taking into account the diversity of technological processes and structural designs of screw transport and technological mechanisms (STTM), this issue requires further research and refinement of various parameters of theoretical and practical importance.

OBJECTIVES

The objective of this work is to substantiate theoretically the screw loaders performance with two branches of pouring bulk materials.

THE MAIN RESULTS OF THE RESEARCH

A number of original screw conveyor-mixers for cutting down power consumption and minimizing the damage of seeds as well as for increasing the reliability of screw working bodies are designed. To use such conveyors it is necessary to solve issues related to the nature of bulk material motion as well as to the practicability of their use.

To mix the bulk material effectively, the conveyor should work in the medium speed mode. This is the characteristic feature of screw conveyor-mixers Fig. 1. Based on experimental research it is proved that the material in the cross section of conveyor casing is lifted to the upper point and falls on the inner surface of the cylindrical casing under the force of gravity, repeating the cycle by the cycle.

The motion trajectories of the given bulk material volume in the cross section of conveyor casing in the fast- and medium speed modes are compared in Fig. 2.

The angular parameter θ is determined by the nature of bulk material motion during the screw conveyor operation. To determine the nature of bulk material transportation, the motion of the given bulk material volume along the coordinates xyz (Fig. 1.) should be considered.

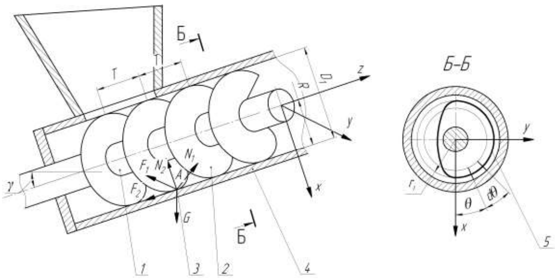

Fig. 1. Computation scheme of transporting the given bulk material volume in the inclined screw conveyor: 1 - drive shaft; 2 – screw working body; 3 – given bulk material volume; 4 – casing; 5 – trajectory of bulk material motion in the medium speed mode (mode of transporting and mixing)

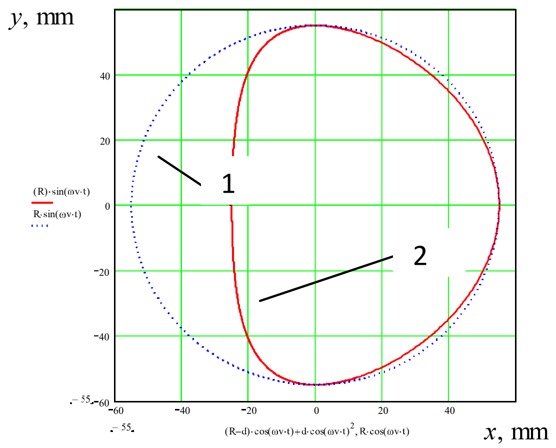

Fig. 2. Motion trajectories of the given bulk material volume in cross section of casing in the fast speed 1 and medium speed 2 modes as compared

When the conveyor operates in the medium speed mode, the bulk material is mixed and transported simultaneously. Taking into account the contact of the given bulk material volume A with the auger's screw surface and the cylindrical surface of the casing, the placement is determined by the radial parameter R and the angular parameter θ.

In parametric form, with sufficient approximation, the coordinates of the given bulk material volume A are determined by the dependences:

$$\begin{aligned} x_A &= (R-d)\cdot\cos\theta + d\cos^2\theta; \\ y_A &= R\cdot\sin\theta; \\ z_A &= \frac{T_0(\omega t-\theta)}{2\pi}, \end{aligned} \tag{1}$$

where: x_A, y_A, z_A, – coordinates of the given bulk material volume, m; R – radial parameter of the given bulk material volume, m; θ – angular parameter of the given bulk material volume, rad; ω – angular speed of working body rotation, rad/s; t – time, s; d – parameter that determines the displacement of motion trajectory of the given bulk material volume in medium speed mode as compared with the fast speed mode, T_0 - step, mm;

Parameter d is the function of angular speed of working body rotation, the inner radius of casing, and the transported material properties. The angular speed of working body rotation increases, the parameter d decreases. The inner radius of casing increases, the parameter d increases as well. In fast speed mode d=0, this parameter can be determined with the use of parametrical dependences based on experimental research.

Motion speeds of the given bulk material volume related to the auger along the axes x, y, z:

$$\begin{cases} \dot{x}_1 = \dot{x}_A - \dot{x}_{1u}; \\ \dot{y}_1 = \dot{y}_A - \dot{y}_{1u}; \\ \dot{z}_1 = \dot{z}_A - \dot{z}_{1u}, \end{cases} \tag{2}$$

where: $\dot{x}_A$, $\dot{y}_A$, $\dot{z}_A$, – projections of motion speed of the given bulk material volume on the axes of coordinates xyz, m/s; $\dot{x}_{1u}$, $\dot{y}_{1u}$, $\dot{z}_{1u}$ – projections of motion speed of the working body on the axes of coordinates xyz, m/s.

As the casing is motionless, the motion speeds of the given bulk material volume related to the casing along the axes x, y, z equal:

$$\begin{cases} \dot{x}_2 = \dot{x}_A; \\ \dot{y}_2 = \dot{y}_A; \\ \dot{z}_2 = \dot{z}_A. \end{cases} \tag{3}$$

The projections of motion speed of the given bulk material volume are defined by differentiating the equation (1) for the general case, when $R \neq const$:

$$\begin{cases} \dot{x}_A = \dfrac{d(R-d)}{dt}\cos\theta - (R-d)\cdot\sin\theta\cdot\dfrac{d\theta}{dt} + \dfrac{d(d)}{dt}\cos^2\theta - 2d\cos\theta\sin\theta\dfrac{d\theta}{dt}; \\ \dot{y}_A = \dfrac{dR}{dt}\sin\theta + R\cdot\cos\theta\cdot\dfrac{d\theta}{dt}; \\ \dot{z}_A = \dfrac{T}{2\pi}\left(\omega - \dfrac{d\theta}{dt}\right). \end{cases} \tag{4}$$

Motion speed of screw working body is determined by dependences:

$$\begin{cases} \dot{x}_{1u} = R\cdot\omega\sin\theta; \\ \dot{y}_{1u} = R\cdot\omega\cos\theta; \\ \dot{z}_{1u} = 0. \end{cases} \tag{5}$$

According to (2) and taking into account the dependences (4) and (5), we develop the formulas:

$$\begin{cases} \dot{x}_1 = \dfrac{d(R-d)}{dt}\cos\theta + R\cdot\sin\theta\cdot\left(\omega - \dfrac{d\theta}{dt}\right) + \\ +d\sin\theta\dfrac{d\theta}{dt} + \dfrac{d(d)}{dt}\cos^2\theta - 2d\cos\theta\sin\theta\dfrac{d\theta}{dt}; \\ \dot{y}_1 = \dfrac{dR}{dt}\sin\theta - R\cdot\cos\theta\cdot\left(\omega - \dfrac{d\theta}{dt}\right); \\ \dot{z}_1 = \dfrac{T_0}{2\pi}\left(\omega - \dfrac{d\theta}{dt}\right). \end{cases} \tag{6}$$

The modules of motion speed of the given bulk material volume are determined by formulas:

$$|\dot{s}_1| = \sqrt{\dot{x}_1^2 + \dot{y}_1^2 + \dot{z}_1^2}\ ; \tag{7}$$

$$|\dot{s}_2| = \sqrt{\dot{x}_A^2 + \dot{y}_A^2 + \dot{z}_A^2}\ . \tag{8}$$

Inserting the equations (4) and (6) into (7) and (8), and hypothesizing that the casing has a cylindrical shape with R = const, d = const, after the cuts, we get the formulas:

$$|\dot{s}_1| = \sqrt{\left(R^2 + \frac{T_0^2}{4\pi^2}\right)\left(\omega - \frac{d\theta}{dt}\right)^2 + 2Rd\sin^2\theta\left(\omega - \frac{d\theta}{dt}\right)\frac{d\theta}{dt}(1-2\cos\theta) + d^2\sin^2\theta\left(\frac{d\theta}{dt}\right)^2(1-2\cos\theta)^2}\ ; \tag{9}$$

$$|\dot{s}_2| = \sqrt{R^2\left(\frac{d\theta}{dt}\right)^2 + \frac{T_0^2}{4\pi^2}\left(\omega - \frac{d\theta}{dt}\right)^2 + 2Rd\sin^2\theta\left(\frac{d\theta}{dt}\right)^2(1-2\cos\theta) + d^2\sin^2\theta\left(\frac{d\theta}{dt}\right)^2(1-2\cos\theta)^2}\ . \tag{10}$$

The acceleration of the given bulk material volume is determined by differentiating the equation (6) when R=const; d=const.

$$\begin{aligned}\ddot{x} &= R\cos\theta\frac{d\theta}{dt}\left(\omega - \frac{d\theta}{dt}\right) - R\sin\theta\frac{d^2\theta}{dt^2} + d\cos\theta\frac{d^2\theta}{dt^2} + d\sin\theta\frac{d^2\theta}{dt^2} + \\ &+ 2d\left(\sin^2(\theta)\frac{d^2\theta}{dt^2} - \cos^2(\theta)\frac{d^2\theta}{dt^2} - 2\cos\theta\sin\theta\frac{d^2\theta}{dt^2}\right); \\ \ddot{y} &= R\sin\theta\frac{d\theta}{dt}\left(\omega - \frac{d\theta}{dt}\right) + R\cos\theta\frac{d^2\theta}{dt^2}; \\ \ddot{z} &= -\frac{T_0}{2\pi}\frac{d^2\theta}{dt^2}.\end{aligned} \tag{11}$$

The numerical and experimental research as well as the research presented in the work [5-6] prove that the stable mode of transportation is set regardless of the initial conditions of transportation after the passage of transitional mode zone.

The minimum force of material feed in a loading zone of a vertical conveyor should be defined; the rational location of a loading conveyor should be specified. To achieve these goals, the analytical model shown in Fig. 3 should be considered.

A particle of the material located on a screw surface of a vertical conveyor in a loading zone is exposed to a horizontal conveyor's action. In the general case of inclined position of screw conveyors axes, the motion of this particle is described by the equations of equilibrium:

$$\begin{cases}\sum X = N_{1x} + F_{1x} + P_{1x} + G_x + F_{ix} = 0; \\ \sum Y = N_{1y} + N_{2y} + F_{1y} + P_{1y} + G_y = 0; \\ \sum Z = N_{1z} + F_{1z} + P_{1z} + G_z = 0,\end{cases} \tag{12}$$

where: N_{1x}, N_{1y}, N_{1z} – projections of a normal reaction from a vertical auger surface to the axes x, y, z, H; F_{1x}, F_{1y}, F_{1z} – projections of frictional forces between a particle and a surface of a screw working body to the axes x, y, z, H; G_x, G_y, G_z –- projections of a weight force to the axes x, y, z, H; P_{1x}, P_{1y}, P_{1z} – projections of a force of feeding the material into a loading zone by a horizontal conveyor to the axes x, y, z, H; F_{ix} – projection of a centrifugal force to the axis x; N_{2y} – projection of a normal reaction from a casing surface to the axis y, H.

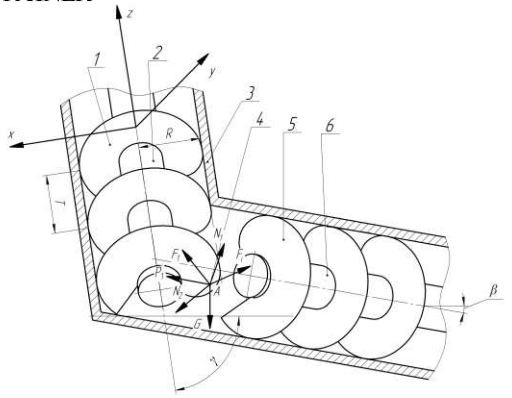

Fig. 3. Analytical model to determine the minimum force of material feed in a loading zone of a vertical conveyor: 1 – screw working body of a vertical conveyor; 2 – shaft of a vertical conveyor; 3 – casing; 4 – a piece of material; 5 – screw working body of a horizontal conveyor; 6 – shaft of a horizontal conveyor

Projections of a normal reaction to the axes are deduced by the formulae:

$$\begin{cases}N_{1x} = -N_1 \cdot \sin\alpha; \\ N_{1y} = -N_1 \cdot \sin\alpha; \\ N_{1z} = N_1 \cdot \cos\alpha,\end{cases} \tag{13}$$

where: α – an angle of helix ascent of a screw working body, rad; N_1 – normal reaction from the screw surface, H.

Projections of a weight force to the axes:

$$\begin{cases}G_x = mg \cdot \cos\gamma; \\ G_y = 0; \\ G_z = -mg \cdot \sin\gamma,\end{cases} \tag{14}$$

where: m – a particle mass, kg; γ – axis inclination angle of a vertical screw working body to the horizontal, rad; g – acceleration of gravity, м/с^2.

The projection of a centrifugal force:

$$F_{ix} = -mR\omega_2^2, \tag{15}$$

where: R – outer radius of a vertical auger, m; ω_2 – angular rate of auger rotation, с$^{-1}$.

Friction F_1 acts oppositely to the vector of a particle absolute rate, and its projections are:

$$\begin{cases}F_{1x} = -f_1 N_1 \cdot \cos\alpha; \\ F_{1y} = -f_1 N_1 \cdot \cos\alpha; \\ F_{1z} = -f_1 N_1 \cdot \sin\alpha,\end{cases} \tag{16}$$

where: f_1 – coefficient of friction between the particle and auger surface.

Projections of a force of material feed into the loading zone by a horizontal conveyor:

$$\begin{cases}P_{1x} = P_1 \cdot \sin(\gamma - \beta); \\ P_{1y} = 0; \\ P_{1z} = P_1 \cdot \cos(\gamma - \beta),\end{cases} \tag{17}$$

Where:β – axis inclination angle of a horizontal screw working body to the horizontal, rad.

The numerical and experimental research as well as the research presented in the work [3, 6] prove that the stable mode of transportation is set regardless of the initial conditions of transportation after the passage of transitional mode zone.

Based on (13-17), the system of equations (12) can be developed:

$$\begin{cases}\sum X=-N_1\sin\alpha-f_1N_1\cos\alpha+P_1\sin(\gamma-\beta)+mg\cos\gamma-mR\omega_2^2=0;\\ \sum Y=-N_1\sin\alpha-f_1N_1\cos\alpha+f_2N_2=0;\\ \sum Z=N_1\cos\alpha-f_1N_1\sin\alpha-mg\sin\gamma+P_1\cos(\gamma-\beta)=0.\end{cases}\qquad(18)$$

where: N_2 – normal reaction of a casing surface, H.

Based on the third equation, the normal reactions of a casing surface can be deduced:

$$N_1=\frac{mg\sin\gamma-P_1\cos(\gamma-\beta)}{\cos\alpha-f_1\sin\alpha}.\qquad(19)$$

Substituting the equation (19) into the first equation of the equations system (18), the following formulae are deduced:

$$\frac{(-mg\sin\gamma+P_1\cos(\gamma-\beta))(\sin\alpha+f_1\cos\alpha)}{\cos\alpha-f_1\sin\alpha}+ \\ +P_1\sin(\gamma-\beta)+mg\cos\gamma-mR\omega_2^2=0.\qquad(20)$$

$$(-mg\sin\gamma+P_1\cos(\gamma-\beta))\,\mathrm{tg}(\alpha+\varphi)+ \\ +P_1\sin(\gamma-\beta)+mg\cos\gamma-mR\omega_2^2=0;$$

$$-mg\sin\gamma\,\mathrm{tg}(\alpha+\varphi)+P_1(\cos(\gamma-\beta)\,\mathrm{tg}(\alpha+\varphi)+ \\ +\sin(\gamma-\beta))+mg\cos\gamma-mR\omega_2^2=0;$$

$$P_1=\frac{mg(\sin\gamma\,\mathrm{tg}(\alpha+\varphi)-\cos\gamma)+mR\omega_2^2}{\cos(\gamma-\beta)\,\mathrm{tg}(\alpha+\varphi)+\sin(\gamma-\beta)},\qquad(21)$$

where: φ – friction angle between the material and auger surface, $\varphi=\mathrm{arctg}\,f_1$.

The force of feeding material into a loading zone by a horizontal conveyor can be deduced from the formula:

$$P_1=P_0-mg(\sin\beta+f_2\cos\beta),\qquad(21)$$

where: P_0 – axial force of material feed, H; f_2 – coefficient of friction between the particle and the surface of a horizontal auger casing.

Substituting the equation (21) into the equation (20), the minimum axial force of material feed can be deduced:

During the study of the technological process of loading a SW, the analytical dependence for determining the value of axial force of a horizontal branch was developed, where:

$$P_o=\frac{mg(\sin\gamma\,\mathrm{tg}(\alpha+\varphi)-\cos\gamma)+mR\omega_2^2}{\cos(\gamma-\beta)\,\mathrm{tg}(\alpha+\varphi)+\sin(\gamma-\beta)}+ \\ +mg(\sin\beta+f_2\cos\beta),\qquad(22)$$

Based on the formula 22, the graphs of dependences of minimum axial force of material feed on inclination angles of the vertical conveyor (Fig. 4) and the horizontal conveyor (Fig. 5) are developed.

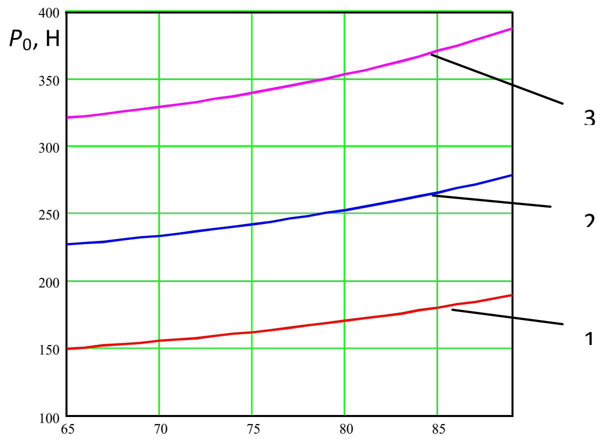

Fig. 4. Graph of the dependence of minimum axial force of material feed on the inclination angle of a conveyor horizontal branch R=0.1м, T=0.2м; β=0grad: 1 – $\omega_2=20c^{-1}$; 2 – $\omega_2=25c^{-1}$; 3 – $\omega_2=30c^{-1}$

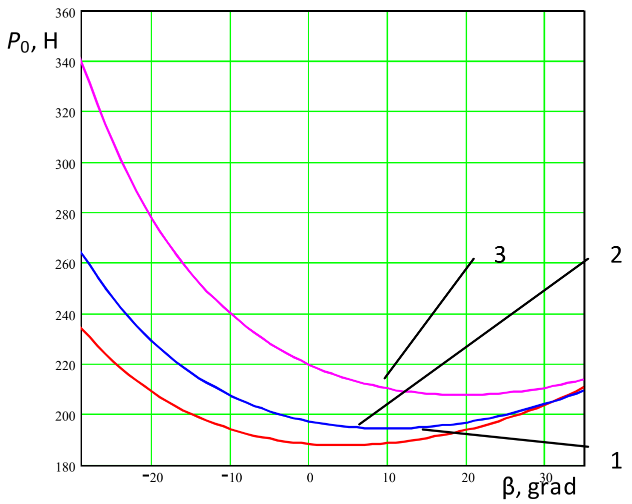

Fig. 5. Graph of the dependence of minimum axial force of material feed on the inclination angle of a horizontal conveyor R = 0.075m, T = 0.15m; = 25s-1 1 – γ = 75grad; 2 – γ = 80grad; 3 –- γ = 90grad

In addition, the graphs in Fig. 3 prove the existence of an optimum inclination angle of a horizontal auger, due to which the axial force of material feed takes the smallest value.

To find the optimum angle β, the equation (23) is differentiated:

$$\frac{dP_0}{d\beta}=\frac{-\left(mg\sin\gamma\,\mathrm{tg}(arctg\frac{T}{2\pi R}+\varphi)-\cos\gamma)+mR\frac{\pi^2n_2^2}{900}\right)}{\left(\cos(-\gamma+\beta)\,\mathrm{tg}(\mathrm{arctg}\frac{T}{2\pi R}+\varphi)-\sin(-\gamma+\beta)\right)^2}\times \\ \times\left(-\sin(-\gamma+\beta)\,\mathrm{tg}(\mathrm{arctg}\frac{T}{2\pi R}+\varphi)-\cos(-\gamma+\beta)\right)+ \\ +mg(\cos\beta-f_2\sin\beta)\qquad(23)$$

Considering the equation (23) equivalent to zero, the optimum angle β can be defined. Nevertheless, this equation has no analytical solution. Therefore, to define the optimum angle β, the graphical method shown in Fig. 3 should be applied.

CONCLUSIONS

1. The engineering technique of determining the nature of loading on the elements in medium speed mode of screw conveyor, on the casing and the screw working body in particular is developed. The speeds of bulk material transportation periodically change when the augers with axis motion are used. This fact improves the process of mixing the bulk materials.

2. The analytical dependences to determine the parameters during transportation of the given bulk material are developed. These dependences can be widely used in designing the screw transport and technological systems.

3. Analysing the graphs in 2 and 3, the following conclusions should be made. First, if the inclination angle of a vertical screw conveyor increases, the minimum axial force of material feed increases as well. Second, to reduce the minimum axial force of material feed by 5-7%, the horizontal auger should be set with a positive inclination angle β of the axis of a horizontal screw working body to the horizontal. The positive inclination angle β ranges within 3-20 degrees. Third, the greater the inclination angle of a vertical auger is, the greater should be the inclination angle of a horizontal auger.

REFERENCES

1. **Grygoryev A.M. 1972.** Screw conveyors / A.M. Grygoryev. – M.: Mechanical Engineering, 184.
2. **Zenkov R.M. 1987.** Continuous transport machines / R.M.Zenkov, I.I.Ivankov, L.N.Kolobov. – M.: Mechanical Engineering, 320.
3. **Rohatynskyi R.M., Hevko I.B., Diachun A.Y. 2014.** The scientific and applied fundamentals of screw transport and technological mechanisms. Ternopil, TNTU, 280.
4. **Pavlyshche V.T. 1993.** The basis of design and machine parts calculation. – K.: "Vyshcha shkola", 555.
5. **Ivanchenko F.K. 1993.** Lifting-and-transport machines. – K.: Vyshcha shkola, 412.
6. **Aleksandrov M. P. 1974.** Lifting and transport machines Mechanical engineering, 503.
7. **All Union State Standards Screw conveyors for feedstuff. Main parameters. 1980.** AUSS 23976 – 80 – M.: Standards publisher, 19. (National standards of Ukraine);
8. **All Union State Standards Augers for agricultural machinery. 1973.** AUSS 2705 - 73. – Standards publisher, 16. (National standards of Ukraine).
9. **Hewko I. 2011**. Model of loading on the screw working bodies (Моделювання характеру навантаження на гвинтові робочі органи) Bulletin TNTU. –V. 16. № 1. 69-77.
10. **Hewko B.M. 1989**. Screw falling mechanisms of agricultural machinery. Higher school, 176.
11. **Rohatynskyi R.M. 1997.** Mechanical and technological backgrounds of interaction of screw working bodies with agricultural raw materials: the thesis of Doctor of Sciences (Engineering) 05.20.01, 05.05.05 / Rohatynskyi Roman Mykhailovych, 502.
12. **Volkov R .A., Gnutov A. N., Diachkov V. K. and others. 1984.** Conveyors: Guide – under the editionship of Y.A. Perten. – Mechanical engineering, 367
13. **Gevko R.B. 2011.** Obgruntuvannya parametriv konstruktsiyi robochogo organu shaybovogo transportera. Visnik Kharkivskogo natsionalnogo tehnichnogo universitetu Imeni Petra Vasilenka. – Vipusk 114. 241-246.
14. **Aleksey Popov 2010.** Новая теория контактной прочности упруго сжатых тел // MOTROL. Commission of Motorization and Power Industry in Agriculture Polish Academy of Sciences Branch of Lublin Ropczyce School of Engineering and Management. – Lublin, – Tom 12A. 223-232.
15. **Loveykin V.S. 2011.** Bagatomasova model dinamiki ruhu kormozmishuvacha gvintovogo tipu zi zminnim oporom // MOTROL. Commis-sion of Motorization and Energetics in Agriculture – Lublin, Vol. 13B. 124-129.
16. **Loveykin V., Javorska A. 2012.** Screw feeder: optimization of motion modes considering that the moments of resistance forces change under linear law Motrol. Motoryzacja i Energetyka Vol. 14/3. 40-46.
17. **Adigamov K.A., Baibara S.N., Chernenko G.V.** 2009. Critical frequency of the vertical screw rotation. Digest of the East-Ukrainian National University named after Volodymyr Dal. – №2 (132). 9-10.
18. **Nilsson L.G. 1971.** On the vertical serew conveyor for non- cohesive bulk materials. Acta polytechnica Scandinavica. 4 Stokholm, 96.
19. **Fernandez J.W, Cleary P.W., Mcbride W., 2009.** Effect of screw design on hopper draw dawn to a horizontal screw feeder, Seventh International Conference on CFD in the Minerals and Process Industries CSIRO, Melbourne, Australia 9-11 Decem.
20. **Lytvynov O., Tana W. 2006.** Towards the dynamic calculation of machines. Motrol. Tom 8A, - pg. 210-223.

MOTROL. Commission of Motorization and Energetics in Agriculture – 2017. Vol.19. No.2. 53-56

TO CALCULATION OF INHOMOGENEOUS GRAIN MIXTURE FLOW IN A CYLINDRICAL SIEVE OF VIBROCENTRIFUGAL

Vasiliy Olshanskiy, Volodymyr Burlaka, Maksym Slipchenko, Olga Malec
Kharkiv Petro Vasylenko National Technical University of Agriculture
Alchevskyh Str., 44, Kharkiv, Ukraine E-mail: teoriyaTMM@gmail.com

Summary Formulas to calculate the kinematic characteristics of vertical motion of steady fine-grained mixture with variable porosity on a cylindrical sieve of vibrocentrifugal which rotates with a constant angular velocity around a vertical axis were derived and tested by calculation.

The change in the concentration of grains along the thickness of the mobile separating layer of the mixture caused by the action of the centrifugal force and the vertical harmonic vibrations of the vibrating screen is approximated by a quadratic three terms whose coefficients depend on the physical and mathematical characteristics of the bulk material, the parameters of the sieve motion and the presence on its surface of the intensifiers of the segregation process in the mixture , riffles, etc.).

The basis of the differential flow equation used is a two-parameter rheological dependence, according to which the shear stress in the mixture is proportional not only to the rate of shear deformations proper to the hydrodynamic models of motion, but also to the residual dry friction or excess internal pressure.

Therefore, the designed continual model of movement of the separating bulk material generalize famous model of motion absolutely vibroliquefied grain mixture, that is hydrodynamics model. Thanks to the introduction of a simple approximation of the change in the specific mass of a grain mixture over the thickness of the moving layer, it was possible to analytically integrate the differential equation of the grain of the flow and obtain computational formulas for calculating the velocity of the mixture and the vibrosieve productivity.

The calculations showed that the results to which the derived formulas lead are in good agreement with those known in the literature, both in terms of the velocity of the grain of the flow and the productivity of the vibrosieve. Numerical examples, calculations, studied the influence of various factors, including the porosity of the mixture and rheological constants, on the kinematic characteristics of the grain flow. Earlier such calculations were carried out by computer integration of nonlinear differential equations. Thus, the analytical method proposed here for calculating the grain flow can be an alternative to known numerical methods. This is the difference between this work and this work from existing developments.

Key words: vertical cylindrical vibrosieve, steady-state grain flow, variable porosity, quadratic approximation of three terms, two-parameter rheological dependence, visco-dry friction, velocity of movement, vibrosieve productivity.

INTRODUCTION

The quality of the vibratory separation of grain mixtures depends from the velocity of the bulk material and the intensity of the segregation process that occurs in it. These factors also effect on the productivity of grain cleaning equipment. Therefore, investigation of the consistent pattern of porosity in a mixture without which segregation is impossible, and also the distribution of the shear rate along the thickness of the moving layer, is to topical problems.

ANALYSIS OF RECENT RESEARCHES AND PUBLICATIONS

From the works in which the motion of grain mixtures of variable porosity in a cylindrical vertical vibrosieve is investigated, we shall distinguish [1 - 4]. In them, to determine the distribution of the concentration of grains over the thickness of the moving layer of the mixture, are take integral from a specially constructed second-order nonlinear differential equation on the computer. Then the received numerical information was used at computer integration of the grain flow equation, carrying out calculations of velocity of movement of a mixture and productivity of a vibrating sieve. So, as basis of the equation of motion was taken a classical one parametric dependence of the tangential stress from the rate of shear deformations, what is accepted in the dynamics of viscous liquids. It is established that the results of such mathematical modeling of the dynamics of an inhomogeneous grain mixture are in good agreement with the results of experimental studies [5].

Unlike the above-mentioned publications, a simplified analytical method has been developed here. Calculation of the grain flow, not associate with the numerical integration of the corresponding differential equations. It is based on the use of quadratic-polynomial approximation of the distribution of the specific mass of a grain mix or the concentration of grains over the thickness of a mobile separated layer. Such an approximation was discussed in [6]. It gives the results close to those of the power approximation [7, 8]. Simplified analytical methods for calculating grain flows through a flat sieve, using power-law approximations of the change in the specific mass of a grain mixture, was developed in [9, 10]. Here we consider the motion of an inhomogeneous mixture along the surface of a vertical cylindrical vibrosieve, where the centrifugal force also influences the kinematic parameters of the grain flow. In contrast to [11], the distribution of the grain concentration along the thickness of the mobile layer of the mixture is approximated by a non-power function rather than a power function, and a square of three terms that changes the design formulas, in addition to the astringent shear resistance, the residual dry friction is additionally taken into account.

Other approaches to modeling the movement of bulk materials of variable porosity along an inclined plane are also known [12, 13]. They are based on the equations of state of a dense gas, coinciding in form with the Klaiperon-Mendeleyev equation.

In a number of studies, the inhomogeneity of a pseudo-liquefied mixture on a vibratory sieve is characterized by a variable coefficient of vibro-viscosity [14 - 16]. For the adopted laws of the vibroviscosity changing equations of oscillations and the velocity of the grain flow in a cylindrical vibrosieve are analytically solved which is expressed in terms of Bessel functions [17 - 19].

Here we construct an analytical solution of the problem in elementary functions.

OBJECTIVES

The aim of the paper is to derive and test a new calculation equals for the calculation of the velocity of the steady-state flow of a mixture of variable porosity along the thickness of the moving layer and the productivity of the cylindrical sieve of the vibrocentrifuge.

THE MAIN RESULTS OF THE RESEARCH

Using the calculation scheme, shown in fig. 1 in [11], the following expression for the rate of grain flow is obtained:

$$u(r)=\frac{\gamma}{\mu}\int_R^r\left[\left(f\Omega^2-\frac{g}{r}\right)\int_{R_0}^r t\nu(t)\,dt\right]dr+u_0. \qquad (1)$$

where: $R_0=R-h$ is the radius of the free surface of the cylindrical layer of the mixture; R – the radius of the sieve; h – thickness of the moving layer; γ – specific gravity of the grain material; μ, f – coefficients of two parametric rheological dependencies, were first characterizes the viscous resistance, and the second - dry friction; g – acceleration of gravity; $\nu(r)$ – concentration of grains in the mixture; r – radial coordinate; Ω – angular velocity of sieve rotation around the vertical axis; u_0 – velocity of sliding of the mixture over the surface of the sieve.

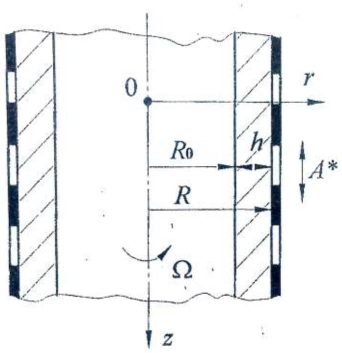

Fig. 1. Calculation scheme

Following [6], the function $\nu(r)$ is given in the form of a square three terms:

$$\nu(r)=\nu_0+a(r-R_0)+b(r-R_0)^2, \qquad (2)$$

where: $a=0{,}3483\frac{\nu_0}{h}\chi^{\lambda}$; $b=0{,}6797\frac{\nu_0}{h^2}\chi^{\lambda}$;

$\lambda=1{,}579$; $\chi=h\left[\frac{\gamma\Omega^2(R-0{,}5h)}{2\alpha\nu_0(\Phi+2)}\right]^{1/3}$; $\Phi=\frac{\sqrt{1+\varphi^2}-\varphi}{\varphi}$;

$\varphi=\frac{f_0}{2}\left(1+e^{-G}\right)$; $G=\frac{A_k\omega^2}{R\Omega^2}$; ν_0 – concentration of grains at the free surface of the mixture; f_0 – coefficient of dry friction in the mixture at rest; A_k – amplitude of the vertical oscillations of the sieve with frequency ω.

The value of the constant α depends on the presence on the surface of the sieve of the activators of the segregation process in the mixture (ribs, rifles) [2, 3].

For the adopted relationship $\nu(r)$, we have:

$$\int_{R_0}^r t\nu(t)\,dt=\frac{b}{4}(r-R_0)^4+\frac{a+bR_0}{3}(r-R_0)^3+$$
$$+\frac{aR_0}{2}(r-R_0)^2+\frac{\nu_0}{2}\left(r^2-R_0^2\right).$$

Substitution of this expression in (1), and further integration, yield a closed formula for the rate of grain flow:

$$u(r)=\frac{\gamma}{\mu}\left[\sum_{j=1}^{5}A_j\left(r^j-R^j\right)+A_0\ln\frac{r}{R}\right]+u_0. \qquad (3)$$

where: $A_0=\frac{gR_0^2}{2}\left(\nu_0-\frac{aR_0}{3}+\frac{bR_0^2}{6}\right)$;

$A_1=\frac{f\Omega^2}{2}R_0^2\left(\frac{aR_0}{3}-\frac{bR_0^2}{6}-\nu_0\right)$; $A_2=\frac{g}{4}\left(aR_0-bR_0^2-\nu_0\right)$;

$A_3=\frac{1}{3}\left[\frac{f\Omega^2}{2}\left(\nu_0+bR_0^2-aR_0\right)+\frac{g}{3}\left(2bR_0-a\right)\right]$;

$A_4=\frac{1}{4}\left[\frac{f\Omega^2}{3}\left(a-2bR_0\right)-\frac{bg}{4}\right]$; $A_5=\frac{f\Omega^2}{20}b.$

Thus, using the approximation (2) makes it possible to express the quadrature in (1) in terms of elementary functions.

If in the formula (3) take $a=b=0$; $\nu_0\gamma=\rho$, then with her as a particular case, we get:

$A_4=A_5=0$; $A_3=\frac{f\Omega^2}{6}\nu_0$; $A_2=-\frac{g\nu_0}{4}$;

$A_1=-\frac{f\Omega^2}{2}R_0\nu_0$; $A_0=\frac{gR_0^2}{2}\nu_0$;

$$u(r)=\frac{\rho}{4\mu}\left\{g\left(R^2-r^2+R_0^2\ln\frac{r^2}{R^2}\right)+\right.$$
$$\left.+2f\Omega^2\left[R_0^2(R-r)-\frac{R^3-r^3}{3}\right]\right\}+u_0.$$

This expression $u(r)$ coincides with that printed in [20], where it was derived to calculate the velocity of motion of a homogeneous mixture.

From (3) when $f = 0$ implies the formula $u\ r$, obtained in [19] on the basis of the hydrodynamic model.

Thus, the solution (3) generalizes the known results.

To find the productivity P of vibrosieve, we need to calculate the integral:

$$P = 2\pi\gamma \int_{R_0}^{R} r\nu\ r\ u\ r\ dr. \qquad (4)$$

After substituting expressions (2) and (3) into, it is also "taken" analytically, but it reduces to a cumbersome formula. Therefore P is more convenient to calculate by numerical methods on the computer.

To verify the reliability of the results obtained, we will perform calculations for: $R = 0.3075\,m$; $\Omega = 11.77\,s^{-1}$; $A_k = 0.006\,m$; $\omega = 95\,s^{-1}$; $\gamma = 1350\,kg/m^3$; $f_0 = 0.47$; $u_0 = 0$; $\alpha = 0.23h$ and various μ, f, ν_0, h. Calculated by the formula (3) value $u\ r$ for $h = 0.018m$; $\mu = 1.9\,Pa\cdot s$; $f = 0{,}1$ and different value of ν_0 in the numerator recorded in table 1.

Table 1. Values $u\ r$ calculated of two ways

$r_* = \dfrac{r - R_0}{h}$	$\nu_0 = 0.3$	$\nu_0 = 0.4$	$\nu_0 = 0.5$
	Values $10u\ r\ , m/s$		
0.0	2.220 / 2.211	2.901 / 2.891	3.576 / 3.565
0.2	2.139 / 2.131	2.793 / 2.784	3.442 / 3.432
0.4	1.891 / 1.885	2.466 / 2.458	3.034 / 3.027
0.6	1.465 / 1.461	1.904 / 1.900	2.339 / 2.335
0.8	0.842 / 0.841	1.091 / 1.090	1.337 / 1.336

In the denominator are shown those values $u\ r$ which theoretically derived in other ways [11].

We got a good consistency theoretical results got in different ways. The discrepancy is within 1%.

The results of calculations $u\ R_0$ for various μ, f and ν_0 recorded in the table 2. At the same time, $h = 0.016m$ and previous other output data were set.

Table 2. Values $u\ R_0$ calculated of two ways

$\mu,\ Pa\cdot s$	f	$\nu_0 = 0.3$	$\nu_0 = 0.4$	$\nu_0 = 0.5$
		Values $10u\ R_0\ , m/s$		
0.9	0.10	3.617 / 3.605	4.742 / 4.727	5.858 / 5.842
0.9	0.15	2.268 / 2.262	2.973 / 2.966	3.675 / 3.666
1.1	0.10	2.959 / 2.949	3.880 / 3.868	4.793 / 4.780
1.1	0.15	1.856 / 1.850	2.432 / 2.427	3.007 / 2.999

Here, too, the numerator calculated by the formula (3), little different from the denominators obtained by other means in [11].

Calculations confirm significant effect on the rate of grain flow parameters μ, f and ν_0.

Table 3 vibrosieve recorded performance values. The results obtained in the numerator numerical integration formula (4), and the denominator – borrowed from [11].

Table 3. Productivity P of vibrosieve calculated in two ways, when $h = 0.012m$

$\mu,\ Pa\cdot s$	f	$\nu_0 = 0.3$	$\nu_0 = 0.4$	$\nu_0 = 0.5$
		Values $P,\ kg/s$		
0.9	0.10	1.324 / 0.319	2.293 / 2.285	3.517 / 3.508
0.9	0.15	0.824 / 0.821	1.428 / 1.423	2.190 / 2.184
1.2	0.10	0.993 / 0.989	1.720 / 1.714	2.638 / 2.631
1.2	0.15	0.618 / 0.616	1.071 / 1.067	1.642 / 1.638

Differences theoretical results in performance vibrosieve obtained in various ways, too, are within 1%. Values μ, f, ν_0 significantly influence the performance of the estimated sieve.

CONCLUSIONS

The comparisons have confirmed the reliability of the calculated formulas derived above, which generalize known dependences obtained earlier for a homogeneous mixture on the basis of a one-parameter hydrodynamic model. The proposed method of modeling makes it possible to approximately calculate the kinematic characteristics of the grain flow of an inhomogeneous mixture without the numerical integration of nonlinear differential equations.

REFERENCES

1. **Tishchenko L.M. 2003.** To the study of the separation of fractions of a grain mixture during separation on a vertical cylindrical vibrocentrifugal sieve. / L.M. Tishchenko, M.V. Piven // Vibrations in technics and technology. – Vinnica. – №5 (31). 40-43. (in Russia).
2. **Piven M.V. 2006.** Rationale of the parameters of the process of sieve separation of grain mixtures: dissert for a science candidate degree of Eng. Science of 05.05.11 "Machinery and means of agricultural production mechanization" / M.V. Piven – Kharkiv, 256. (in Russia).
3. **Tishchenko L.M. 2010.** Modeling of processes of grain separators / L.M. Tishchenko, D.I. Mazorenko, M.V. Piven and other – Kharkov: Miskdruk, 360. (in Russia).
4. **Tishchenko L.M. 2013.** Rationale process of segregation at grain mixtures separatory sieves vibrocentrifugal / L.M. Tishchenko, M.V. Piven, V.V. Bredixin // Motrol. Motorization and power industry in agriculture Lublin-Rzesow. – Vol.15. No 7. 105-112. (in Russia).
5. **Tishchenko L.M. 2016.** Experimental studies of intralayer processes in grain mixtures separated by cylindrical vibrating centrifugal sieves / L.M. Tishchenko, M.V. Piven // Mechanization of agricultural production: Bulletin Khntusg: Kharkov. – Vol. 173. 153-160. (in Russia).

6. **Olshanskyi V.P. 2016.** About quadratic approximation of the distribution of the specific mass in the layer of vibroseparated grain mixture / V.P. Olshanskyi, O.V. Olshanskyi // Engineering of storage and product industries. – Kharkov. – №2 (2). 66-70. (in Ukranian).
7. **Olshanskyi V.P. 2016.** Tabular calculation of the porosity of the grain-mix layer in a cylindrical vibrosieve / V.P. Olshanskyi, S.V. Olshanskyi, M.V. Slipchenko // Vibrations in technics and technology. – Vinnica. – №3 (83). 195-201. (in Ukranian).
8. **Olshanskyi V. 2016.** Analytacal method for determining porosity in the layer of vibro separation grain mixture / V. Olshanskii, A. Olshanskii, S. Kharchenko, F. Kharchenko // TEKA. Commission of motorization and energetics in agriculture – Poland: Lublin-Rzeszow. – Vol. 16. № 4. 49-56. (in English).
9. **Olshanskyi V.P. 2016** On the movement of a grain mixture of variable porosity on a flat vibrosieve / V.P. Olshanskyi, O.V. Olshanskyi // Engineering of storage and product industries – Kharkov. – №2 (2). 61-65. (in Ukranian).
10. **Olshanskyi V.P. 2016**. On the nonlinear model of the motion of a grain mixture of variable porosity on a flat vibrosieve / V.P. Olshanskyi, V.V. Burlaka, M.V. Slipchenko, S.O. Kharchenko // Bulletin of SNAU: Mechanization and automation of production processes – Sumy. – №10/1 (29). 107-112. (in Ukranian).
11. **Olshanskyi V.P. 2016.** About motion of grain mixture of variable porosity in the cylindrical sieve of vibrocentrifuge / V. Olshanskii, A. Olshanskii, S. Kharchenko, F. Kharchenko // TEKA. Commission of motorization and energetics in agriculture – Poland: Lublin-Rzeszow – Vol. 15. № 3. 87-93. (in English).
12. **Dolgunin V.N. 1995.** Segregation modeling of particle rapid gravity flow / V.N. Dolgunin, A.A. Ukolov // Powder Technology – Vol. 83. 95-103. (in English).
13. **Dolgunin V.N. 2005.** Rapid gravitational flows of granular materials: a technique of measurement, regularities, technological application / V.N. Dolgunin, V. Ya. Borshchev – M: Mashinostroenie, 73. (in Russia).
14. **Tishchenko L.M. 2011.** Vibrosieve separation of grain mixtures / L.M. Tishchenko, V.P. Olshanskyi, S.V. Olshanskyi – Kharkov: Miskdruk, 280. (in Russia).
15. **Tishchenko L. 2011** On velocity profiles of on inhomogeneous vibrofluidized grain on shaker / L. Tishchenko, V. Olshanskyi, S. Olshanskyi // Journal of Engineering Physics and Thermophysics – Vol. 84 №3. 509-514. (in English).
16. **Tishchenko L.** Vibroseparation by a flat sieve of an inhomogeneous layer of grain / L. Tishchenko // Motrol. Motorization and power industry in agriculture – Poland: Lublin-Rzesow –Vol. 14D. 21-30. (in Russia).
17. **Tishchenko L.M. 2012.** Fluctuations in grain flows on vibrosieve / L.M. Tishchenko, V.P. Olshanskyi, S.V. Olshanskyi – Kharkov: Miskdruk, 267. (in Russia).
18. **Tishchenko L. 2012.** Vibrational processes in grain mixtures on sieve vibrating centrifugal separators / L. Tishchenko // Motrol. Motorization and power industry in agriculture – Poland: Lublin-Rzesow – Vol. 14D. 30-39. (in Russia).
19. **Tishchenko L.M. 2013.** Dynamics of vibratory centrifugal grain cleaning / L.M. Tishchenko, V.P. Olshanskyi, S.V. Olshanskyi and other – Kharkov: Miskdruk, 440. (in Russia).
20. **Olshanskyi V.P. 2016.** Mathematical models of grain flows on vibrosieve // V.P. Olshanskyi, O.V. Olshanskyi – Kharkiv: Miskdruk, 140. (in Ukrainian).

MOTROL. Commission of Motorization and Energetics in Agriculture – 2017. Vol.19. No.2. 57-60

FRUIT PLANTATIONS PROTECTION OF INTENSIVE TYPE FROM SPRING FROSTS BY MEANS OF LIQUID ATOMIZATION

Ganna Rudnytska, Alexander Anikeev, Michael Tsyganenko, Kirill Sirovitskiy, Evgen Gaek
Kharkiv Petro Vasylenko National Technical University of Agriculture
Moskovskiy Str., 45, Kharkiv, Ukraine, E-mail: kafedra_emtp@ukr.net

Summary. The model of the thermal state of the leaf was refined. The possible condensation of moisture on the leaves upon their cooling was taken into account. When considering radiative heat-exchange, it is necessary to take into account the fact that bodies not only emit their own, but also reflect the energy received from outside. The sum of the body's own emission and reflected emission is called effective radiation. In this paper, we propose to delay the radiative cooling of the soil by installing a foggy screen and to estimate the "lifetime" of this veil against to the environmental conditions. When considering radiative heat-exchange, it is necessary to take into account the fact that bodies not only emit their own, but also reflect the energy received from outside. The sum of the body's own emission and reflected emission is called effective radiation. The obtained results give an approximate estimate of the heat exchange rate between soil and air, because the convective heat exchange between the soil, air and the accumulated heat of the soil is not taken into account. The force of the aerodynamic resistance is directed opposite to the drop movement vector. In our case it is directed opposite to gravity force.

Key words: fruits, protection, atomization, method, temperature, intensive, spring frosts.

INTRODUCTION

According to the recommendations of physicians, annually an adult should consume at least 80 kg of fruit and berries. These products are of particular value as a source of vitamins. They play a major role in human activity because of increasing the body's vital tone, its physical and mental efficiency, and disease resistance. A sufficiently high level of consumption of these products (in the range 100...160 kg per person in a year) has established in the developed countries of the world. In Ukraine this level is very low and does not exceed 25...30 kg.

During 1991-2007 the area of fruit and berry plantations in Ukraine has decreased by 73,3%. To date, their areas in agricultural enterprises make up 109,4 thousand of hectare. Reducing the scale of operations of this product is occurring not only due to the reduction of areas of fruit plantations, but also due to the reduction of their yields. The main reasons of this are the lack of proper logistical support, non-compliance of land treatment, and high labour coefficient of production. One of the reasons of the low yield of fruit trees is the loss of their generative organs during spring frosts.

Frosts are observed at night in the spring, during the flowering and fruit-setting. The temperature of the air drops below zero, lasts for 3...4 hours and more, what leads to damage or destruction of the generative organs (0...-1^{0}C).

Many methods are known to protect spring planting of an intensive type from spring frosts. The most common are the covering of trees, smoking, air heating in the row-spacing, the mixing of air layers with helicopters and stationary propellers, and irrigation. But today in Ukraine they do not find wide application in the production either because of their low efficiency, or because of high costs of energy resources. Despite of the development of a number of measures, the task of fruit plantations protecting has not resolved. Today there is no efficient and economical method of protecting from this phenomenon of nature.

ANALYSIS OF RESEARCHES AND PUBLICATIONS

Spray irrigation has been used for a long time to protect gardens from frosts [1-3]. The phenomenon of radiative frost is considered in the literature [4]. The main cause of it is the predominance of the thermal radiative flow from the soil over the incoming heat flow from warmer air. Also the phenomenon of latent frost is considered [4]. It can be attended by below the maximum permissible value of the temperature the leaf or flower for the current phase of vegetation. In that time the air temperature can be several times higher than the maximum permissible value of the temperature.

The model of the thermal state of the leaf was refined. The possible condensation of moisture on the leaves upon their cooling was taken into account [5, 11].

OBJECTIVES

There is a part of the garden correctly geometry and relief. The structure of the planting is known, as well as the geometry of the row-spacing and the height of plants. The rated value of air temperatures which dose not damage plants and provide their survival is given. There are known climatic conditions of the region where fruits are cultivated. At the same time, providing the predetermined thermal regime of the open agroecosystem (gardens and nursery-garden of seedlings which are cultivated on the open ground) at extreme seasons of a year is the urgent problem. Especially these questions worry gardeners in the three main extreme seasons of the year: during the first autumn frosts (-5^{0}C, -10^{0}C and below); during the winter season (-15^{o}C, -20 ^{0}C and below); during the first spring frosts (-1^{o}C, -2^{o}C and below). Short-term frosts are not as dangerous as long-term frosts. Although they are less significant in strength.

THE MAIN RESULTS OF THE RESEARCH

In the case of radiation freezing, the temperature lowering of the sheet can occur due to heat-exchange of radiation with colder bodies as are soil and sky. As the reflectivity (albedo) of the soil is usually worse than that of the leaves, so, according to the laws of Stefan-Boltzmann and Kirchhoff [6, 7, 12-16], by the same temperature, the body with a smaller reflectivity radiates more than the body with greater reflectivity. In our case this means that the soil will chill faster than the leaves, and the leaves will be more strongly chill from radiation heat-exchange with the soil than with the atmosphere. If we manage to stop or delay the radiative cooling of the soil, then frost may not occur.

In this paper, we propose to delay the radiative cooling of the soil by installing a foggy screen and to estimate the "lifetime" of this veil against to the environmental conditions [17-19].

We will try to estimate the loss of thermal energy by soil due to radiation in the cloudless sky on basis of the approaches which were described in the literature [4, 5, 20, 21]. In this article, the reflectivity values were taken as equal 0,05 for the soil and 0,15 for the leaves and flowers. Though, permissible temperature of the leaf (which equals + 2°C) is slightly higher than the maximum permissible temperature for flowers and leaves of apple and pear. This temperature rise provides certain reserve for carrying out frost protection measures.

The specific radiation heat flow rate of the emitting surface is determined on the basis of the Stefan-Boltzmann law [6, 7]:

$$q_r = \varepsilon \cdot \sigma_0 \cdot T^4, \qquad (1)$$

where: ε – the rate of the body blackness, according to Kirchhoff's law (ε = 1-A); A – Albedo (reflectivity) of the surface; T – surface temperature, K; σ_0 – the Stefan-Boltzmann radiation constant of an absolutely black body ($\sigma_0 = 5{,}67 \cdot 10^{-8}$ W/(м^2·K^4).

The specific heat flow rate of soil intrinsic radiation:

$$q_{rsoil} = \varepsilon_{soil} \cdot \sigma_0 \cdot T_{soil}^4, \qquad (2)$$

where: T_{soil} – Kelvin temperature; ε_{soil} – coefficient of soil blackness.

The specific heat flow rate of the intrinsic radiation of a sheet is written as follows:

$$q_{rleaf} = \varepsilon_{leaf} \cdot \sigma_0 \cdot T_{leaf}^4, \qquad (3)$$

where: T_{leaf} – Kelvin temperature; ε_{leaf}– Blackness factor of sheet surface.

In a cloudless sky, the specific radiation heat flow from the atmosphere per unit surface area will be written as [8]:

$$q_{ra} = \varepsilon_a \cdot \sigma_0 \cdot T_a^4 = \sigma_0 \cdot (0{,}526 + 0{,}065 \cdot \sqrt{P_{va}}) \cdot T_a^4, \qquad (4)$$

where: P_{va} –the partial vapour pressure (Pa) in atmospheric air by the counterpart of humidity.

When considering radiative heat-exchange, it is necessary to take into account the fact that bodies not only emit their own, but also reflect the energy received from outside. The sum of the body's own emission and reflected emission is called effective radiation. The resulting heat flow which is establishing between the bodies is equal to the difference of the effective heat flows from the bodies. For two opaque infinite parallel plates, the specific resultant heat flow will be written so:

$$q_{r12} = \varepsilon_{12} \cdot (\sigma_0 \cdot T_1^4 - \sigma_0 \cdot T_2^4), \qquad (5)$$

where: ε_{12} – the reduced rate of the bodies system blackness, equal to:

$$\varepsilon_{12} = \frac{1}{1/\varepsilon_1 + 1/\varepsilon_2 - 1}. \qquad (6)$$

As the formula (5) indicates when the bodies temperatures are equal – the resultant heat flow equals zero.

In the case when one of the plane-parallel bodies does not reflect the incident on it radiation. That is, it can only flow and emit heat flow. The resulting heat flow will be written as follows (the body 1 reflects and absorbs, the body 2 only absorbs):

$$q_{r12} = \varepsilon_1 \cdot (\sigma_0 \cdot T_1^4 - \varepsilon_1 \cdot \sigma_0 \cdot T_2^4). \qquad (7)$$

For our problem, atmospheric air has the properties of body 2. According to the ratio (7), as a result we will obtain the next formula for the resulting heat flow between soil and air:

$$q_{rsa} = \varepsilon_{soil} \cdot (\sigma_0 \cdot T_{soil}^4 - \varepsilon_a \cdot \sigma_0 \cdot T_a^4), \qquad (8)$$

Using the ratios (1)-(8), the results presented in fig. 1 are obtained.

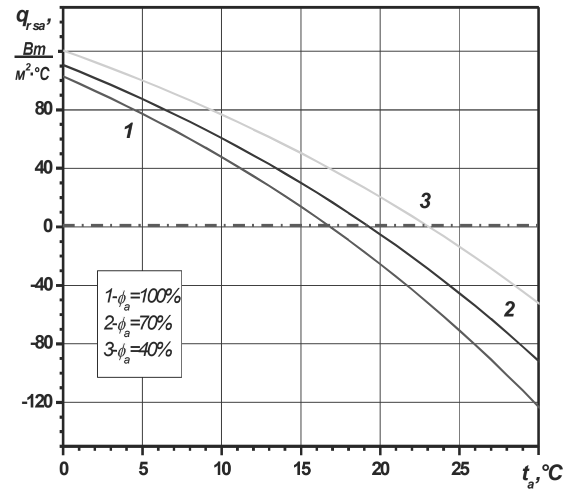

Fig. 1. The specific resultant heat flow from air, soil and leaf, depending on air temperature and relative humidity. 1, 2, 3 - air when relative humidity is 100%, 70%, 40% properly

Figure 1 presents the specific resultant radiative heat flow rate between atmospheric air and the soil surface, at different relative humidity of atmospheric air and at soil temperature equal to the leaf temperature.

As we can see from figure 1, for the resultant radiative heat flow between soil (when the temperature is + 2°C) and air was zero - the air temperature (when a relative air humidity is 40%, 70%, 100%) should be equals 23°C, 19°C and 17°C properly.

The obtained results give an approximate estimate of the heat exchange rate between soil and air, because the convective heat exchange between the soil, air and the accumulated heat of the soil is not taken into account.

One of the effective methods of reducing the radiation flow from the soil to the atmosphere on application of measures for the garden protection (open agro ecosystem) from frost is smoking [1-3, 22, 23].

It is known that for small particle sizes (atmospheric fog), infrared radiation scatters less than visible radiation (which is used in infrared photography). And for large drop size (thick fog), infrared radiation scatters as much as visible radiation.

We propose to install a heat-radiating foggy screen to protect the garden from radiation frost. One of the important characteristics of a foggy environment is the drop size, their rate of sedimentation, and evaporation time.

The drop deposition rate is the free-fall velocity, which is achieved when balance of all forces acting on the drop is reached [9].

In our case (fig. 2) the next forces impact on a drop:

1) gravity force – F_g,
2) force of aerodynamic resistance – F_d,
3) buoyancy force – F_{Ar}.

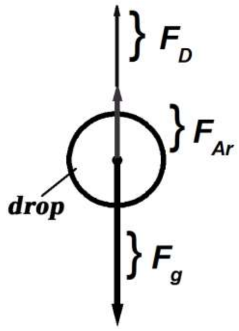

Fig.2. Forces acting on a drop in free fall

The force of the aerodynamic resistance is directed opposite to the drop movement vector. In our case it is directed opposite to gravity force. The buoyancy force is also directed opposite to the vector of gravity force [9]:

$$\overline{F_g} = \overline{F_D} + \overline{F_{Ar}}. \tag{9}$$

Let's take a drop for a solid sphere. The rate of the drop gravity force (10), the buoyancy force (11), and the force of aerodynamic resistance (12) will be written as follows:

$$F_g = m_d \cdot g = V_d \cdot \rho_d \cdot g = \frac{\pi \cdot d^3}{6} \cdot \rho_d \cdot g, \tag{10}$$

$$F_{Ar} = V_d \cdot \rho_0 \cdot g = \frac{\pi \cdot d^3}{6} \cdot \rho_0 \cdot g, \tag{11}$$

$$F_D = A_d \cdot C_D \cdot \frac{\rho_0 \cdot (W_d - W_0)^2}{2}, \tag{12}$$

where: m_d, V_d, A_d – mass, volume, cross-section area of a drop (inferior index d); ρ_d, ρ_0 – density of a drop and atmosphere air; W_d – rate of drop sedimentation; W_0 – traverse speed of environmental air, in our case, equals zero.

The coefficient of aerodynamic resistance is a function of the dimensionless Reynolds number and for a solid sphere in the region of friction flow is equal [9]:

$$C_D = \frac{24}{\mathrm{Re}_d}, \tag{13}$$

where: the ratio $\mathrm{Re}_d = \frac{\rho_0 \cdot |W_d - W_0| \cdot d}{\mu_0}$, expresses the relation between the forces of inertia and the forces of viscosity. From the relations (9)-(13), Stokes [9] obtained a formula for calculating the drop sedimentation rate:

$$W_d = \frac{d^2 \cdot (\rho_d - \rho_0) \cdot g}{18 \cdot \mu_d}. \tag{14}$$

The rate of evaporation is estimated by the Maxwell formula [10]:

$$I = 2 \cdot \pi \cdot d \cdot D \cdot (c_d - c_0), \tag{15}$$

where: D – diffusion coefficient; c_d – concentration of water vapour by drop; c_0 – concentration of water vapour in atmosphere air.

Table 1 presents the sedimentation rate, the passage time of 1 m (the lifetime of the fog screen), and the rate of drops evaporation of different diameters in the air with a 90% relative humidity.

It can be seen that as the diameter of the drop increases, the drop sedimentation increases. And thereby the possible lifetime of the foggy screen decreases because of falling of the drops to the ground.

Table 1. Drop sedimentation rate, passage time and drops evaporation rate of different diameters

d, мсм	W_d, м/s	τ, s	I, кgs
2,5	$1{,}9673 \cdot 10^{-4}$	5083,19	$3{,}3067 \cdot 10^{-13}$
5,0	$7{,}8691 \cdot 10^{-4}$	1270,80	$6{,}6135 \cdot 10^{-13}$
10,0	$3{,}1476 \cdot 10^{-3}$	317,70	$1{,}3227 \cdot 10^{-12}$
20,0	$1{,}2591 \cdot 10^{-2}$	79,42	$2{,}6454 \cdot 10^{-12}$
40,0	$5{,}0362 \cdot 10^{-2}$	19,86	$5{,}2908 \cdot 10^{-12}$
80,0	$2{,}0145 \cdot 10^{-1}$	4,96	$1{,}0582 \cdot 10^{-11}$
100,0	$3{,}1476 \cdot 10^{-1}$	3,18	$1{,}3227 \cdot 10^{-11}$

CONCLUSION

The obtained results (the specific resultant radiative heat flow from air, soil and leaf, depending on air temperature and relative humidity) give an approximate estimate of the heat exchange rate between soil and air, whereas convective heat exchange between soil and air and the accumulated heat of the soil are not taken into account.

In order to resultant radiation heat flow between the soil (when the temperature is + 2°C) and air equalled zero the air temperature (with relative air humidity of 40%, 70%, 100%) should be 23°C, 19°C and 17°C, properly.

The sedimentation rate, the passage time of 1 m and the rate of drop evaporation of various diameters in air (with a relative humidity of 90%) are calculated. When the diameter of the drop increases, the sedimentation rate increases. And, thereby, the possible lifetime of the foggy screen decreases because of falling of the drops to the ground.

The obtained data allow to substantiate the choice of the spraying equipment for installing a foggy screen.

REFERENCES

1. **Goltsberg I.A. 1961.** Agroclimatic characteristics of frosts in the USSR and methods of combating them / Goltsberg Ida. – L.: Gidrometeoizdat, 198. (Russian).
2. **Olkhovsky G.G. 1919.** Fighting frosts. – M.: Narkomizdat, 41. (Russian).
3. **Krasikov P.N. 1948.** Fighting frost with smoke and fog // Proceedings of the Main Geophysical Observatory. – Issue. 72-74. – L.: Gidrometeoizdat. 84-99. (Russian).
4. **Chudnovsky A.F. 1949.** Frosts / Abram Chudnovsky. Ed. Acad. AF Ioffe. – M.: Gidrometeoizdat, 124. (Russian).
5. **Pastukhov V.I. 2010.** Estimating the power of the heat source for support the thermal regime of the agroecosystem / V.I. Pastukhov, M.G. Sandomirsky, A.V. Rudnitskaya, A.V. Minyachikhin, E.N. Rudnitskiy // Herald of KhNTUSG. Issue 93 "Mechanization of agriculture" Kharkiv. – Issue.1. 63-71. (Russian).
6. **Isachenko V.P. 1975.** Heat transfer / Isachenko V.P., Osipova V.A., Sukomel A.S. // Textbook for high schools, Izd. 3rd revision., Add. - Moscow: Energia, 488. (Russian).
7. **Mikheev M.A. 1977.** Fundamentals of heat transfer / M.A. Mikheev, I.M. Mikheeva - Izd. 2 nd, the stereotype. – Moscow: Energia, 344. (Russian).
8. **Brovka G.P. 2000.** Comprehensive analysis and modelling of interrelated processes of heat, moisture and water-soluble compounds transfer in soils / Brovka G.P., Dedyulya I.V., Rovdan E.N., Sychevsky V.A. // Proceedings of the IV Minsk International Forum on Heat and Mass Transfer (May 22-26, 2000). Volume 8. Heat-mass exchange in capillary-porous bodies. – Minsk: ANC " A.V. Lykov ITMO" NASB. 135-144. (Russian).
9. **Straus V. 1981.** Industrial purification of gases / Werner Strauss. Moscow: Chemistry, 616. (Russian).
10. **Fuks N.A. 1958.** Evaporation and growth of drops in a gaseous medium / Nikolai Fuchs. – Moscow: Publishing House of the Sciences Academy of the USSR, 90. (Russian).
11. **Anikeev A.I. 2016.** To the question of improving the efficiency of harvesting corn by implementing agrologistics elements / A.I. Anikeev, M.O. Tsyganenko, K.G. Sirovitskiy, A.R. Koval // MOTROL. Commission of Motorization and Energetics in Agriculture – Vol. 18. No. 7. 49-54. (Poland).
12. **Melnik V.I. 2015.** Economic efficiency of elements exact farming systems / V.I. Melnik, A.I. Anikeev, M.O. Tsyganenko, K.G. Sirovitskiy // MOTROL. Commission of Motorization and Energetics in Agriculture –Vol.17. No.7. 61-66 (Poland).
13. **Kharchenko S.O. 2015.** Direction in development of agricultural technologies of block-variant systems for farms of different technological levels / S.O. Kharcenko, A.I. Anikeev, M.O. Tsiganenko, A.D. Kalujniy, A.G. Rudnitskaya, V.V. Kachanov, A.M. Krasnorutskiy, S.A. Chigrina, K.G. Sirovitskiy, E.A. Gaek // Herald of KhNTUSG. Issue 156 "Mechanization of agriculture" Kharkiv. 174-179. (Russian).
14. **Kalyzhniy A.D. 2016.** Justification of rational scientific methods of acquisition tractor units as part of the tractor with a continuously variable transmission / A.D. Kalyzhniy, K.G. Sirovitskiy, S.N. Vasjuk, A.R. Koval // Engineering of nature management. Kharkiv –№ 1 (5). 113-117 (Ukraine).
15. **Pastukhov V.I. 2010.** Justification of the heat source power for providing thermal models of agroecosystems regimes / V.I. Pastukhov, A.V. Rudnitskaya, A.V. Sergeeva // Herald of TDATU. Issue 8. Melitopol. 120-131. (Ukraine).
16. **Borisovskiy S.G. 2007.** Methods of combating spring frost in fruit-bearing gardens / S.G. Borisovsliy, A.A. Firshev, V.I. Pastukhov, A.V. Rudnitskaya // Herald of KhNTUSG. Issue 59 "Mechanization of agriculture" Kharkiv. 20-24. (Ukraine).
17. **Kharchenko S.A. 2015.** Raising quality of work indicators for implementation of tillage hinged units / S.A. Kharchenko, A.V. Rudnytskaya, A.D. Kalyuzhny, V.V. Kachanov, I.S. Tishchenko, G.V. Fesenko // Engineering of nature management. Kharkiv –№ 2 (4). 92-95 (Ukraine).
18. **Zaika P.M. 2001.** Free motion of a material point in a calm isotropic gaseous medium / P.M. Zaika, V.I. Melnik, A.I. Anikeev // Herald of NTU "KhPI". Issue 1 "Dynamics and reliability of machines" Kharkiv. 153-154. (Ukraine).
19. **Kharchenko S.A. 2015.** Modeling the dynamics of the grain mixtures with the screening on cylindrical vibrating sieve separators / S.A. Kharchenko // TEKA. Commission of Motorization and Energetics in Agriculture – Vol.15. No.3. 87-92. (Poland).
20. **Gaek E.A. 2016.** The algorithm of mathematical modeling of dispersed phase particles of dusty air flow / E.A. Gaek // MOTROL. Commission of Motorization and Energetics in Agriculture –Vol. 18. No. 7. 79-83. (Poland).
21. **Pankova O.V. 2015.** Prolonged effect of optical radiation of a red range during the germination of seeds / O.V. Pankova, A.M. Fesenko, V.V. Bezpalko, N.L. Lysychenko, L. Golovan, T. Romanova // MOTROL. Commission of Motorization and Energetics in Agriculture –Vol. 17. No. 7. 29-34. (Poland).
22. **Gutyanskyi R.A. 2016.** Formation soybean yields in the meteorological conditions of eastern steppe of ukraine / R.A. Gutyanskyi, O.V. Pankova, A.M. Fesenko, V.V. Bezpalko // MOTROL. Commission of Motorization and Energetics in Agriculture –Vol. 18. No. 7. 43-47. (Poland).
23. **Fesenko A.M. 2017.** Application of no-till sunflower cultivation: technical, environmental and economic aspects / A.M. Fesenko, O.V. Pankova, V.V. Bezpalko, R.A. Gutyanskyi // MOTROL. Commission of Motorization and Energetics in Agriculture –Vol. 19. No. 1. 15-20. (Poland).

C O N T E N T S

List of the Reviewers

1.	R. Kuzminskyi	5.	S. Kovalyshyn
2.	I. Palamarchuk	6.	O. Kalahan
3.	V. Tymochko	7.	M. Student
4.	V. Shevchuk	8.	Z. Duryahina

Editors of the “MOTROL” magazine of the Commission of Motorization and Power Industry in Agriculture would like to inform both the authors and readers that an agreement was signed with the Interdisciplinary Centre for Mathematical and Computational Modelling at the Warsaw University referred to as “ICM”. Therefore, ICM is the owner and operator of the IT system needed to conduct and support a digital scientific library accessible to users via the Internet called the “ICM Internet Platform”, which ensures the safety of development, storage and retrieval of published materials provided to users. ICM is obliged to put all the articles printed in the “MOTROL” on the ICM Internet Platform. ICM develops metadata, which are then indexed in the “Agro” database.

We are pleased to announce that the magazine “MOTROL – Motorization and Energetics in Agriculture” (ISSN 1730-8658) has undergone a positive evaluation of the IC Journals Master List 2013, the result of which is granting the ICV Index (Index Copernicus Value) 6.56 pts. The resulting score was calculated on the basis of a survey submitted by the Editorial Team as well as assessments made by the professionals from Index Copernicus. We invite you to familiarize yourself with the methodology of IC Journals Master List evaluation:

http://journals.indexcopernicus.com/masterlist.php?q=motrol

Impact factor of the “MOTROL” journal according of the Commission of Motorization and Energetics in Agriculture is 3,6 (July 2017).

GUIDELINES FOR AUTHORS (2017)

The journal publishes the original research papers. The papers (min. 8 pages) should not exceed 12 pages including tables and figures. Acceptance of papers for publication is based on two independent reviews commissioned by the Editor.

Authors are asked to transfer to the Publisher the copyright of their articles as well as written permissions for reproduction of figures and tables from unpublished or copyrighted materials.

Articles should be submitted electronically to the Editor and fulfill the following formal requirements:
- Clear and grammatically correct script in English,
- Format of popular Windows text editors (A4 size, 12 points Times New Roman font, single interline, left and right margin of 2,5 cm),
- Every page of the paper including the title page, text, references, tables and figures should be numbered,
- SI units should be used.

Please organize the script in the following order (without subtitles):
Title, Author(s) name (s), Affiliations, Full postal addresses, Corresponding author's e-mail
Abstract (up to 200 words), Keywords (up to 5 words), Introduction, Materials and Methods, Results, Discussion (a combined Results and Discussion section can also be appropriate), Conclusions (numbered), References, Tables, Figures and their captions

Note that the following should be observed:
An informative and concise title; Abstract without any undefined abbreviations or unspecified references; No nomenclature (all explanations placed in the text); References cited by the numbered system (max 5 items in one place); Tables and figures (without frames) placed out of the text (after References) and figures additionally prepared in the graphical file format jpg or cdr.

Make sure that the tables do not exceed the printed area of the page. Number them according to their sequence in the text. References to all the tables must be in the text. Do not use vertical lines to separate columns. Capitalize the word 'table' when used with a number, e.g. (Table1).

Number the figures according to their sequence in the text. Identify them at the bottom of line drawings by their number and the name of the author. Special attention should be paid to the lettering of figures – the size of lettering must be big enough to allow reduction (even 10 times). Begin the description of figures with a capital letter and observe the following order, e.g. Time(s), Moisture (%, vol), (%, m^3m^{-3}) or (%, gg^{-1}), Thermal conductivity (W $m^{-1}K^{-1}$).

Type the captions to all figures on a separate sheet at the end of the manuscript.

Give all the explanations in the figure caption. Drawn text in the figures should be kept to a minimum. Capitalize and abbreviate 'figure' when it is used with a number, e.g. (Fig. 1).

Colour figures will not be printed.

Make sure that the reference list contains about 30 items. It should be numbered serially and arranged alphabetically by the name of the first author and then others, e.g.
7. Kasaja O., Azarevich G. and Bannel A.N. 2009. Econometric Analysis of Banking Financial Results in Poland. Journal of Academy of Business and Economics (JABE), Vol. IV. Nr 1, 202–210.

References cited in the text should be given in parentheses and include a number e.g. [7].

Any item in the References list that is not in English, French or German should be marked, e.g. (in Italian), (in Polish).

Leave ample space around equations. Subscripts and superscripts have to be clear. Equations should be numbered serially on the right-hand side in parentheses. Capitalize and abbreviate 'equation' when it is used with a number, e.g. Eq. (1). Spell out when it begins a sentence. Symbols for physical quantities in formulae and in the text must be in italics. Algebraic symbols are printed in upright type.

Acknowledgements will be printed after a written permission is sent (by the regular post, on paper) from persons or heads of institutions mentioned by name.